

HINDERED ROTATION VERSUS RACEMISATION IN AXIALLY CHIRAL
THIOHYDANTOIN DERIVATIVES

by

Oya ARICA

B.S., Chemistry, Yıldız Technical University, 2012

Submitted to the Institute for Graduate Studies in
Science and Engineering in partial fulfillment of
the requirements for the degree of
Master of Science

Graduate Program in Chemistry

Boğaziçi University

2016

ACKNOWLEDGEMENTS

I would like to thank my thesis supervisor, Prof. İlknur Doğan for her guidance, support and advice during my research.

I also wish to thank Prof. Viktorya Aviyente and Prof. Nüket Öcal for being my thesis jury members and for their final comments on the thesis.

I would like to thank Sevgi Sarıgül, for her great help during my research in the laboratory. I would like to thank the other members in my laboratory as well, Şenel Teke Tuncel, Şule Erol Günel and Ari Hakkör for their assistance and help during my project.

I would like to express my thanks to my mother Şule Arıca, my father Atilla Arıca and my sister Beril Arıca, for their endless encouragement and support.

I owe great thanks to my friends, Özlem Kambay, Ayşe Hazal Pekcan, Gökhan Aydemir, Duygu Tuncel, and Didem Erkut for their support in every stage of this project.

I am grateful to the all the members of the chemistry department. I also would like to thank Begüm Alaybeyoğlu and Ayla Türkekul for recording the NMR spectra.

ABSTRACT

HINDERED ROTATION VERSUS RACEMISATION IN AXIALLY CHIRAL THIOHYDANTOIN DERIVATIVES

In this project 5-benzyl-3-(aryl)-2-thiohydantoin and 5-isobutyl-3-(aryl)-2-thiohydantoin derivatives have been synthesized by reacting aryl isothiocyanates with S-phenylalanine methyl ester hydrochloride or with S-leucine methyl ester hydrochloride in the presence of triethylamine (TEA). The synthesized compounds have a chirality center at C5 of the heterocyclic ring. The 3-phenyl derivatives **1** and **4** have been found to exist in **R** or **S** enantiomeric forms. When the phenyl ring carried an *ortho* substituent (compounds **2**, **3**, **5** and **6**), the compounds were shown to become axially chiral, the N3-C_(aryl) bond being the chirality axis. The axially chiral derivatives were shown to exist in unequal amounts of **SM**, **SP**, **RM** and **RP** stereoisomeric forms. Although the syntheses started with an optically pure amino acid ester, the products were found to get racemized at C5 during the reactions. However for the axially chiral derivatives, a high prevalence of the **P** isomers over the **M** isomers have been obtained. The isomeric assignments were done by comparing the ¹H NMR spectra with the HPLC chromatograms. The stereoisomers were resolved micropreparatively by HPLC on chiral stationary phases. The conversion type (racemization or rotation) of each separated isomer has been determined by HPLC analyses. It has been found that although the stereoisomers converted to each other only by rotation in toluene, in ethanol racemization was accompanied with rotation depending on the temperature of the thermal interconversion experiment. The energy barriers for the rotation and racemization processes have been determined. The resolved enantiomer of 5-isobutyl-3-phenyl-2-thiohydantoin was found to racemize at a faster rate than that of the 5-benzyl derivative. The occurrence of racemization was further proved through Hydrogen/Deuterium exchange reactions via ¹H NMR experiments done in CD₃OD. The synthesized compounds will further be exploited in sterically controlled face-selective enolate reactions.

ÖZET

EKSENSEL KİRAL TİYOHİDANTOİN TÜREVLERİNDE RASEMİKLEŞMEYE KARŞI ENGELLİ DÖNME

Bu projede 5-benzil-3-(aril)-2-tiyohidantoin ve 5-izobütil-3-(aril)-2-tiyohidantoin türevleri, trietilamin (TEA) varlığında aril izotiyosiyanatlar ile S-fenil alanin metil ester hidroklorür veya S-lösin metil ester hidroklorürün reaksiyonu ile sentezlenmiştir. Sentezlenen bileşiklerin heterosiklik halkadaki C5'te kiral merkezleri vardır. 3-fenil türevleri olan **1** ve **4**, **R** veya **S** enantiyomerleri halinde bulunmuştur. Fenil halkası *orto*-süstitüent taşıdığında, (bileşikler **2**, **3**, **5** ve **6**) N3-C_(aril) bağı kiral eksen olacak şekilde, bileşiklerin eksensel kiral oldukları görülmüştür. Eksensel kiral türevler, farklı miktarlarda **SM**, **SP**, **RM** ve **RP** stereoizomerleri halinde gözlemlenmiştir. Sentezlere, optik saf amino asit esterler ile başlanmasına rağmen, ürünlerin reaksiyon sırasında C5'te rasemikleştiği bulunmuştur. Ancak, eksensel kiral türevler için, **M** izomerlerine kıyasla yüksek yaygınlıkta **P** izomerleri elde edilmiştir. İzomerik belirlemeler, ¹H NMR spektrumlarının HPLC kromatogramlarının karşılaştırılmasıyla yapılmıştır. Stereoizomerler, HPLC'de kiral sabit fazlar üzerinde mikro preparatif şekilde ayrılmıştır. Ayrılmış olan her izomerin dönüşüm tipi (rasemikleşme veya dönme) HPLC analizleri ile belirlenmiştir. Toluende, birbirlerine karşı sadece dönme gösteren stereoizomerlerin, etanolde termal ara-dönüşüm deneyinin sıcaklığına bağlı olarak, dönmenin rasemikleşmeye eşlik ettiği bulunmuştur. Dönme ve rasemikleşme süreçleri için enerji bariyerleri belirlenmiştir. 5-İzobütil-3-fenil-2-tiyohidantoin'in ayrılmış enantiyomerinin 5-benzil türevinden daha hızlı bir oranla rasemikleştiği bulunmuştur. Rasemikleşmenin varlığı daha sonrasında dötero-metanolde ¹H NMR deneyleri vasıtasıyla Hidrojen/Döteryum değişim reaksiyonları aracılığıyla kanıtlanmıştır. Sentezlenen türevlerden daha sonrasında sterik kontrollü yön-seçici enolat reaksiyonlarında faydanılacaktır.

TABLE OF CONTENTS

| | |
|---|-------|
| ACKNOWLEDGEMENTS..... | iii |
| ABSTRACT..... | iv |
| ÖZET..... | v |
| LIST OF FIGURES..... | ix |
| LIST OF TABLES..... | xvi |
| LIST OF SYMBOLS..... | xvii |
| LIST OF ACRONYMS/ABBREVIATIONS..... | xviii |
| 1. INTRODUCTION..... | 1 |
| 2. THEORY..... | 4 |
| 2.1. Chirality..... | 4 |
| 2.2. Atropisomerism and Hindered Rotation in 5-Benzyl-3-aryl-2-thiohydantoins and 5-Isobutyl-3-aryl-2-thiohydantoins..... | 5 |
| 2.3. Nomenclature..... | 5 |
| 2.4. Stereoisomers of 5-Benzyl-3-aryl-2-thiohydantoin and 5-Isobutyl-3- aryl-2-thiohydantoin derivatives..... | 6 |
| 2.5. Asymmetric Synthesis of 5-Benzyl-3-aryl-2-thiohydantoin and 5-Isobutyl-3- aryl-2-thiohydantoin derivatives by Using the Chiral Pool Approach..... | 8 |
| 2.6. Chromatographic Separation of Stereoisomers..... | 9 |
| 2.6.1. HPLC Technique in Chiral Separations..... | 9 |
| 2.6.2. Separation of Stereoisomers by HPLC on Chiral Stationary Phases..... | 10 |
| 2.7. Determination of the Kinetic and the Thermodynamic Constants of the Internal Rotation and Racemisation Process for 5-Benzyl-3-aryl-2- thiohydantoin and 5-Isobutyl-3-aryl-2-thiohydantoin derivatives..... | 11 |
| 2.7.1. Reaction Kinetics for 5-Benzyl-3-aryl-2-thiohydantoin and 5- Isobutyl-3-aryl-2-thiohydantoin derivatives for Reversible Reactions of Rotation and Racemisation..... | 11 |
| 2.7.2. Hydrogen-Deuterium Exchange at C-5 for 5-Benzyl- 3-aryl-2-thiohydantoin and 5-Isobutyl-3-aryl-2-thiohydantoin derivatives by ¹ H-NMR..... | 13 |

| | |
|---|----|
| 3. EXPERIMENTAL..... | 15 |
| 3.1. Organic Synthesis of 5-Benzyl-3-aryl-2-thiohydantoins..... | 15 |
| 3.1.1. General Procedure for the Synthesis of 5-Benzyl-3-aryl-2-thiohydantoins..... | 15 |
| 3.1.1.1. 5-Benzyl-3-phenyl-2-thiohydantoin..... | 15 |
| 3.1.1.2. 5-Benzyl-3-(<i>o</i> -tolyl)-2-thiohydantoin..... | 16 |
| 3.1.1.3. 5-Benzyl-3-(<i>o</i> -bromophenyl)-2-thiohydantoin..... | 17 |
| 3.2. Organic Synthesis of 5-Isobutyl-3-aryl-2-thiohydantoins..... | 18 |
| 3.2.1. General Procedure for the Synthesis of 5-Isobutyl-3-aryl-2-thiohydantoins..... | 19 |
| 3.2.1.1. 5-Isobutyl-3-phenyl-2-thiohydantoin..... | 19 |
| 3.2.1.2. 5-Isobutyl-3-(<i>o</i> -tolyl)-2-thiohydantoin..... | 20 |
| 3.2.1.3. 5-Isobutyl-3-(<i>o</i> -bromophenyl)-2-thiohydantoin..... | 21 |
| 3.3. Apparatus..... | 22 |
| 3.4. List of Chemicals..... | 23 |
| 3.5. Thermal Interconversion of 5-Benzyl-3-aryl-2-thiohydantoin and 5-Isobutyl-3-aryl-2-thiohydantoin derivatives..... | 23 |
| 4. RESULTS AND DISCUSSION..... | 25 |
| 4.1. Overview..... | 25 |
| 4.2. ¹ H NMR Spectra of the Compounds..... | 27 |
| 4.3. Determination of Barriers of Rotation and/or Racemisation for 5-Benzyl-3-aryl-2-thiohydantoin and 5-Isobutyl-3-aryl-2-thiohydantoin derivatives by HPLC on Chiral Stationary Phases..... | 29 |
| 4.3.1. Determination of Racemisation at C-5 Barrier (S → R Conversion) for 5-Benzyl-3-phenyl-2-thiohydantoin Enantiomers..... | 29 |
| 4.3.2. Determination of the Rotation around N3 _(sp²) -C _(aryl) bond (SP → SM and RP → RM Conversion) and Racemisation at C-5 Barrier (SM → RM and RM → SM Conversion) for 5-Benzyl-3-(<i>o</i> -tolyl)-2-thiohydantoin stereoisomers..... | 30 |
| 4.3.2.1. Solvent Effect on the Interconversions Between the Stereoisomers of 5-Benzyl-3-(<i>o</i> -tolyl)-2-thiohydantoin..... | 32 |

| | |
|--|----|
| 4.3.3. Determination of the Rotation around $N3_{(sp^2)}-C_{(aryl)}$ bond (RP → RM Conversion) and Racemisation at C-5 Barrier (RM ⇌ SM and RP ⇌ SP Conversion) for 5-Benzyl-3- (<i>o</i> -bromophenyl)-2-thiohydantoin stereoisomers..... | 38 |
| 4.3.3.1. Solvent Effect on the Interconversions Between the Stereoisomers of 5-Benzyl-3-(<i>o</i> -bromophenyl)- 2-thiohydantoin..... | 42 |
| 4.3.4. Determination of Racemisation at C-5 Barrier (S → R Conversion) for 5-Isobutyl-3-phenyl-2-thiohydantoin Enantiomers..... | 53 |
| 4.3.5. Determination of the Rotation around $N3_{(sp^2)}-C_{(aryl)}$ bond (RM → RP Conversion) and Racemisation at C-5 Barrier (RM ⇌ SM and RP ⇌ SP Conversion) for 5-Isobutyl-3-(<i>o</i> -tolyl)- 2-thiohydantoin stereoisomers..... | 55 |
| 4.3.5.1. Solvent Effect on the Interconversions Between the Stereoisomers of 5-Isobutyl-3-(<i>o</i> -tolyl)-2-thiohydantoin..... | 55 |
| 4.3.6. Determination of the Rotation around $N3_{(sp^2)}-C_{(aryl)}$ bond (SP → SM Conversion) and Racemisation at C-5 Barrier (RM ⇌ SM and RP ⇌ SP Conversion) for 5-Isobutyl-3- (<i>o</i> -bromophenyl)-2-thiohydantoin stereoisomers..... | 56 |
| 4.3.6.1. Solvent Effect on the Interconversions Between the Stereoisomers of 5-Isobutyl-3-(<i>o</i> -bromophenyl)-2thiohydantoin... | 63 |
| 4.4. Deuteration of 5-Benzyl-3-aryl-2-thiohydantoins and 5-Isobutyl-3-aryl-2-thiohydantoins..... | 64 |
| 4.5. Separation Factors (α) for the Synthesized Derivatives..... | 70 |
| 5. CONCLUSION..... | 78 |
| REFERENCES..... | 81 |
| APPENDIX A: 1H -NMR SPECTRA OF THE COMPOUNDS..... | 84 |

LIST OF FIGURES

| | | |
|-------------|--|----|
| Figure 1.1. | Hindered internal rotation around C _{aryl} -N _{sp2} bond in aryl substituted heterocyclic compounds..... | 1 |
| Figure 1.2. | Sterically hindered biphenyl derivatives..... | 1 |
| Figure 2.1. | Rotational isomers of 5-benzyl-3-aryl-2-thiohydantoin and 5-isobutyl-3-aryl-2-thiohydantoin derivatives..... | 6 |
| Figure 2.2. | Descriptors for axially chiral 5-benzyl-3-aryl-2-thiohydantoin and 5-isobutyl-3-aryl-2-thiohydantoin derivatives..... | 7 |
| Figure 2.3. | Stereoisomers of axially chiral 5-benzyl-3-aryl-2-thiohydantoin and 5-isobutyl-3-aryl-2-thiohydantoin derivatives..... | 8 |
| Figure 2.4. | (S)-phenyl alanine methyl ester and (S)-leucine methyl ester structures..... | 8 |
| Figure 2.5. | Enolisation mechanism of synthesized derivatives..... | 13 |
| Figure 3.1. | The synthesis of 5-benzyl-3-aryl-thiohydantoin..... | 15 |
| Figure 3.2. | The synthesis of 5-isobutyl-3-aryl-thiohydantoin..... | 19 |
| Figure 4.1. | Structure of 5-benzyl-3-phenyl-2-thiohydantoin (a) and 5-isobutyl-3-phenyl-2-thiohydantoin (b)..... | 28 |
| Figure 4.2. | The plot of $\ln\left(\frac{[S]_0 - [S]_{eq}}{[S] - [S]_{eq}}\right)$ versus time at 313 K for 5-benzyl-3-phenyl-2-thiohydantoin | 30 |

| | | |
|--------------|---|----|
| Figure 4.3. | HPLC chromatograms for racemisation of 5-benzyl-3-phenyl-2-thiohydantoin in ethanol at 313 K..... | 31 |
| Figure 4.4. | The plot of $\ln\left(\frac{[\mathbf{SM}]_o - [\mathbf{SM}]_{eq}}{[\mathbf{SM}] - [\mathbf{SM}]_{eq}}\right)$, $\ln\left(\frac{[\mathbf{RM}]_o - [\mathbf{RM}]_{eq}}{[\mathbf{RM}] - [\mathbf{RM}]_{eq}}\right)$ and versus time at 298 K for 5-benzyl-3-(<i>o</i> -tolyl)-2-thiohydantoin..... | 33 |
| Figure 4.5. | HPLC chromatograms for racemisation of SM -5-benzyl-3-(<i>o</i> -tolyl)-2-thiohydantoin to RM in ethanol at 298 K..... | 34 |
| Figure 4.6. | HPLC chromatograms for racemisation of RM -5-benzyl-3-(<i>o</i> -tolyl)-2-thiohydantoin to SM in ethanol at 298 K..... | 35 |
| Figure 4.7. | HPLC chromatograms for rotation of SP -5-benzyl-3-(<i>o</i> -tolyl)-2-thiohydantoin to SM in ethanol at 298 K..... | 36 |
| Figure 4.8. | HPLC chromatograms for rotation of RP -5-benzyl-3-(<i>o</i> -tolyl)-2-thiohydantoin to RM in ethanol at 298 K..... | 37 |
| Figure 4.9. | The plot of $\ln\left(\frac{[\mathbf{SP}]_o - [\mathbf{SP}]_{eq}}{[\mathbf{SP}] - [\mathbf{SP}]_{eq}}\right)$ and $\ln\left(\frac{[\mathbf{RP}]_o - [\mathbf{RP}]_{eq}}{[\mathbf{RP}] - [\mathbf{RP}]_{eq}}\right)$ versus time at 298 K for 5-benzyl-3-(<i>o</i> -tolyl)-2-thiohydantoin..... | 38 |
| Figure 4.10. | HPLC chromatograms for rotation of SM -5-benzyl-3-(<i>o</i> -tolyl)-2-thiohydantoin to SP in toluene at 313 K..... | 39 |
| Figure 4.11. | HPLC chromatograms for rotation of RP -5-benzyl-3-(<i>o</i> -tolyl)-2-thiohydantoin to RM in toluene at 313 K..... | 40 |
| Figure 4.12. | The plot of $\ln\left(\frac{[\mathbf{RP}]_o - [\mathbf{RP}]_{eq}}{[\mathbf{RP}] - [\mathbf{RP}]_{eq}}\right)$ and $\ln\left(\frac{[\mathbf{SM}]_o - [\mathbf{SM}]_{eq}}{[\mathbf{SM}] - [\mathbf{SM}]_{eq}}\right)$ versus time at 313 K for 5-benzyl-3-(<i>o</i> -tolyl)-2-thiohydantoin | 41 |

- Figure 4.13. The plot of $\ln\left(\frac{[\mathbf{RM}]_o - [\mathbf{RM}]_{eq}}{[\mathbf{RM}] - [\mathbf{RM}]_{eq}}\right)$, $\ln\left(\frac{[\mathbf{SP}]_o - [\mathbf{SP}]_{eq}}{[\mathbf{SP}] - [\mathbf{SP}]_{eq}}\right)$, $\ln\left(\frac{[\mathbf{RP}]_o - [\mathbf{RP}]_{eq}}{[\mathbf{RP}] - [\mathbf{RP}]_{eq}}\right)$, versus time at 298 K for 5-benzyl-3-(*o*-bromophenyl)-2-thiohydantoin.....43
- Figure 4.14. HPLC chromatograms for racemisation of **SP**-5-benzyl-3-(*o*-bromophenyl)-2-thiohydantoin to **RP** in ethanol at 298K.....44
- Figure 4.15. HPLC chromatograms for racemisation of **RP**-5-benzyl-3-(*o*-bromophenyl)-2-thiohydantoin to **SP** in ethanol at 298 K.....45
- Figure 4.16. HPLC chromatograms for racemisation of **RM**-5-benzyl-3-(*o*-bromophenyl)-2-thiohydantoin to **SM** in ethanol at 298 K.....46
- Figure 4.17. The plot of $\ln\left(\frac{[\mathbf{RM}]_o - [\mathbf{RM}]_{eq}}{[\mathbf{RM}] - [\mathbf{RM}]_{eq}}\right)$, $\ln\left(\frac{[\mathbf{SP}]_o - [\mathbf{SP}]_{eq}}{[\mathbf{SP}] - [\mathbf{SP}]_{eq}}\right)$, $\ln\left(\frac{[\mathbf{RP}]_o - [\mathbf{RP}]_{eq}}{[\mathbf{RP}] - [\mathbf{RP}]_{eq}}\right)$, versus time at 313 K for 5-benzyl-3-(*o*-bromophenyl)-2-thiohydantoin.....47
- Figure 4.18. HPLC chromatograms for racemisation of **SP**-5-benzyl-3-(*o*-bromophenyl)-2-thiohydantoin to **RP** in ethanol at 313 K.....48
- Figure 4.19. HPLC chromatograms for racemisation of **RP**-5-benzyl-3-(*o*-bromophenyl)-2-thiohydantoin to **SP** in ethanol at 313 K.....49
- Figure 4.20. HPLC chromatograms for racemisation of **RM**-5-benzyl-3-(*o*-bromophenyl)-2-thiohydantoin to **SM** in ethanol at 313 K.....50
- Figure 4.21. HPLC chromatograms for rotation of **RP**-5-benzyl-3-(*o*-bromophenyl)-2-thiohydantoin to **RM** in toluene at 383 K.....51
- Figure 4.22. The plot of $\ln\left(\frac{[\mathbf{RP}]_o - [\mathbf{RP}]_{eq}}{[\mathbf{RP}] - [\mathbf{RP}]_{eq}}\right)$ versus time at 383 K for 5-benzyl-3-(*o*-bromophenyl)-2-thiohydantoin.....52

| | | |
|--------------|---|----|
| Figure 4.23. | The plot of $\ln K$ versus $1/T$ for 5-benzyl-3-(<i>o</i> -bromophenyl)-2-thiohydantoin..... | 52 |
| Figure 4.24. | The plot of $\ln([S]_o/[S]_{eq})$ versus time at 313 K for 5-isobutyl-3-phenyl-2-thiohydantoin | 53 |
| Figure 4.25. | HPLC chromatograms for racemisation of 5-isobutyl-3-phenyl-2-thiohydantoin in ethanol at 313 K..... | 54 |
| Figure 4.26. | The plot of $\ln([SM]_o/[SM]_{eq})$, $\ln([SP]_o/[SP]_{eq})$, $\ln([RM]_o/[RM]_{eq})$, $\ln([RP]_o/[RP]_{eq})$, versus time at 298 K for 5-isobutyl-3-(<i>o</i> -tolyl)-2-thiohydantoin..... | 57 |
| Figure 4.27. | HPLC chromatograms for racemisation of SM -5-isobutyl-3-(<i>o</i> -tolyl)-2-thiohydantoin to RM in ethanol at 298 K..... | 58 |
| Figure 4.28. | HPLC chromatograms for racemisation of RM -5-isobutyl-3-(<i>o</i> -tolyl)-2-thiohydantoin to SM in ethanol at 298 K..... | 59 |
| Figure 4.29. | HPLC chromatograms for racemisation of SP -5-isobutyl-3-(<i>o</i> -tolyl)-2-thiohydantoin to RP in ethanol at 298 K..... | 60 |
| Figure 4.30. | HPLC chromatograms for racemisation of RP -5-isobutyl-3-(<i>o</i> -tolyl)-2-thiohydantoin to SP in ethanol at 298 K..... | 61 |
| Figure 4.31. | HPLC chromatograms for rotation of RM -5-isobutyl-3-(<i>o</i> -tolyl)-2-thiohydantoin to RP in toluene at 313 K..... | 62 |
| Figure 4.32. | The plot of $\ln([RM]_o/[RM]_{eq})$ versus time at 313 K for 5-isobutyl-3-(<i>o</i> -tolyl)-2-thiohydantoin..... | 63 |

- Figure 4.33. The plot of $\ln\left(\frac{[\mathbf{RP}]_o - [\mathbf{RP}]_{eq}}{[\mathbf{RP}] - [\mathbf{RP}]_{eq}}\right)$, $\ln\left(\frac{[\mathbf{SP}]_o - [\mathbf{SP}]_{eq}}{[\mathbf{SP}] - [\mathbf{SP}]_{eq}}\right)$, $\ln\left(\frac{[\mathbf{RM}]_o - [\mathbf{RM}]_{eq}}{[\mathbf{RM}] - [\mathbf{RM}]_{eq}}\right)$, versus time at 313 K for 5-isobutyl-3-(*o*-bromophenyl)-2-thiohydantoin.....65
- Figure 4.34. HPLC chromatograms for racemisation of **RP**-5-isobutyl-3-(*o*-bromophenyl)-2-thiohydantoin to **SP** in ethanol at 313 K.....66
- Figure 4.35. HPLC chromatograms for racemisation of **SP**-5-isobutyl-3-(*o*-bromophenyl)-2-thiohydantoin to **RP** in ethanol at 313 K.....67
- Figure 4.36. HPLC chromatograms for racemisation of **RM**-5-isobutyl-3-(*o*-bromophenyl)-2-thiohydantoin to **SM** in ethanol at 313 K.....68
- Figure 4.37. HPLC chromatograms for rotation of **SP**-5-isobutyl-3-(*o*-bromophenyl)-2-thiohydantoin to **SM** in toluene at 383 K.....69
- Figure 4.38. The plot of $\ln\left(\frac{[\mathbf{SP}]_o - [\mathbf{SP}]_{eq}}{[\mathbf{SP}] - [\mathbf{SP}]_{eq}}\right)$ versus time at 383 K for 5-isobutyl-3-(*o*-bromophenyl)-2-thiohydantoin.....70
- Figure 4.39. $\ln(C-5/CH_3)$ versus time graphic for calculation of racemisation barrier of 5-benzyl-3-(*o*-tolyl)-2-thiohydantoin by $^1\text{H-NMR}$70
- Figure 4.40. Exchange of deuterium with hydrogen atom at C-5 of the 5-benzyl-3-(*o*-tolyl)-2-thiohydantoin in time by $^1\text{H-NMR}$71
- Figure 4.41. 5-isobutyl-3-(*o*-tolyl)-2-thiohydantoin C-5 hydrogen signal change in time in CD_3OD72
- Figure 4.42. 5-benzyl-3-(*o*-tolyl)-2-thiohydantoin C-5 hydrogen signal change in time in CD_3OD73
- Figure 4.43. 5-benzyl-3-(*o*-bromophenyl)-2-thiohydantoin C-5 hydrogen signal change in time in CD_3OD74

| | | |
|--------------|--|----|
| Figure 4.44. | 5-isobutyl-3-phenyl-2-thiohydantoin C-5 hydrogen signal change in time in CD ₃ OD..... | 75 |
| Figure 4.45. | 5-isobutyl-3-(<i>o</i> -bromophenyl)-2-thiohydantoin C-5 hydrogen signal change in time in CD ₃ OD..... | 76 |
| Figure A.1. | The 400 MHz ¹ H NMR spectrum of recrystallized 5-benzyl-3-phenyl-2-thiohydantoin in CDCl ₃ | 84 |
| Figure A.2. | The coupling constants of recrystallized 5-benzyl-3-phenyl-2-thiohydantoin in CDCl ₃ | 85 |
| Figure A.3. | The 400 MHz ¹ H NMR spectrum of recrystallized 5-isobutyl-3-phenyl-2-thiohydantoin in CDCl ₃ | 86 |
| Figure A.4. | The coupling constants of recrystallized 5-isobutyl-3-phenyl-2-thiohydantoin in CDCl ₃ | 87 |
| Figure A.5. | The 400 MHz ¹ H NMR spectrum of 5-benzyl-3-(<i>o</i> -tolyl)-2-thiohydantoin in CDCl ₃ , not used for assignment..... | 88 |
| Figure A.6. | The coupling constants of 5-benzyl-3-(<i>o</i> -tolyl)-2-thiohydantoin in CDCl ₃ , not used for assignment..... | 89 |
| Figure A.7. | The 400 MHz ¹ H NMR spectrum of recrystallized 5-benzyl-3-(<i>o</i> -bromophenyl)-2-thiohydantoin in CDCl ₃ , used for assignment | 90 |
| Figure A.8. | The coupling constants of recrystallized 5-benzyl-3-(<i>o</i> -bromophenyl)-2-thiohydantoin in CDCl ₃ , used for assignment..... | 91 |
| Figure A.9. | The 400 MHz ¹ H NMR spectrum of recrystallized 5-isobutyl-3-(<i>o</i> -tolyl)-2-thiohydantoin in CDCl ₃ , used for assignment..... | 92 |

- Figure A.10. The coupling constants of recrystallized 5-isobutyl-3-(*o*-tolyl)-2-thiohydantoin in CDCl₃, used for assignment.....93
- Figure A.11. The 400 MHz ¹H NMR spectrum of recrystallized 5-isobutyl-3-(*o*-bromophenyl)-2-thiohydantoin in CDCl₃, used for assignment94
- Figure A.12. The coupling constants of recrystallized 5-isobutyl-3-(*o*-bromophenyl)-2-thiohydantoin in CDCl₃, used for assignment.....95
- Figure A.13. The 400 MHz ¹H NMR spectrum of crude 5-benzyl-3-(*o*-tolyl)-2-thiohydantoin in CD₃OD, used for assignment.....96
- Figure A.14. The 400 MHz ¹H NMR spectrum of recrystallized 5-benzyl-3-(*o*-tolyl)-2-thiohydantoin in CD₃OD, used for assignment.....97
- Figure A.15. The 400 MHz ¹H NMR spectrum of 5-benzyl-3-(*o*-bromophenyl)-2-thiohydantoin in C₆D₆, not used for assignment.....98
- Figure A.16. The 400 MHz ¹H NMR spectrum of recrystallized 5-isobutyl-3-(*o*-tolyl)-2-thiohydantoin in C₆D₆, used for assignment.....99
- Figure A.17. The 400 MHz ¹H NMR spectrum of crude 5-isobutyl-3-(*o*-tolyl)-2-thiohydantoin in CDCl₃, used for assignment.....100
- Figure A.18. The 400 MHz ¹H NMR spectrum of recrystallized 5-isobutyl-3-(*o*-bromophenyl)-2-thiohydantoin in C₆D₆, used for assignment.....101

LIST OF TABLES

| | | |
|------------|--|----|
| Table 1.1. | The synthesized derivatives of 5-benzyl-3-aryl-2-thiohydantoins and 5-isobutyl-3-aryl-2-thiohydantoins..... | 2 |
| Table 3.1. | Chemicals used in this study..... | 23 |
| Table 4.1. | Relative proportions of the isomers determined by HPLC with a chiral stationary phase..... | 25 |
| Table 4.2. | Calculated ΔG^\ddagger (kJ/mole) and k values for 5-benzyl-3- <i>o</i> -tolyl-2-thiohydantoin..... | 33 |
| Table 4.3. | Calculated ΔG^\ddagger (kJ/mole) and k values for 5-benzyl-3-(<i>o</i> -bromophenyl)-2 thiohydantoin..... | 42 |
| Table 4.4. | Calculated ΔG^\ddagger (kJ/mole) and k values for 5-isobutyl-3- <i>o</i> -tolyl-2-thiohydantoin..... | 56 |
| Table 4.5. | Calculated ΔG^\ddagger (kJ/mole) and k values for 5-isobutyl-3-(<i>o</i> -bromophenyl)-2-thiohydantoin..... | 64 |
| Table 4.6. | Calculated separation factors (α) for the synthesized derivatives for HPLC..... | 77 |
| Table 5.1. | Summary of the results of racemisations and rotations observed within the stereoisomers of the compounds studied | 79 |

LIST OF SYMBOLS

| | |
|---------------------|---|
| A_m | Amount of the compound in the mobile phase |
| A_s | Amount of the compound in the stationary phase |
| C_m | Concentration of the compound in mobile phase |
| C_s | Concentration of the compound in stationary phase |
| F | Flow rate |
| h | Planck's constant |
| Hz | Hertz |
| J | Joule |
| K | Equilibrium constant |
| k' | Capacity factor |
| k_b | Boltzman constant |
| k_f | Rate constant for forward reaction |
| k_r | Rate constant for reverse reaction |
| t | Time |
| T | Temperature |
| t_R | Retention time |
| V_0 | Dead volume |
| V_n | Net retention volume |
| V_R | Retention volume |
| α | Separation factor |
| ΔG^\ddagger | Free energy of activation |
| ΔH° | Standard enthalpy change |
| ΔS° | Standard entropy change |

LIST OF ACRONYMS/ABBREVIATIONS

| | |
|----------|-------------------------------------|
| C_6D_6 | Deutero-benzene |
| $CDCl_3$ | Deutero-chloroform |
| CD_3OD | Deutero-methanol |
| CSP | Chiral stationary phase |
| HPLC | High Pressure Liquid Chromatography |

INTRODUCTION

In heterocyclic compounds when an sp^2 nitrogen heteroatom is bonded to an *o*-aryl ring, (Figure 1.1) hindered rotation around C-N bond is observed if the *ortho*-substituent Z and the exo cyclic groups O and Y are too bulky to pass each other [1-4]. This hindered rotation is worth to consider due to the fact that these compounds are heterocyclic analogues of biphenyl derivatives (Figure 1.2) which are well known with the hindered rotation around $C_{sp^2}-C_{sp^2}$ bond [5-9].

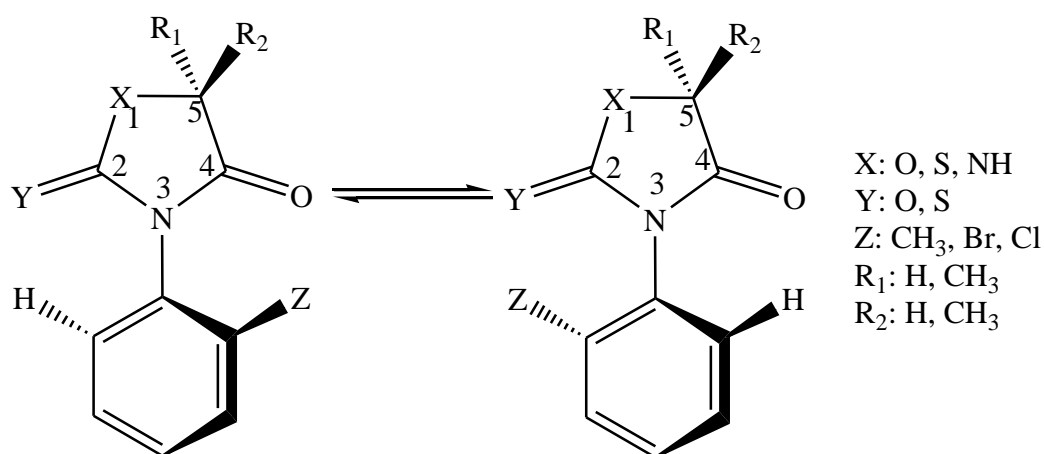


Figure 1.1. Hindered internal rotation around $C_{\text{aryl}}-N_{\text{sp}^2}$ bond in aryl substituted heterocyclic compounds.

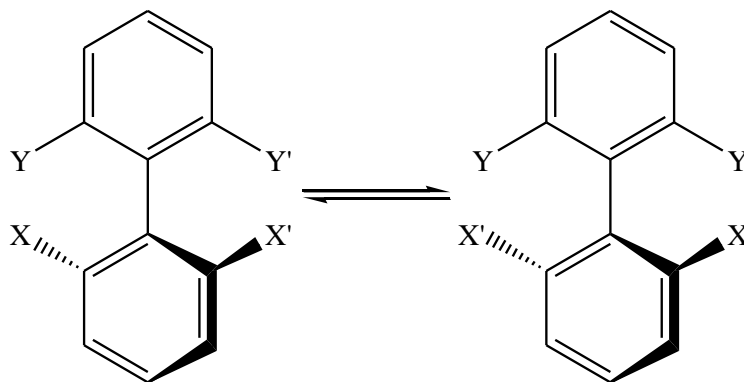


Figure 1.2. Sterically hindered biphenyl derivatives.

The experiments on *N*-*o*-aryl substituted heterocyclic molecules such as thiazolidinediones [4], 2-thioxo-4-thiazolidinones [2] and 2-thioxo-4-oxazolidinones [2] showed that these compounds are axially chiral due to the hindered rotation around the C-N bond. The reason for that is, the carbonyl and/or thiocarbonyl groups on the heteroring prevent the free rotation of the *o*-aryl group substituted on N-3 so that axial chirality occurs and C-N bond becomes a chiral axis. Hindered rotation around the C_{aryl}-N_{sp2} has also been observed in 3-arylhydantoins and thiohydantoins [10-12], azoline-2-thiones [13] and *N*-arylpyrrole derivatives [14].

Axially chiral compounds have significant importance in modern synthetic chemistry and particularly valuable in drug discovery and development [15]. Some hydantoin and thiohydantoin derivatives exhibit a wide range of biological activities, including anticonvulsant, antiarrhythmic, anti-inflammatory, and antidiabetic properties, as well as herbicidal and fungicidal activity [16]. Additionally, 2-thiohydantoins have been used as reference standards for the development of C-terminal protein sequencing [17] as reagents for the development of dyes and in textile printing, metal cation complexation and polymerization catalysis [18].

In this study, axially chiral thiohydantoin derivatives (compound **2**, **3**, **5** and **6**), which are diastereomeric compounds because of the chiral center at C-5 of the heterocyclic ring and the N_{sp2}-C_{aryl} chiral axis, and non-axially chiral derivatives (compound **1** and **4**) were synthesized (Table 1.1).

Table 1.1. The synthesized derivatives of 5-benzyl-3-aryl-2-thiohydantoins and 5-isobutyl-3-aryl-2-thiohydantoins

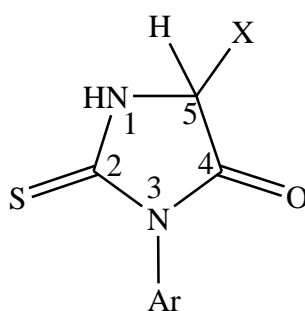


Table 1.1. The synthesized derivatives of 5-benzyl-3-aryl-2-thiohydantoins and 5-isobutyl-3-aryl-2-thiohydantoins (continued).

| No | Ar | X |
|-----------|-----------------------|----------|
| 1 | phenyl | benzyl |
| 2 | <i>o</i> -tolyl | benzyl |
| 3 | <i>o</i> -bromophenyl | benzyl |
| 4 | phenyl | isobutyl |
| 5 | <i>o</i> -tolyl | isobutyl |
| 6 | <i>o</i> -bromophenyl | isobutyl |

The method developed by Reyes and Burgess has been applied with some modifications to synthesize thiohydantoin derivatives with benzyl and isobutyl substituents at C-5 of the heterocyclic ring [19].

The aims of this project are the followings:

- To synthesize derivatives of 5-benzyl-3-aryl-2-thiohydantoins and 5-isobutyl-3-aryl-2-thiohydantoins
- To prove the presence of diastereomeric species using ^1H NMR,
- To investigate the hindered rotations and racemisations if they exist, by HPLC or by NMR.
- To calculate kinetic and thermodynamic constants of the internal rotation and the racemisation processes.

2. THEORY

2.1. Chirality

Stereoisomers are isomers which differ from each other by the spatial arrangements of atoms, and not by the order of atomic connectivity. One type of such isomerism is the mirror-image stereoisomers, a non-superimposable set of two molecules that are mirror images of each other. The existence of these molecules is determined by the concept known as chirality. The word "chiral" was derived from the Greek word for "hand", because hands are good examples of chirality since they are non-superimposable mirror images of each other. These non-superimposable isomers are called "enantiomers". These molecules have same chemical and physical properties such as; identical melting and boiling points, same solubility in same solvents, same nuclear magnetic resonance and infrared shifts in spectra. However, they differ in rotating the plane polarized light to opposite directions. They can show different chemical reactions with other enantiomeric substances as well.

Chiral molecules, which have two or more chirality centers, may be either enantiomers or diastereomers. Diastereomers are stereoisomers that are not mirror images of each other. These molecules have different chemical and physical properties.

Four main types of chirality are; central chirality, axial chirality, planar chirality and helical chirality.

Central chirality occurs when four different types of atoms are attached to a tetrahedral atom. This atom is called as the "stereocenter" and the most known example is a carbon atom. However, sulphur, tetrahedral nitrogen and phosphorus would also be a stereocenter.

Atropisomers are stereoisomers arising because of hindered rotation about a single bond, where energy differences due to steric strain or other contributors create a barrier to rotation that is high enough to allow for isolation of individual conformers. M. Oki defined atropisomers taking into account the temperature-dependence associated with the

interconversion of conformers, specifying that atropisomers interconvert with a half-life of at least 1000 seconds at a given temperature, corresponding to an energy barrier of 93 kJ mol⁻¹ (22 kcal mol⁻¹) at 300 K (27 °C) [20]. Thus atropisomerism results from restricted rotation around carbon-carbon single bond and atropisomers display axial chirality.

Helical chirality occurs when a special case of chirality axis appears in molecules with a helical shape. This type of molecule can adopt either right- or left-handed twist.

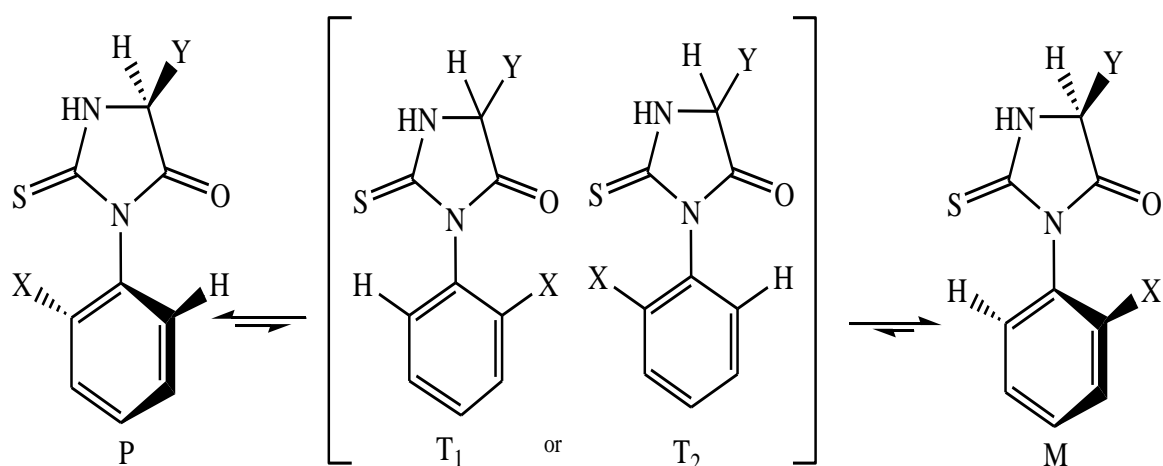
2.2. Atropisomerism and Hindered Rotation in 5-Benzyl-3-aryl-2-thiohydantoins and 5-Isobutyl-3-aryl-2-thiohydantoins

The biphenyls constitute classical examples of atropisomeric compounds. In these compounds, the bond's rotation, which is between the aromatic rings, is restricted. The rotation around carbon-carbon single bond is restricted due to the presence of *ortho* substituents at the aromatic rings of the biphenyl molecule. Therefore, two enantiomeric stereoisomers exist and rings remain orthogonal to each other.

The synthesized derivatives of 2-thiohydantoin in this study, have restricted rotation due to the presence of the *ortho* substituted phenyl ring at N-3 position of the thiohydantoin ring and due to the presence of exocyclic oxygen and sulphur atoms (Figure 2.1). As a result, interconvertible stereoisomers of 5-benzyl-3-aryl-2-thiohydantoins and 5-isobutyl-3-aryl-2-thiohydantoins exist (Figure 2.3).

2.3. Nomenclature

To name the conformation of axially chiral stereoisomers, Cahn-Ingold-Prelog system is used where chiralities are defined in terms of the helicities as **M** or **P** [21]. In this system, first an axis is drawn through the single bond around which conformation is defined and smallest torsion angle formed between the carbon atoms bearing the groups of the highest priority is used to define helix.



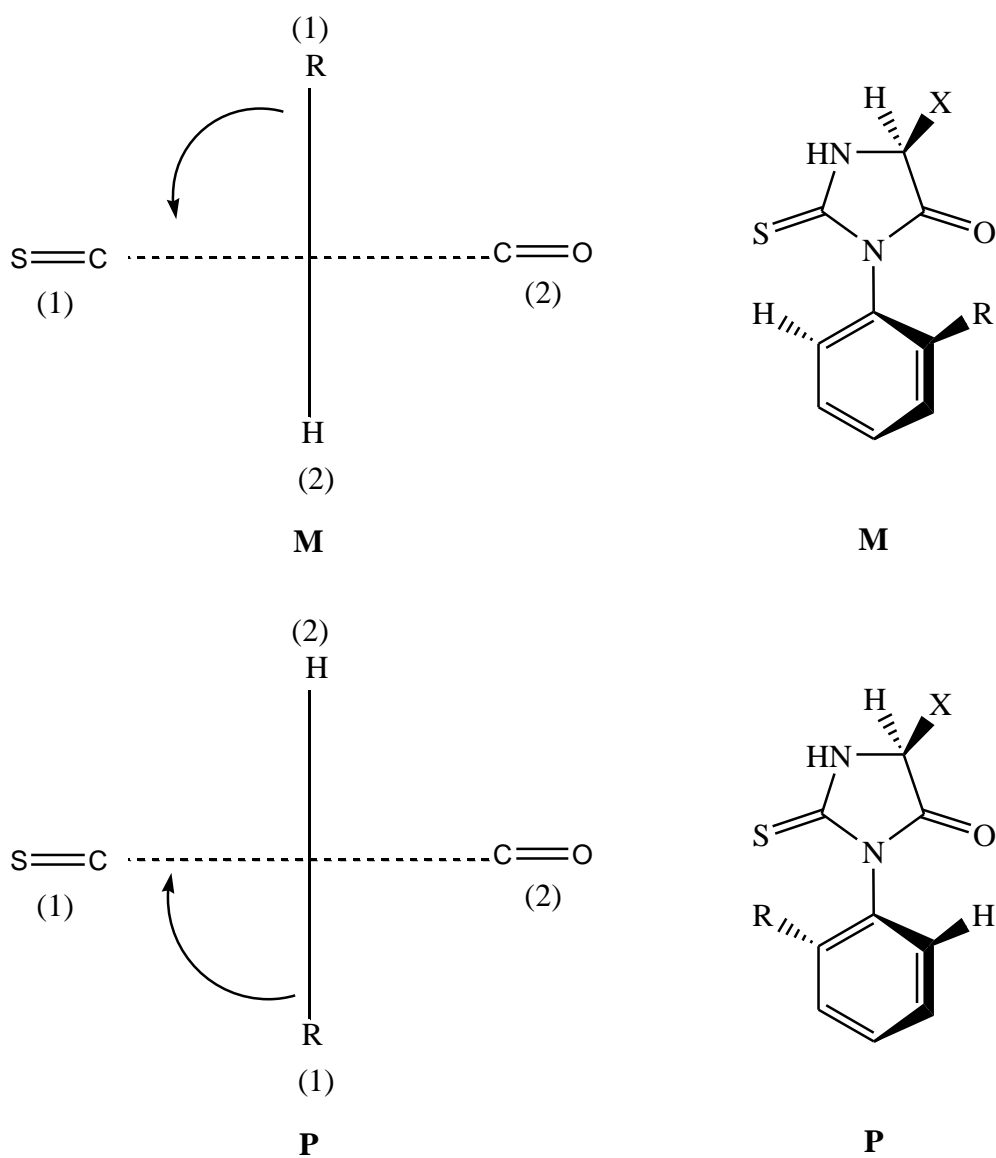
Y: benzyl, isobutyl; X: H, CH₃, Br

Figure 2.1. Rotational isomers of 5-benzyl-3-aryl-2-thiohydantoin and 5-isobutyl-3-aryl-2-thiohydantoin derivatives.

The clockwise rotation is assigned as “**P**” (plus) and the counter clockwise rotation is assigned as “**M**” (minus) (Figure 2.2).

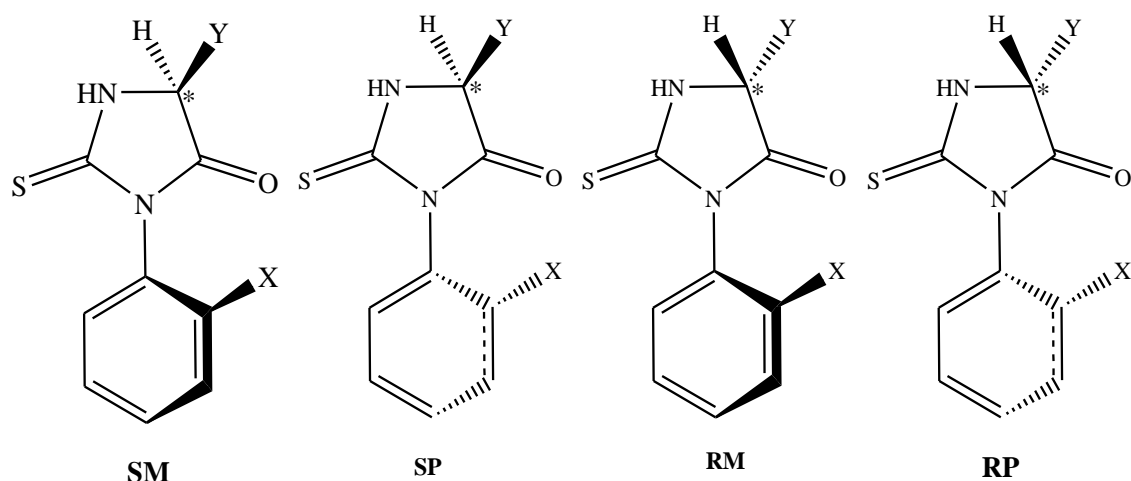
2.4. Stereoisomers of 5-Benzyl-3-aryl-2-thiohydantoin and 5-Isobutyl-3-aryl-2-thiohydantoin derivatives

For 5-benzyl-3-aryl-2-thiohydantoin and 5-isobutyl-3-aryl-2-thiohydantoin derivatives, if the N-3 position has been substituted with *o*-bromophenyl or *o*-tolyl, the derivatives become axially chiral due to hindered rotation around C_{aryl}-N_{sp²} bond forming **P** and **M** stereoisomers. In addition, C-5 of the thiohydantoin is a chiral center. Therefore, 4 types of stereoisomers may be observed at the end of the synthesis reactions for axially chiral 5-benzyl-3-aryl-2-thiohydantoin and 5-isobutyl-3-aryl-2-thiohydantoin (Figure 2.3) derivatives, such as: **SP**, **RP**, **SM** and **RM**.



X: benzyl, isobutyl; R: CH₃, Br

Figure 2.2. Descriptors for axially chiral 5-benzyl-3-aryl-2-thiohydantoin and 5-isobutyl-3-aryl-2-thiohydantoin derivatives.



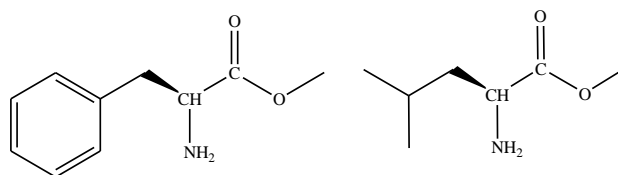
(2) : X= CH₃ , Y= Benzyl ; (3) : X= Br , Y= Benzyl

(5) : X=CH₃ , Y= Isobutyl ; (6) : X=Br , Y= Isobutyl

Figure 2.3. Stereoisomers of axially chiral 5-benzyl-3-aryl-2-thiohydantoin and 5-isobutyl-3-aryl-2-thiohydantoin derivatives.

2.5. Asymmetric Synthesis of 5-Benzyl-3-aryl-2-thiohydantoin and 5-Isobutyl-3-aryl-2-thiohydantoin derivatives by Using the Chiral Pool Approach

One of the common methods of synthesis for chiral molecules is via the chiral pool approach. In this method, an enantiopure starting material is used in order to receive only the enantiopure stereoisomer at the end of the organic reaction. In this study, 5-benzyl-3-aryl-2-thiohydantoin and 5-isobutyl-3-aryl-2-thiohydantoin derivatives have been synthesized using the chiral pool approach. As starting materials (S)- phenyl alanine methyl ester and (S)- leucine methyl ester have been used (Figure 2.4).



(S)- phenyl alanine methyl ester ; (S)- leucine methyl ester

Figure 2.4. (S)- phenyl alanine methyl ester and (S)- leucine methyl ester structures.

2.6. Chromatographic Separation of Stereoisomers

2.6.1. HPLC Technique in Chiral Separations

Chromatographic methods on chiral stationary phases are considered most useful for enantiomeric resolutions for a number of reasons. The most important reason is the ease of separation. Of various chromatographic methods, high pressure liquid chromatography (HPLC) is one of the most powerful separation techniques. HPLC is used for identification and separation of enantiomers. The chromatographic separation of enantiomers can be achieved via chiral stationary phases. Enantiomers can be resolved by the formation of diastereomeric complexes between the solute and a chiral molecule that is bound to the stationary phase.

Strongly retained stereoisomers move slowly while weakly held stereoisomers travel rapidly on chiral stationary phases.

The retention of a component on a column can be expressed by its retention time (t_R), retention volume ($V_R = t_R \times F$, where F is the flow rate) or the capacity ratio (k'), which is directly related to its equilibrium distribution constant (K) in the stationary-mobile phase system. The capacity ratio is defined by:

$$k' = A_s/A_m \quad (2.1)$$

where A_s and A_m denote the amount of the compound in the stationary and the mobile phase, respectively. Let V_s and V_m be the volumes of the respective phases; then

$$k' = C_s V_s / C_m V_m = K V_s / V_m \quad (2.2)$$

V_m is commonly written as V_0 and represents the dead volume in the column, which does not contribute to the separation. Consequently, the net retention volume, V_n can be written as $V_n = V_R - V_0$, and since $K = V_n / V_s$ combination with equation (2.2) gives:

$$k' = (V_R - V_0)/V_0 \quad (2.3)$$

This expression permits the determination of the capacity factor from the chromatogram. The chromatographic separation of two components (1 and 2) depends on the separation factor (α) of a column. It can be written as $k_2'/k_1' = K_2/K_1 = \alpha$. From Equation (2.3), α can be formulated as:

$$\alpha = (V_{R2} - V_0)/(V_{R1} - V_0) \quad (2.4)$$

Thus the separation factor is simply the ratio of the net retention volumes of the two components. If the dead volume V_0 , has been determined, the separation factor is easily calculated from Equation (2.4).

2.6.2. Separation of Stereoisomers by HPLC on Chiral Stationary Phases

Enantiomers have identical chemical and physical properties so it is not possible to separate enantiomers by an ordinary HPLC. Therefore, to separate enantiomers, HPLC columns packed with chiral stationary phases (CSPs) are used.

In chiral stationary phases, there is an optically pure chiral selector which forms diastereomeric complexes between the analyte stereoisomers. The retention time is related to these temporary diastereomeric complexes on chiral stationary phases due to the energy differences between the complexes. The enantiomers, which form more stable diastereomeric complexes will differ in energy and will be most retained while the less stable diastereomer will leave the chiral stationary phase first. Some of the chiral stationary phases are generated from polysaccharide derivatives, particularly their carbamate derivatives, such as cellulose carbamate and amylose carbamate, and they can separate a wide range of racemic compounds into optical stereoisomers due to their exhibition of high chiral recognition.

In this study, separation of stereoisomers was succeeded with Chiralpak IC, Chiralpak IB and Chiralpak IA columns, packed with cellulose tris (3,5-dichlorophenyl)

carbamate, cellulose tris (3,5-dimethylphenyl) carbamate and amylose tris (3,5-dimethylphenyl) carbamate as chiral stationary phases.

2.7. Determination of the Kinetic and the Thermodynamic Constants of the Internal Rotation and Racemisation Process for 5-Benzyl-3-aryl-2-thiohydantoin and 5-Isobutyl-3-aryl-2-thiohydantoin derivatives

2.7.1. Reaction Kinetics for 5-Benzyl-3-aryl-2-thiohydantoin and 5-Isobutyl-3-aryl-2-thiohydantoin derivatives for Reversible Reactions of Rotation and Racemisation

The reversible reaction $\mathbf{SM} \rightleftharpoons \mathbf{RM}$ is first order in both forward (f) and the reverse direction (r), so that $r_f = k_f[\mathbf{SM}]$ and $r_r = k_r[\mathbf{RM}]$. If $(d[\mathbf{SM}]/dt)_f$ denotes the rate of change of $[\mathbf{SM}]$ due to forward reaction, then $-(d[\mathbf{SM}]/dt)_f = r_f = k_f[\mathbf{SM}]$. The rate of formation of $[\mathbf{SM}]$ by the reverse reaction is $-(d[\mathbf{SM}]/dt)_r = r_r = k_r[\mathbf{RM}]$. So,

$$(d[\mathbf{SM}]/dt) = -k_f[\mathbf{SM}] + k_r[\mathbf{RM}] \quad (2.5)$$

We have $\Delta[\mathbf{RM}] = -\Delta[\mathbf{SM}]$, so $[\mathbf{RM}] - [\mathbf{RM}]_0 = -([\mathbf{SM}] - [\mathbf{SM}]_0)$. Substitution of $[\mathbf{RM}] = [\mathbf{RM}]_0 + [\mathbf{SM}]_0 - [\mathbf{SM}]$ into Equation (2.5) gives,

$$d[\mathbf{SM}]/dt = k_r[\mathbf{RM}]_0 + k_r[\mathbf{SM}]_0 - (k_f + k_r)[\mathbf{SM}] \quad (2.6)$$

At equilibrium the rates of the forward and reverse reactions become equal, the concentration of each species being constant, thus $d[\mathbf{SM}]/dt$ is 0. Let $[\mathbf{SM}]_{\text{eq}}$ be the equilibrium concentration of \mathbf{SM} . Setting $d[\mathbf{SM}]/dt=0$ and $[\mathbf{SM}]=[\mathbf{SM}]_{\text{eq}}$ in Equation (2.6), we get,

$$k_r[\mathbf{RM}]_0 + k_r[\mathbf{SM}]_0 = (k_f + k_r)[\mathbf{SM}]_{\text{eq}} \quad (2.7)$$

The use of Equation (2.7) in Equation (2.6) gives $d[\mathbf{SM}]/dt = (k_f + k_r)([\mathbf{SM}]_{\text{eq}} - [\mathbf{SM}])$. Using the identity $\int (x+s)^{-1} dx = \ln(x+s)$ to integrate this equation we get,

$$\ln\left(\frac{[\text{SM}] - [\text{SM}]_{\text{eq}}}{[\text{SM}]_0 - [\text{SM}]_{\text{eq}}}\right) = -(k_f + k_r)t \quad (2.8)$$

Since $k_f = k_r$ for the racemisation of enantiomers, Equation (2.8) could be written as Equation (2.9) for the racemisation of enantiomers

$$\ln\left(\frac{[\text{SM}] - [\text{SM}]_{\text{eq}}}{[\text{SM}]_0 - [\text{SM}]_{\text{eq}}}\right) = -2kt \quad (2.9)$$

By using Equation (2.9), a plot of $\ln\left(\frac{[\text{SM}] - [\text{SM}]_{\text{eq}}}{[\text{SM}]_0 - [\text{SM}]_{\text{eq}}}\right)$ versus time gives a straight line, the slope being equal to $-2k$. Having determined k , the free energy of activation can be calculated using the Eyring Equation (2.10),

$$\Delta G^\ddagger = RT \ln(k_b \cdot T / k \cdot h) \quad (2.10)$$

where $R=8.3143 \text{ J/mol.K}$, $T=$ temperature (Kelvin) at which the interconversion takes place, k_b (Boltzmann constant) = $1.3805 \cdot 10^{-23} \text{ J/K}$, h (Planck constant) = $6.6256 \cdot 10^{-34} \text{ J.s}$, $k=$ the rate constant for racemisation reaction. These reversible calculations are compatible for **SP \rightleftharpoons RP**, **SP \rightleftharpoons SM**, **RP \rightleftharpoons RM**. Therefore, all reversible reactions' kinetics are determined with Eyring Equation (2.10).

Also at temperature T , the standart free energy change, ΔG° , is given by:

$$\Delta G^\circ = -RT \ln K = \Delta H^\circ - T \Delta S^\circ \quad (2.11)$$

Where K is the equilibrium constant at temperature T (K). ΔH° is the standard enthalpy change and ΔS° is the standard entropy change. Thus:

$$\ln K = -\Delta H^\circ / RT + \Delta S^\circ / R \quad (2.12)$$

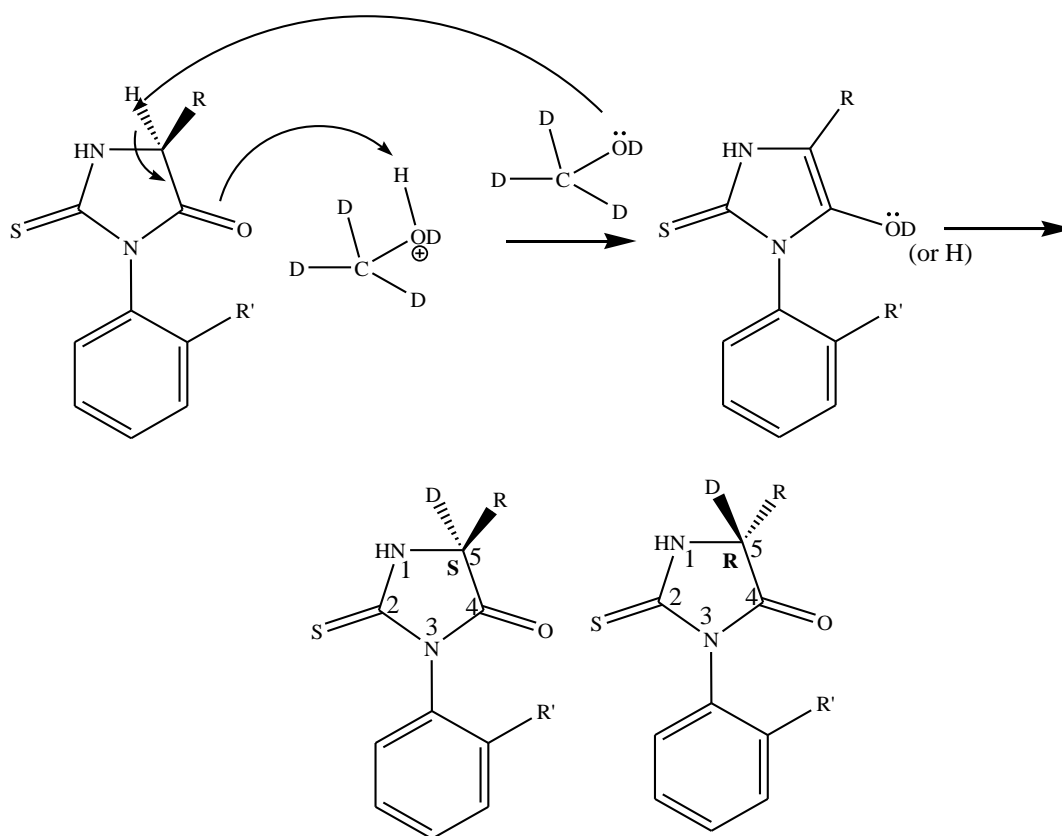
Assuming that ΔH° and ΔS° are constant and comparing the two equilibrium constants K_1 and K_2 at temperatures T_1 and T_2 the following equation (Van't Hoff Equation) results:

$$\ln(K_2/K_1) = (\Delta H^\circ / R)(1/T_1 - 1/T_2) \quad (2.13)$$

from which ΔH° and ΔS° of the process can be obtained.

2.7.2. Hydrogen-Deuterium Exchange at C-5 for 5-Benzyl-3-aryl-2-thiohydantoin and 5-Isobutyl-3-aryl-2-thiohydantoin derivatives by $^1\text{H-NMR}$

To observe the racemisation for the synthesized derivatives, the hydrogen-deuterium exchange reaction is an indicator. For synthesized derivatives; the enolisation mechanism shows that, exchange of deuterium at C-5 hydrogen generates **S** and **R** enantiomers at C-5 (Figure 2.5). Therefore, the racemisation may be detected if exist; with the deuterium-hydrogen exchange at C-5 by $^1\text{H-NMR}$. With following the disappearance of C-5 hydrogen signal in time intervals, the rate of the racemisation can be detected.



(2) : $\text{R}' = \text{CH}_3$, $\text{R} = \text{Benzyl}$; (3) : $\text{R}' = \text{Br}$, $\text{R} = \text{Benzyl}$

(5) : $\text{R}' = \text{CH}_3$, $\text{R} = \text{Isobutyl}$; (6) : $\text{R}' = \text{Br}$, $\text{R} = \text{Isobutyl}$

Figure 2.5. Enolisation mechanism of synthesized derivatives.

For synthesized derivatives, since both conversions of rotation and racemisation may be observed when the derivatives are dissolved in deuterio-methanol, the rate of the deuterium exchange in deuterio-methanol can be calculated (for compounds **2** and **5**) from;

$$\ln((C-5)/(CH_3)) \quad (2.14)$$

because the intensity of the CH₃ signals of **SM**, **RM**, **RP** and **SP** should remain the same however C-5 signal should be decreasing depending on time. From time versus $\ln((C-5)/(CH_3))$ the slope can be obtained and from the Eyring Equation (2.10) the racemisation ΔG^\ddagger energy barrier can be calculated.

3. EXPERIMENTAL

3.1 Organic Synthesis of 5-Benzyl-3-aryl-2-thiohydantoin

To synthesize 5-benzyl-3-aryl-2-thiohydantoin, the reaction of (S)-Phenyl alanine methyl ester salt with aryl isothiocyanates was used in the presence of triethylamine (TEA) (Figure 3.1).

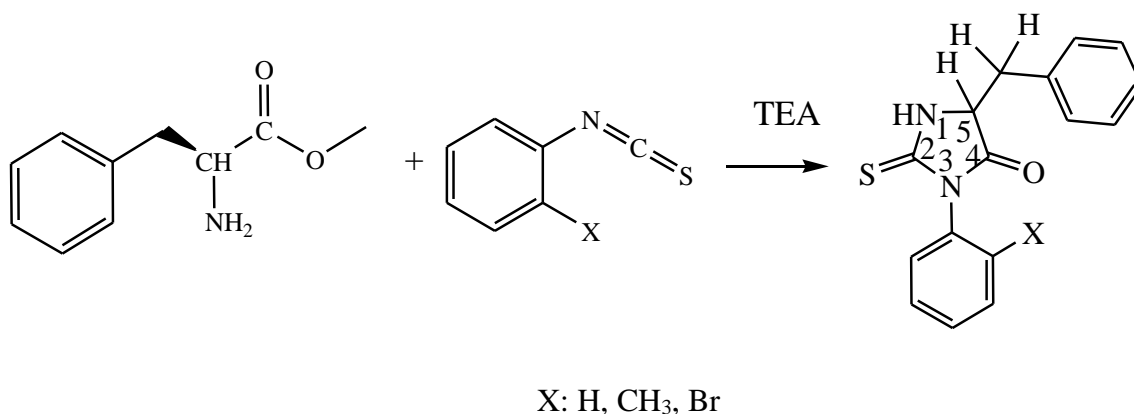


Figure 3.1. The synthesis of 5-benzyl-3-aryl-thiohydantoin.

3.1.1. General Procedure for the Synthesis of 5-Benzyl-3-aryl-2-thiohydantoin

The appropriate (S)-phenylalanine methyl ester salt was refluxed with selected aryl-isothiocyanate and triethylamine in dichloromethane for 1 to 4 hours. To eliminate the remaining triethylamine used in the synthesis, extraction with distilled water was done for five times. After evaporation of the dichloromethane, the crude product was crystallised using ethyl acetate and hexane mixture.

3.1.1.1. 5-Benzyl-3-phenyl-2-thiohydantoin (1). The compound was synthesized as a racemic mixture according to the general procedure using phenyl isothiocyanate.

Starting materials:

- (S)-Phenyl alanine methyl ester salt: 0.5 g (2.32 mmol)
- Triethylamine: 0.32 ml (2.32 mmol)

- Phenyl isothiocyanate: 0.27 ml (2.32 mmol)
- Dichloromethane: 10 ml

Yield: 0.44 g (67.1%)

Melting point: 184-186 °C

¹H NMR (400 MHz) data (ppm):

- Solvent: CDCl₃
- Aromatic protons: 7.0-7.6 (m)
- C-5 Hydrogen: 4.5 (d of d)
- -CH₂ protons (H_a and H_b): 3.15- 3.4 (d of d)
- H_{C5} : J_{H,H_a} = 3.6 Hz. , J_{H,H_b} = 7.8 Hz.
- H_A : J_{H_a,H} = 3.6 Hz. , J_{H_a,H_b} = 13.8 Hz.
- H_B : J_{H_b,H} = 7.8 Hz. , J_{H_b,H_a} = 13.8 Hz.

3.1.1.2. 5-Benzyl-3-(*o*-tolyl)-2-thiohydantoin (2). The compound was synthesized according to the general procedure using *o*-tolyl isothiocyanate. The synthesis was as a mixture of four diastereomers.

Starting materials:

- (S)-Phenyl alanine methyl ester salt: 0.5 g (2.32 mmol)
- Triethylamine: 0.32 ml (2.32 mmol)
- *o*-tolyl isothiocyanate: 0.31 ml (2.32 mmol)
- Dichloromethane: 10 ml

Yield: 0.55 g (79.4%)

Melting point: 146 °C

¹H NMR (400 MHz) data (ppm):

- Solvent: CDCl₃
- Aromatic protons: 6.6-7.4 (m)

- C-5 hydrogen: 4.58 (m)
- -CH₂ protons (H_a and H_b): 3.04-3.44 (d of d)
- -CH₃ (**SM+RP**) protons: 1.82 (s)
- -CH₃ (**SP+RM**) protons: 2.18 (s)
- -NH proton: 7.6 (s)
- H_{C5}: J_{H,H_a} = 4 and 3.6 Hz. , J_{H,H_b} = 7.6 and 6.8 Hz. (for **SM+RP** and **RM+SP**)
- H_A: J_{H_a,H} = 4 and 3.6 Hz. , J_{H_a,H_b} = 13.4 and 13.6 Hz. (for **SM+RP** and **RM+SP**)
- H_B: J_{H_b,H} = 7.6 and 6.8 Hz. , J_{H_b,H_a} = 13.4 and 13.6 Hz. (for **SM+RP** and **RM+SP**)

Isomer ratio:

- -crude: **SM+RP/RM+SP**= 2.22
- -after crystallised: **SM+RP/RM+SP**= 5.65

¹H NMR (400 MHz) data (ppm):

- Solvent: CD₃OD
- Aromatic protons: 6.0-7.4 (m)
- C-5 Hydrogen: 4.7 (m)
- -CH₂ protons: 3.1-3.3 (m)
- -CH₃ (**SM+RP**) protons: 1.35 (s)
- -CH₃ (**SP+RM**) protons: 2.1 (s)

3.1.1.3. 5-Benzyl-3-(o-bromophenyl)-2-thiohydantoin (**3**). The compound was synthesized according to the general procedure using 2-bromophenyl isothiocyanate. The synthesis was as a mixture of four diastereomers.

Starting materials:

- (S)-Phenyl alanine methyl ester salt: 0.5 g (2.32 mmol)
- Triethylamine: 0.32 ml (2.32 mmol)
- 2-bromophenyl isothiocyanate: 0.31 ml (2.32 mmol)
- Dichloromethane: 10 ml

Yield: 0.63 g (75.6%)

Melting point: 150 °C

¹H NMR (400 MHz) data (ppm):

- Solvent: CDCl₃
- Aromatic protons: 6.8-7.8 (m)
- -NH proton: 7.2 (s)
- C-5 Hydrogen: 4.5-4.7 (d of d)
- -CH₂ protons (H_a and H_b): 3.0-3.6 (d of d)
- H_{C5}: J_{H,H_a} = 4 and 4 Hz. , J_{H,H_b} = 8 and 10 Hz. (for **SM+RP** and **RM+SP**)
- H_A: J_{H_a,H} = 4 and 4 Hz. , J_{H_a,H_b} = 14 and 14 Hz. (for **SM+RP** and **RM+SP**)
- H_B: J_{H_b,H} = 8 and 10 Hz. , J_{H_b,H_a} = 14 and 14 Hz. (for **SM+RP** and **RM+SP**)

Isomer ratio:

- -crude from HPLC: **SM+RP/RM+SP** = 0.77
- -after crystallised: **SM+RP/RM+SP** = 0.88

¹H NMR (400 MHz) data (ppm):

- Solvent: C₆D₆
- Aromatic protons: 6.5-7.4 (m)
- C-5 Hydrogen: 3.5-3.7 (m)
- -CH₂ protons: 2.5-3.0 (m)

3.2 Organic Synthesis of 5-Isobutyl-3-aryl-2-thiohydantoins

To synthesize 5-isobutyl-3-aryl-2-thiohydantoins, the reaction of (S)-Leucine methyl ester salt with aryl isothiocyanates was used in the presence of triethylamine (TEA). (Figure 3.2)

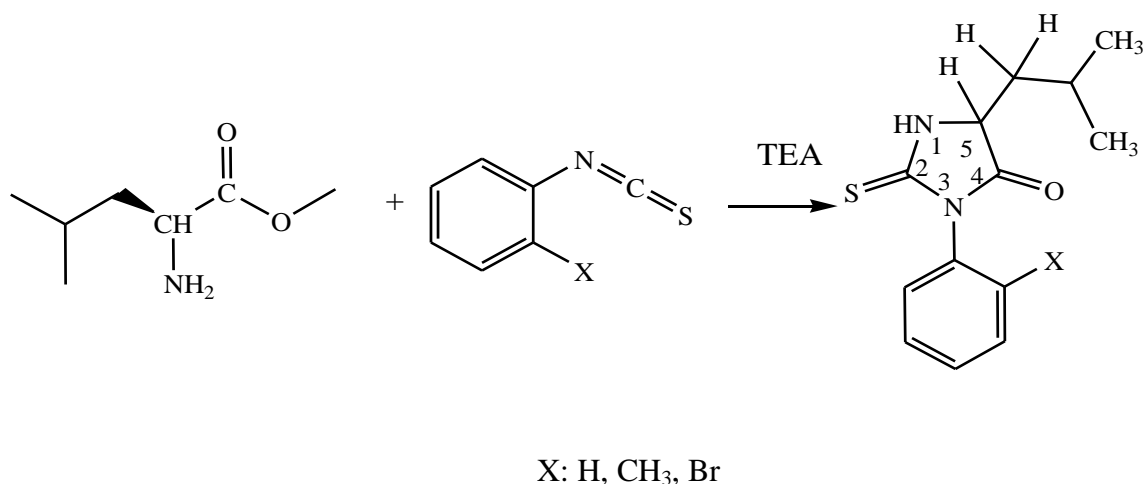


Figure 3.2. The synthesis of 5-isobutyl-3-aryl-thiohydantoin.

3.2.1. General Procedure for the Synthesis of 5-Isobutyl-3-aryl-2-thiohydantoin

The appropriate (S)-leucine methyl ester salt was refluxed with selected aryl-isothiocyanate and triethylamine in dichloromethane for 4 hours. To eliminate the remaining triethylamine used in the synthesis, extraction with distilled water was done for five times. After evaporation of the dichloromethane, the crude product was crystallised using ethyl acetate and hexane mixture.

3.2.1.1. 5-Isobutyl-3-phenyl-2-thiohydantoin (4). The compound was synthesized as a racemic mixture according to the general procedure using phenyl isothiocyanate.

Starting materials:

- (S)-Leucine methyl ester salt: 0.5 g (2.75 mmol)
- Triethylamine: 0.38 ml (2.75mmol)
- Phenyl isothiocyanate: 0.33 ml (2.75 mmol)
- Dichloromethane: 10 ml

Yield: 0.48 g (70.6%)

Melting point: 178 °C

^1H NMR (400 MHz) data (ppm):

- Solvent: CDCl_3
- Aromatic protons: 7.2 -7.5 (m)
- -NH proton: 7.55 (s)
- C-5 Hydrogen: 4.25 (d of d)
- $-\text{CH}_2$ (H_a and H_b) and $-\text{CH}$ (H_c) protons: 1.6 -1.9 (m)
- $-\text{CH}_3$ protons: 0.9 (m)
- H_{C5} : $J_{\text{H,H}_a} = 2.8 \text{ Hz}$, $J_{\text{H,H}_b} = 9 \text{ Hz}$.
- H_A : $J_{\text{H}_a,\text{H}} = 2.8 \text{ Hz}$, $J_{\text{H}_a,\text{H}_b} = 11.8 \text{ Hz}$.
- H_B : $J_{\text{H}_b,\text{H}} = 9 \text{ Hz}$, $J_{\text{H}_b,\text{H}_a} = 11.8 \text{ Hz}$.
- H_C : $J_{\text{H}_c,\text{H}_a} = 8.8 \text{ Hz}$, $J_{\text{H}_c,\text{H}_b} = 8.8 \text{ Hz}$

3.2.1.2. 5-Isobutyl-3-(*o*-tolyl)-2-thiohydantoin (**5**). The compound was synthesized according to the general procedure using *o*-tolyl isothiocyanate. The synthesis was as a mixture of four diastereomers.

Starting materials:

- (S)-Leucine methyl ester salt: 0.5 g (2.75 mmol)
- Triethylamine: 0.38 ml (2.75mmol)
- *o*-tolyl isothiocyanate: 0.37 ml (2.75 mmol)
- Dichloromethane: 10 ml

Yield: 0.51 g (71.2%)

Melting point: 136 °C

^1H NMR (400 MHz) data (ppm):

- Solvent: CDCl_3
- Aromatic protons: 7.0-7.35 (m)
- -NH proton: 7.6 (s)
- C-5 Hydrogen: 4.2-4.3 (d of d)
- $-\text{CH}_2$ (H_a and H_b) and $-\text{CH}$ (H_c) protons: 1.7-1.9 (m)

- -CH₃ protons: 0.9 (m)
- *o*-tolyl -CH₃ (**SP+RM**) protons: 2.1 (s)
- *o*-tolyl -CH₃ (**SM+RP**) protons: 2.12 (s)
- H_{C5}: J_{H₁,H_a} = 4 and 3.6 Hz. , J_{H₁,H_b} = 9.8 and 10.4 Hz. (for **SM+RP** and **RM+SP**)
- H_A: J_{H_a,H} = 4 and 3.6 Hz. , J_{H_a,H_b} = 11.6 and 11.6 Hz. (for **SM+RP** and **RM+SP**)
- H_B: J_{H_b,H} = 9.8 and 10.4 Hz. , J_{H_b,H_a} = 11.6 and 11.6 Hz. (for **SM+RP** and **RM+SP**)
- H_C: J_{H_c,H_b} = 9.2 and 8.8 Hz. , J_{H_c,H_a} = 9.2 and 8.8 Hz. (for **SM+RP** and **RM+SP**)

Isomer ratio:

- -crude: **SM+RP/RM+SP**= 0.56
- -after crystalised: **SM+RP/RM+SP**= 0.39

¹H NMR (400 MHz) data (ppm):

- Solvent: C₆D₆
- Aromatic protons: 6.9-7.4 (m)
- C-5 Hydrogen: 3.3-3.5 (m)
- -CH₂ and -CH protons: 1.15-1.5 (m)
- -CH₃ protons: 0.5-0.7 (m)
- *o*-tolyl -CH₃ (**SP+RM**) protons: 2.1 (s)
- *o*-tolyl -CH₃ (**SM+RP**) protons: 2.2 (s)

3.2.1.3. 5-Isobutyl-3-(*o*-bromophenyl)-2-thiohydantoin (6). The compound was synthesized according to the general procedure using 2-bromophenyl isothiocyanate. The synthesis was as a mixture of four diastereomers.

Starting materials:

- (S)-Leucine methyl ester salt: 0.5 g (2.75 mmol)
- Triethylamine: 0.38 ml (2.75mmol)
- 2-bromophenyl isothiocyanate: 0.37 ml (2.75 mmol)
- Dichloromethane: 10 ml

Yield: 0.48 g (53.3%)

Melting point: 138 °C

¹H NMR (400 MHz) data (ppm):

- Solvent: CDCl₃
- Aromatic protons: 7.25-7.7 (m)
- -NH proton: 7.5 (s)
- C-5 Hydrogen: 4.3-4.5 (m)
- -CH₂ (H_a and H_b) and -CH (H_c) protons: 1.7-2.0 (m)
- -CH₃ protons: 1.0 (m)
- H_{C5}: J_{H₁,H_a} = 4 and 3.6 Hz. , J_{H₁,H_b} = 10.2 and 10.6 Hz. (for **SM+RP** and **RM+SP**)
- H_A: J_{H_a,H} = 4 and 3.6 Hz. , J_{H_a,H_b} = 15.6 and 15.6 Hz. (for **SM+RP** and **RM+SP**)
- H_B: J_{H_b,H} = 10.2 and 10.6 Hz. , J_{H_b,H_a} = 15.6 and 15.6 Hz. (for **SM+RP** and **RM+SP**)
- H_C: J_{H_c, H_b} = 8 and 10 Hz. , J_{H_c,H_a} = 8 and 10 Hz. (for **SM+RP** and **RM+SP**)

Isomer ratio:

- from crude HPLC: **SM+RP/RM+SP**= 0.75
- -after crystallised: **SM+RP/RM+SP**= 0.67

¹H NMR (400 MHz) data (ppm):

- Solvent: C₆D₆
- Aromatic protons: 6.6-7.4 (m)
- -NH proton: 6.5 (s)
- C-5 Hydrogen: 3.3-3.7 (m)
- -CH₂ and -CH protons: 1.15-1.6 (m)
- -CH₃ protons : 0.5-0.7 (m)

3.3. Apparatus

¹H NMR spectra were recorded on the Varian-Mercury VX-400 MHz-BB.

Melting points were measured using Bibby Stuart Scientific melting point apparatus.

Liquid chromatography analyses were performed using Chiral IC column (Daicel Ltd., partical size: 5 μ m, column size: 250 \times 4.6 mm) , IB column (Daicel Ltd., partical size: 5 μ m, column size: 250 \times 4.6 mm) or IA column (Daicel Ltd., partical size: 5 μ m, column size: 250 \times 4.6 mm), Lab Alliance Series III pump and Water Assoc. UV absorbance detector.

3.4. List of Chemicals

Table 3.1. Chemicals used in this study.

| Name | Formula | Supplier | % Purity |
|--------------------------------------|---|---------------|--------------|
| (S)-Phenyl Alanine methyl ester salt | C ₁₀ H ₁₃ NO ₂ | Sigma-Aldrich | 98% |
| (S)-Leucine methyl ester salt | C ₇ H ₅ NO ₂ | Sigma-Aldrich | 98% |
| Phenyl isothiocyanate | C ₇ H ₅ NS | Merck | \geq 98% |
| <i>o</i> -tolyl isothiocyanate | C ₈ H ₇ NS | Sigma-Aldrich | 99% |
| 2-bromophenyl isothiocyanate | C ₇ H ₄ BrNS | Sigma-Aldrich | 98% |
| Triethylamine | C ₆ H ₁₅ N | Merck | \geq 98% |
| Dichloromethane | CH ₂ Cl ₂ | Merck | \geq 99,8% |
| Ethanol for HPLC | C ₂ H ₅ OH | J. T. Baker | |
| Hexane for HPLC | CH ₃ (CH ₂) ₄ CH ₃ | J. T. Baker | 95% |
| Ethyl Acetate | CH ₃ COOC ₂ H ₅ | Merck | \geq 99,5% |
| Toluene | C ₆ H ₅ CH ₃ | Merck | 99% |

3.5. Thermal Interconversion of 5-Benzyl-3-aryl-2-thiohydantoin and 5-Isobutyl-3-aryl-2-thiohydantoin derivatives

5-Benzyl-3-aryl-2-thiohydantoin and 5-isobutyl-3-aryl-2-thiohydantoin derivatives' stereoisomers were separated on chiral stationary phases. After separation, stereoisomers were dissolved either in toluene or ethanol. The temperature was stabilized either with

water bath or oil bath. At a constant temperature, the solution was injected to HPLC within time periods until equilibrium in order to plot the $\ln \left(\frac{[\mathbf{SM}] - [\mathbf{SM}]_{\text{eq}}}{[\mathbf{SM}]_0 - [\mathbf{SM}]_{\text{eq}}} \right)$ versus time graphic for the **SM** derivative. With the slope of the plotted $\ln \left(\frac{[\mathbf{SM}] - [\mathbf{SM}]_{\text{eq}}}{[\mathbf{SM}]_0 - [\mathbf{SM}]_{\text{eq}}} \right)$ versus time graphic rate constant, k , was determined. Using k , in the Eyring Equation (2.10) the ΔG^\ddagger for rotation or racemisation was calculated. For reversible reactions of **RP**, **SP** and **RM** in order to determine rate constant of the ΔG^\ddagger energy barriers, $\ln \left(\frac{[\mathbf{RP}] - [\mathbf{RP}]_{\text{eq}}}{[\mathbf{RP}]_0 - [\mathbf{RP}]_{\text{eq}}} \right)$, $\ln \left(\frac{[\mathbf{SP}] - [\mathbf{SP}]_{\text{eq}}}{[\mathbf{SP}]_0 - [\mathbf{SP}]_{\text{eq}}} \right)$, $\ln \left(\frac{[\mathbf{RM}] - [\mathbf{RM}]_{\text{eq}}}{[\mathbf{RM}]_0 - [\mathbf{RM}]_{\text{eq}}} \right)$ was respectively plotted versus time.

4. RESULTS AND DISCUSSION

4.1. Overview

5-Benzyl-3-aryl-2-thiohydantoin and 5-isobutyl-3-aryl-2-thiohydantoin derivatives were synthesized by using *S*-phenyl alanine methyl ester and *S*-leucine methyl ester hydrochloride with aryl isothiocyanates in the presence of triethylamine. Compounds **1** and compound **4** (Table 1.1) were obtained as racemic mixtures of enantiomers at the end of the reactions. The compounds **2**, **3**, **5** and **6** are axially chiral, the C_{aryl}-N_{sp2} bond being the chiral axis. Because of the presence of also a chiral center at C-5, these compounds were synthesized as diastereomeric mixtures of, **SM**, **SP**, **RM** and **RP** stereoisomers (Figure 2.3). The stereoisomers were resolved by HPLC on chiral stationary phases. The isomer distributions are given in Table 4.1.

Table 4.1. Relative proportions of the isomers determined by HPLC with a chiral stationary phase.

| Compound | SM: RP: SP: RM (Crude) | SM: RP: SP: RM (After recrystallization) |
|----------------------|---------------------------|---|
| 2^a | 8 : 61 : 25 : 6 | 38 : 45 : 12 : 5* |
| 3^b | 2 : 41 : 51 : 5 | 2 : 40 : 47 : 11** |
| 5^c | 2 : 39 : 41 : 18 | 2 : 25 : 47 : 26** |
| 6^d | 3 : 40 : 49 : 8 | 1 : 42 : 49 : 8** |
| | S:R (Crude) | S:R (After recrystallization) |
| 1^b | 52:48 | 53:47** |
| 4^b | 49:51 | 50:50** |

Table 4.2. Relative proportions of the isomers determined by HPLC with a chiral stationary phase (continued).

| | | | | |
|--|-----------------|----------|-------------------|----------|
| | | | | |
| Compound | X | R | Reaction Time (h) | Yield(%) |
| 1 | H | benzyl | 1 | 67 |
| 2 | CH ₃ | benzyl | 2 | 79 |
| 3 | Br | benzyl | 4 | 76 |
| 4 | H | isobutyl | 4 | 70 |
| 5 | CH ₃ | isobutyl | 4 | 71 |
| 6 | Br | isobutyl | 4 | 53 |
| <p>* 2 was recrystallized from ethyl acetate and hexane mixture and washed with toluene ** Compounds were recrystallized from ethyl acetate/hexane ^a ChiralPak IB as the stationary phase, 95:5 Hex:EtOH as eluent, flow rate : 1.0 ml/min ^b ChiralPak IC as the stationary phase, 95:5 Hex:EtOH as eluent, flow rate : 0.8 ml/min ^c ChiralPak IB as the stationary phase, 95:5 Hex:EtOH as eluent, flow rate : 0.8 ml/min. ^d ChiralPak IA as the stationary phase, 95:5 Hex:EtOH as eluent, flow rate : 0.8 ml/min.</p> | | | | |

The assignments of the HPLC peaks to **SM**, **SP**, **RM** and **RP** stereoisomers were done by comparing the HPLC chromatograms with the ¹H-NMR spectra.

The micropreparatively resolved **SP** isomers were found to interconvert to **SM** isomers via rotation around the C_{aryl}-N_{sp²} chiral axis in toluene. Similarly **RP** rotated to give **RM** in toluene. Time course experiments were done for them to find out the activation barriers for rotation.

However, when the solvent was changed to ethanol, that is, when the resolved **SP** stereoisomers of compounds **3**, **5** and **6** were kept in ethanol instead of toluene, **SP** was found to convert to **RP**. Thus racemisation at C-5 of the heteroring occurred in ethanol. In this solvent also **RM** converted to **SM** and **SM** to **RM**. Kinetics of the racemisation processes were also determined.

Racemisations were also proved by hydrogen-deuterium exchange experiments by ¹H-NMR in deuterio-methanol.

4.2. ¹H NMR Spectra of the Compounds

Synthesized 5-benzyl-3-phenyl-2-thiohydantoin (**1**) and 5-isobutyl-3-phenyl-2-thiohydantoin (**4**) (Figure 4.1) are not axially chiral. Due to phenyl group at third position, chirality axis was not generated. Therefore, only two types of stereoisomers were possible at the end of the reaction which were **S** and **R** enantiomers.

Since, NMR cannot separate the enantiomer signals, (S)-5-benzyl-3-phenyl-2-thiohydantoin and (R)-5-benzyl-3-phenyl-2-thiohydantoin gave same ¹H NMR shifts (Figure A.1). The ¹H-NMR of compound **4** is shown in Figure A.2.

5-Benzyl-3-(*o*-tolyl)-2-thiohydantoin and 5-benzyl-3-(*o*-bromophenyl)-2-thiohydantoin derivatives are axially chiral because of the *o*-tolyl group at the third position of the thiohydantoin ring (Figure 2.3). The restricted rotation around carbon-nitrogen bond generates **M** and **P** stereoisomers. Therefore, 4 types of stereoisomers may occur at the end of the synthesis which are **RM**, **RP**, **SP** and **SM**. Even though, enantiomeric signals are not separable from each other in NMR, diastereoisomeric NMR signals may be separated due to their different chemical shifts. **RM** and **SP** stereoisomers are enantiomers of each other so they give same chemical shift in ¹H-NMR as well as **RP** and **SM**. However, **RM** and **RP** are diastereoisomers of each other as well as **SM** and **SP**. As a result, 2 types of chemical shifts were observed for 5-benzyl-3-(*o*-tolyl)-2-thiohydantoin derivative (Figure A.3) and for 5-benzyl-3-(*o*-bromophenyl)-2-thiohydantoin derivative (Figure A.4).

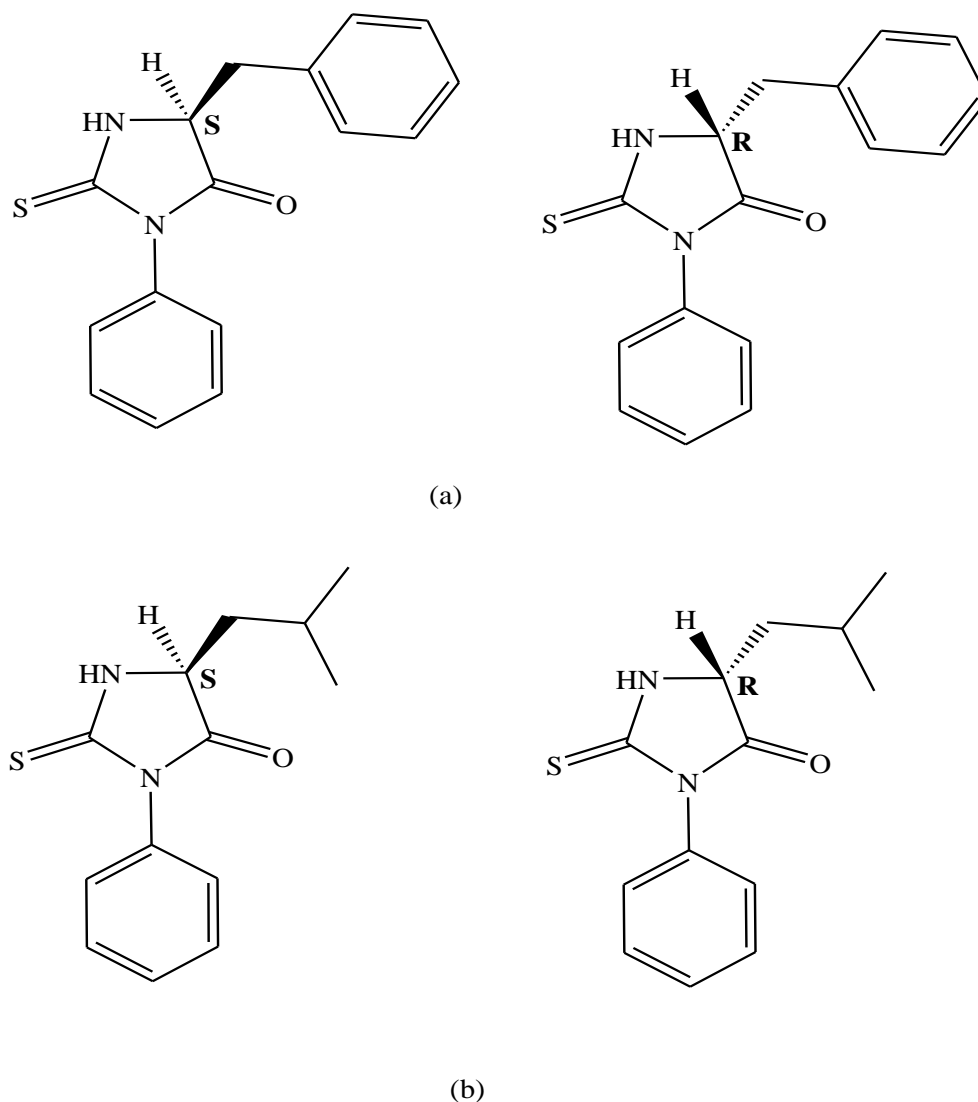


Figure 4.1. Structure of 5-benzyl-3-phenyl-2-thiohydantoin (a) and 5-isobutyl-3-phenyl-2-thiohydantoin (b).

5-Isobutyl-3-(*o*-tolyl)-2-thiohydantoin and 5-isobutyl-3-(*o*-bromophenyl)-2-thiohydantoin derivatives are also axially chiral derivatives (Figure 2.3) so that there are four types of possible stereoisomers for each derivative at the end of the reactions which are **RM**, **SM**, **RP** and **SP**. As a result, 2 types of chemical shifts were observed for 5-isobutyl-3-(*o*-tolyl)-2-thiohydantoin derivative (Figure A.5) and for 5-benzyl-3-(*o*-bromophenyl)-2-thiohydantoin derivative (Figure A.6). The $^1\text{H-NMR}$ spectrum of compound **2** showed that the benzyl group at C-5 shields the *o*-aryl-aromatic hydrogen to 6.6 ppm. On the other hand, the *ortho* hydrogen of 5-isobutyl-3-*o*-tolyl-2-thiohydantoin appeared more deshielded and observed at 7.1 ppm.

In 5-benzyl-3-*o*-tolyl-2-thiohydantoin synthesis when the product was rinsed with toluene it was observed that toluene dissolved **SP** + **RM** more than **SM** + **RP**. The *o*-tolyl methyl group at N-3 position in 2-thiohydantoin ring, gave singlet peaks in ¹H-NMR and **SM/RP** methyl singlet was more shielded than **SP/RM** due to the anisotropic effect of the benzylic group at C-5 of 2-thiohydantoin (Figure A.3).

Assignments of the synthesized derivatives were completed with the comparison of HPLC and ¹H-NMR. For compounds **2**, **3**, **5** and **6**, diastereomeric ratios were determined by ¹H-NMR and each stereoisomer's ratios were also determined with HPLC.

All the ¹H-NMR spectra of the synthesized derivatives and coupling constants are given in Appendix section.

4.3. Determination of Barriers of Rotation and/or Racemisation for 5-Benzyl-3-aryl-2-thiohydantoin and 5-Isobutyl-3-aryl-2-thiohydantoin derivatives by HPLC on Chiral Stationary Phase

4.3.1. Determination of Racemisation at C-5 Barrier (S→R Conversion) for 5-Benzyl-3-phenyl-2-thiohydantoin Enantiomers

The **R** and **S** enantiomers of 5-benzyl-3-phenyl-2-thiohydantoin were separated on Chiralpak IC column in hexane 95% + ethanol 5% mixture. Even though the separation was successful, it was not possible to assign the stereoisomers as **S** or **R** because X-ray is required for the absolute configuration assignment. The rate constant for racemisation was determined for one stereoisomer from the slope of $\ln \left(\frac{([S]_0 - [S]_{eq})}{[S] - [S]_{eq}} \right)$ versus time (slope = -2k) (Figure 4.2). The ΔG^\ddagger for racemisation was calculated from the Eyring Equation (2.10). The k found as $1.5 \times 10^{-6} \text{ s}^{-1}$. The ΔG^\ddagger thermal racemisation energy barrier found as; $\Delta G^\ddagger = 111.7 \text{ kJ/mole}$ at 40°C in ethanol. From HPLC chromatograms it was proved that there was racemisation for benzyl-3-phenyl-2-thiohydantoin in ethanol at 40 °C (Figure 4.3). At 25°C no racemisation was observed.

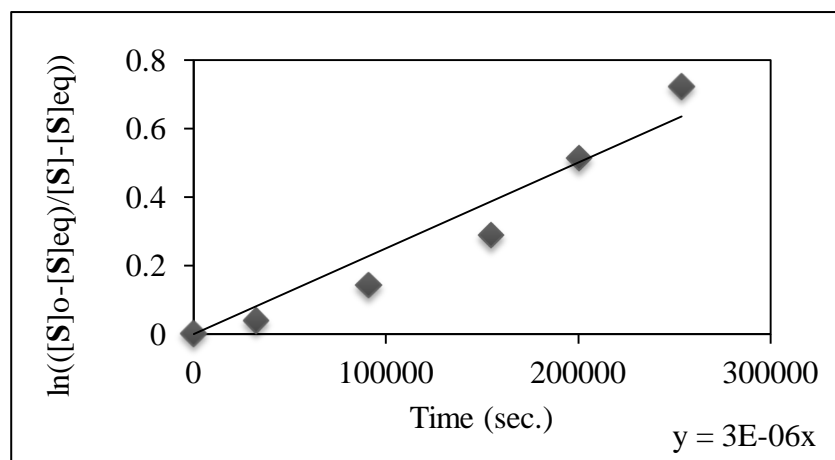


Figure 4.2. The plot of $\ln\left(\frac{[S]_o - [S]_{eq}}{[S] - [S]_{eq}}\right)$ versus time at 313 K for 5-benzyl-3-phenyl-2-thiohydantoin.

4.3.2. Determination of the Rotation around $N3_{(sp^2)}-C_{(aryl)}$ bond (SP→SM and RP→RM Conversion) and Racemisation at C-5 Barrier (SM→RM and RM→SM Conversion) for 5-Benzyl-3-(*o*-tolyl)-2-thiohydantoin stereoisomers

For the micropreparatively resolved single stereoisomers of 5-benzyl-3-*o*-tolyl-2-thiohydantoin, ΔG^\ddagger energy barriers were attempted to be determined at 40°C, but racemisation was observed to occur together with rotation for all 4 stereoisomers. In order to understand the conversion type the temperature was decreased to 25 °C to decrease the rate of rotation. It was observed that **SM** and **RM** stereoisomers gave racemisation at C-5 however **SP**, **RP** stereoisomers gave more rotation than racemisation in ethanol at 25 °C.

5-Benzyl-3-*o*-tolyl-2-thiohydantoin stereoisomers were separated on Chiralpak IB column in hexane 95% and ethanol 5% mixture. The resolved stereoisomers; **RP**, **SP**, **RM** and **SM** were kept at 25°C in ethanol and injected to HPLC in time intervals to observe the type of conversion and to determine the rate constants and ΔG^\ddagger energy barriers. It was observed that, **SM** stereoisomer converted into **RM** with time at 25°C in ethanol.

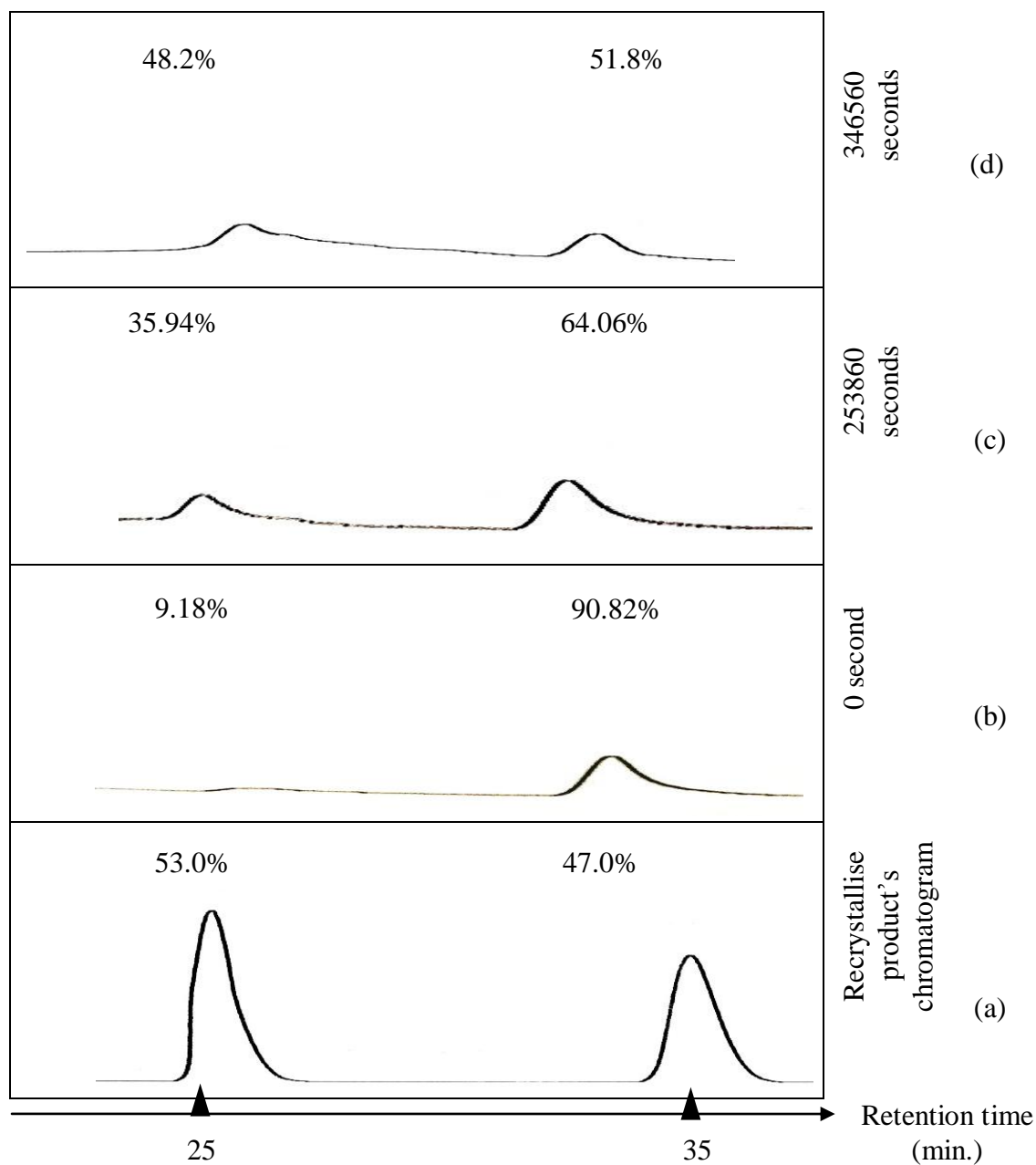


Figure 4.3. 5-Benzyl-3-phenyl-2-thiohydantoin HPLC chromatograms (ChiralPak IC as the stationary phase, 95:5 Hex:EtOH as the eluent, flow rate: 0.8 ml/min, column temperature : 7 °C) for: (a) the racemic recrystallised product, (b) the micropreparatively resolved second eluted enantiomer, (c-d) the thermal racemisation experiment; the conversion of the resolved enantiomer to its counterpart in **ethanol** with time at 313 K.

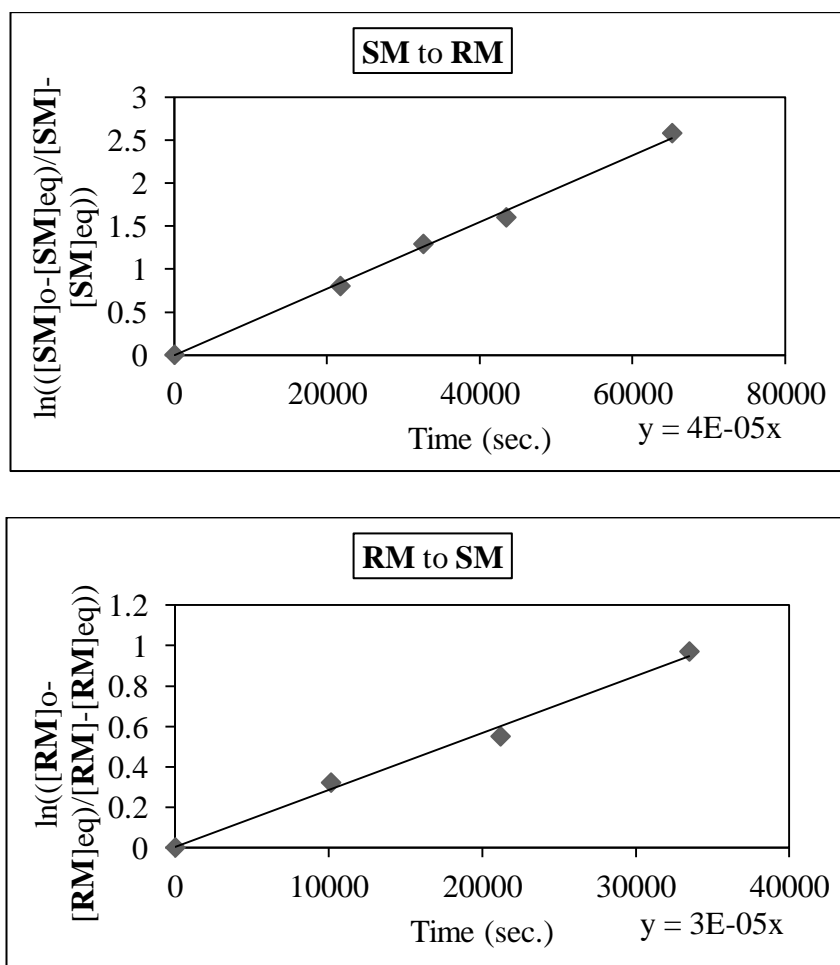
When **RM** was resolved and kept at 25 °C in ethanol, it gave racemisation and formed **SM**. Therefore, the calculation of the ΔG^\ddagger racemisation energy barrier was determined from reversible reaction kinetics due to **RM** \rightleftharpoons **SM**. For **SM** time versus $\ln \left(\frac{[\mathbf{SM}] - [\mathbf{SM}]_{\text{eq}}}{[\mathbf{SM}]_0 - [\mathbf{SM}]_{\text{eq}}} \right)$ and for **RM** time versus $\ln \left(\frac{[\mathbf{RM}] - [\mathbf{RM}]_{\text{eq}}}{[\mathbf{RM}]_0 - [\mathbf{RM}]_{\text{eq}}} \right)$ was plotted (Figure 4.4). The concentration changes of **SM** to **RM** HPLC chromatograms are given in Figure 4.5. For resolved **RM** stereoisomer, the concentration changes of **RM** to **SM** HPLC chromatograms are given in Figure 4.6. When **SP** or **RP** were resolved and subjected to thermal interconversion in ethanol at 25°C, it was observed that these stereoisomers gave rotation predominantly as **SP**→**SM** and **RP**→**RM**. The rotation of **SP** to **SM** HPLC chromatograms and rotation of **RP** to **RM** HPLC chromatograms are given in Figures 4.7 and Figure 4.8 respectively. For **SP** and **RP** time versus $\ln \left(\frac{[\mathbf{SP}] - [\mathbf{SP}]_{\text{eq}}}{[\mathbf{SP}]_0 - [\mathbf{SP}]_{\text{eq}}} \right)$ and $\ln \left(\frac{[\mathbf{RP}] - [\mathbf{RP}]_{\text{eq}}}{[\mathbf{RP}]_0 - [\mathbf{RP}]_{\text{eq}}} \right)$ were plotted respectively (Figure 4.9). The slow conversion of **SP**→**SM** was neglected. The slopes obtained gave the rate constant for the conversion of **SP** to **SM** and **RP** to **RM** respectively. The ΔG^\ddagger rotational energy barriers were calculated from Eyring Equation (2.10) using the rate constants found from the slopes.

4.3.2.1. Solvent Effect on the Interconversions Between the Stereoisomers of 5-Benzyl-3-(*o*-tolyl)-2-thiohydantoin. **SM** stereoisomer was resolved and kept in toluene at a constant temperature to determine the rate constants and ΔG^\ddagger energy barriers; it was observed that, **SM** rotated to **SP** in toluene at 40°C (Figure 4.10). When the **RP** stereoisomer was resolved and kept in toluene, at 40°C, it rotated to **RM** (Figure 4.11). For **SM** and **RP** time versus $\ln \left(\frac{[\mathbf{SM}] - [\mathbf{SM}]_{\text{eq}}}{[\mathbf{SM}]_0 - [\mathbf{SM}]_{\text{eq}}} \right)$ and time versus $\ln \left(\frac{[\mathbf{RP}] - [\mathbf{RP}]_{\text{eq}}}{[\mathbf{RP}]_0 - [\mathbf{RP}]_{\text{eq}}} \right)$ gave the first order rate constants (Figure 4.12). From the slopes, k_f and k_r values were determined. The calculated corresponding ΔG^\ddagger values for 5-benzyl-3-*o*-tolyl-2-thiohydantoin stereoisomers are given in Table 4.2.

Thus for 5-benzyl-3-*o*-tolyl-2-thiohydantoin in ethanol at 25°C, **SM** and **RM** stereoisomers gave racemisation however **SP** and **RP** gave rotation. At 40°C, in ethanol both racemisation and rotation was observed. However in toluene at 40°C, only rotation was observed for both **SM** and **RP**.

Table 4.2. Calculated ΔG^\ddagger (kJ/mole) and k values for 5-benzyl-3-*o*-tolyl-2-thiohydantoin.

| Solvent | T (°C) | Stereoisomer conversion | ΔG_f^\ddagger (kJ/mole) | ΔG_r^\ddagger (kJ/mole) | k_f (s ⁻¹) | k_r (s ⁻¹) |
|---------|--------|-------------------------|---------------------------------|---------------------------------|--------------------------|--------------------------|
| Ethanol | 25 | SP to SM | 105.5±1.2 | - | 2 x 10 ⁻⁶ | - |
| Ethanol | 25 | RP to RM | 105.5±1.2 | - | 2 x 10 ⁻⁶ | - |
| Ethanol | 25 | SM to RM | 100.4±1.2 | 99.3±1.2 | 1.59 x 10 ⁻⁵ | 2.41 x 10 ⁻⁵ |
| Ethanol | 25 | RM to SM | 100.5±1.2 | 100.5±1.2 | 1.51 x 10 ⁻⁵ | 1.49 x 10 ⁻⁵ |
| Toluene | 40 | SM to SP | 103.4±1.2 | 102.9±1.2 | 3.59 x 10 ⁻⁵ | 4.4 x 10 ⁻⁵ |
| Toluene | 40 | RP to RM | 105.4±1.2 | 104.6±1.2 | 1.7 x 10 ⁻⁵ | 2.3 x 10 ⁻⁵ |

Figure 4.4. The plot of $\ln\left(\frac{[SM]_0 - [SM]_{eq}}{[SM] - [SM]_{eq}}\right)$, $\ln\left(\frac{[RM]_0 - [RM]_{eq}}{[RM] - [RM]_{eq}}\right)$ and versus time at 298 K for 5-benzyl-3-*o*-tolyl-2-thiohydantoin.

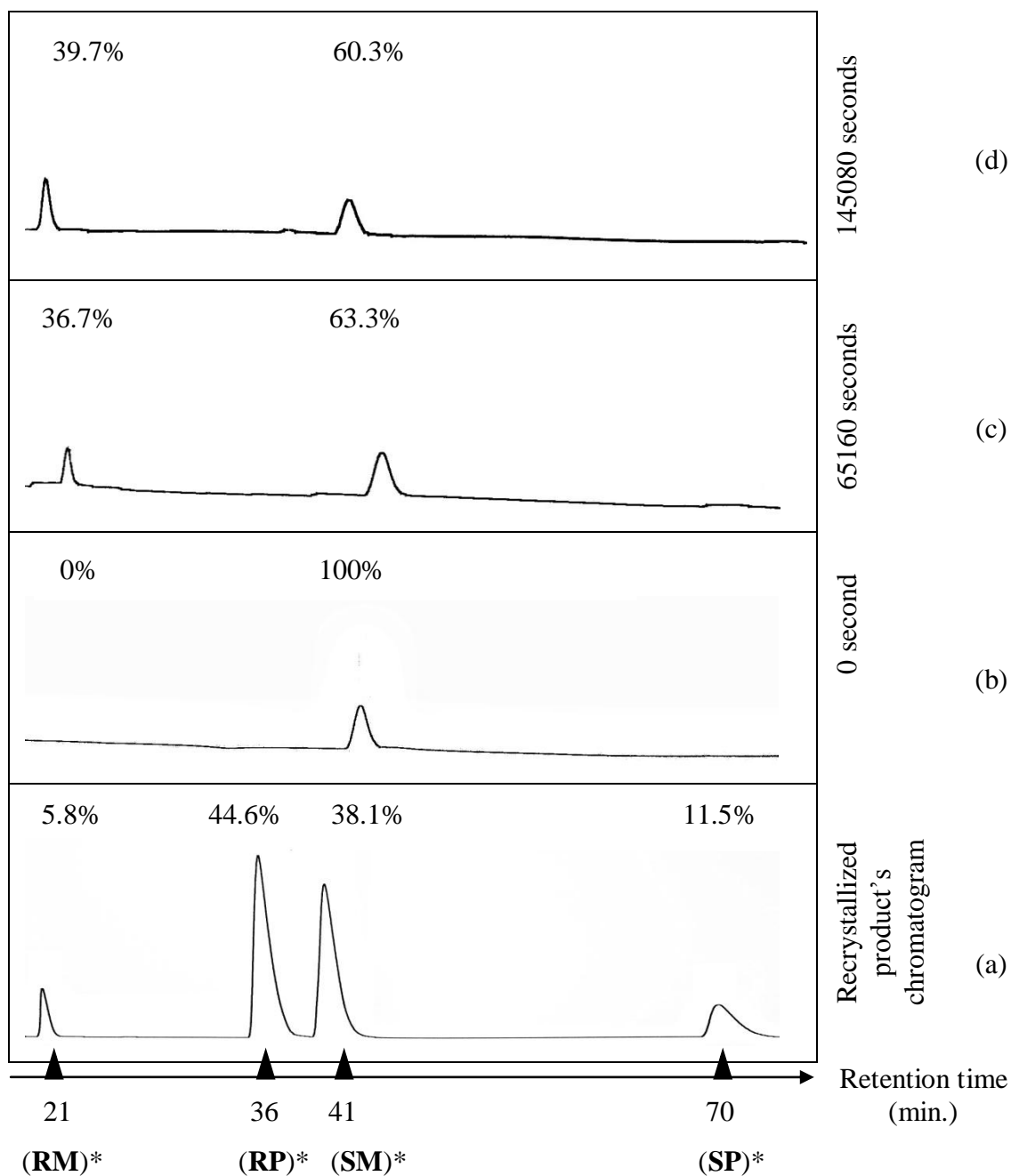


Figure 4.5. 5-Benzyl-3-(*o*-tolyl)-2-thiohydantoin HPLC chromatograms (ChiralPak IB as the stationary phase, 95:5 Hex:EtOH as the eluent, flow rate : 1.0 ml/min, column temperature : 7°C) for: (a) of the recrystallized product which shows the presence of four isomers, (b) the micropreparatively resolved **SM**, (c-d) conversion of **SM** to **RM** with time in **ethanol** at 298 K. (*) The assignments have been done with comparison by the $^1\text{H-NMR}$ spectrum.

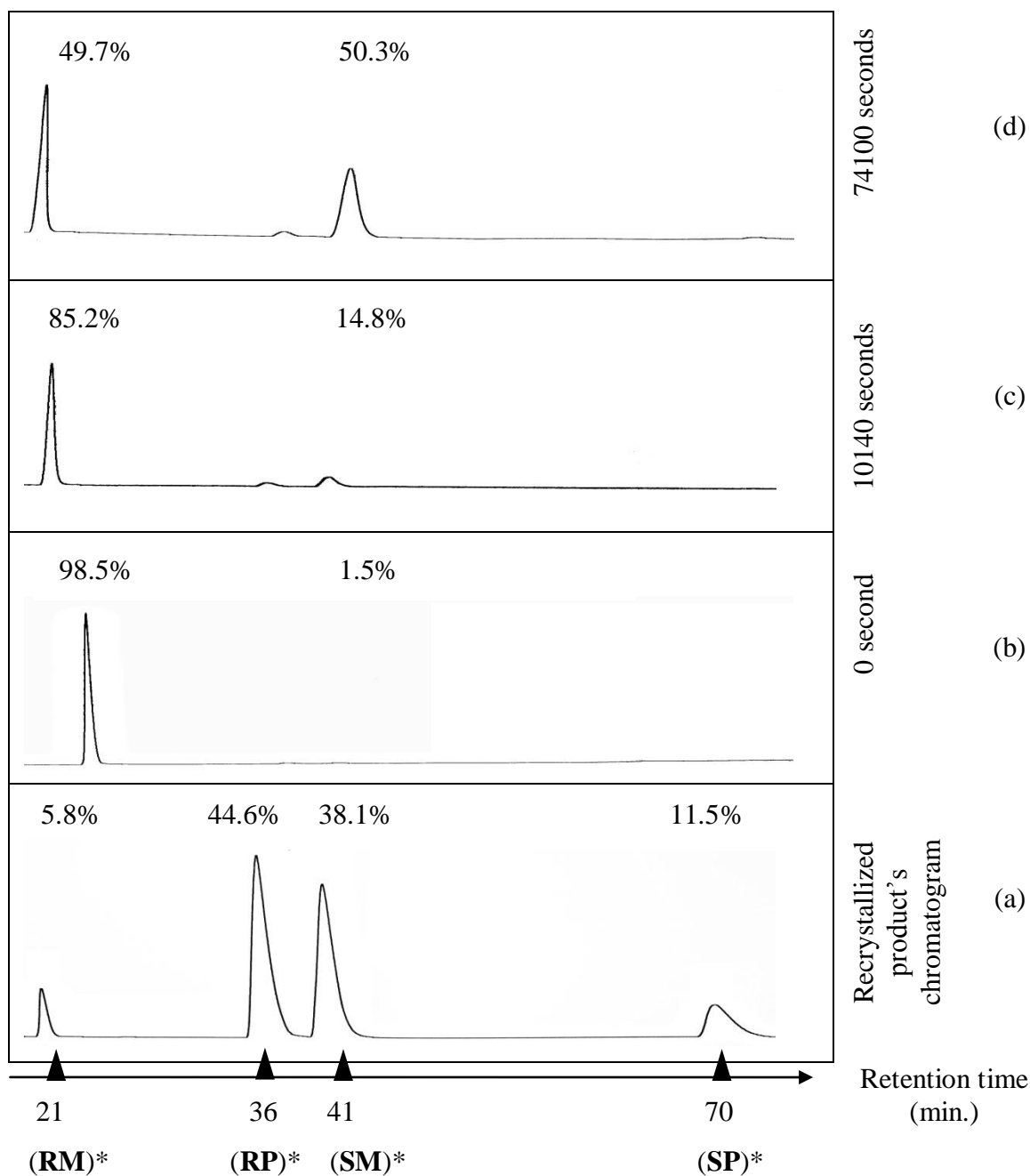


Figure 4.6. 5-Benzyl-3-(*o*-tolyl)-2-thiohydantoin HPLC chromatograms (ChiralPak IB as the stationary phase, 95:5 Hex:EtOH as the eluent, flow rate : 1.0 ml/min, column temperature : 7°C) for: (a) of the recrystallized product which shows the presence of four isomers, (b) the micropreparatively resolved **RM**, (c-d) conversion of **RM** to **SM** with time in **ethanol** at 298 K. (*) The assignments have been done with comparison by the ¹H-NMR spectrum.

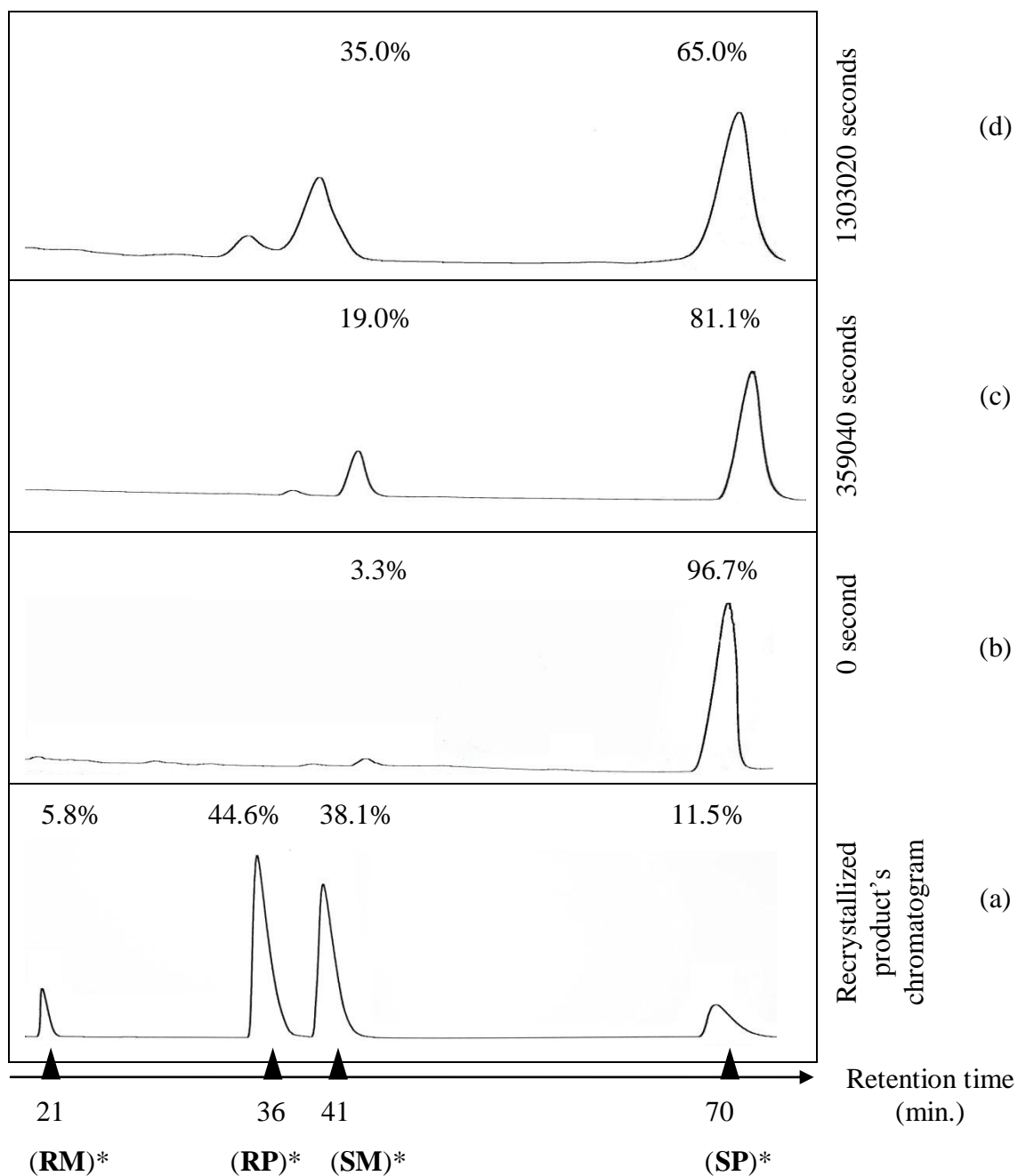


Figure 4.7. 5-Benzyl-3-(*o*-tolyl)-2-thiohydantoin HPLC chromatograms (ChiralPak IB as the stationary phase, 95:5 Hex:EtOH as the eluent, flow rate : 1.0 ml/min, column temperature : 7°C) for: (a) of the recrystallized product which shows the presence of four isomers, (b) the micropreparatively resolved **SP**, (c-d) conversion of **SP** to **SM** with time in **ethanol** at 298 K. (*) The assignments have been done with comparison by the $^1\text{H-NMR}$ spectrum.

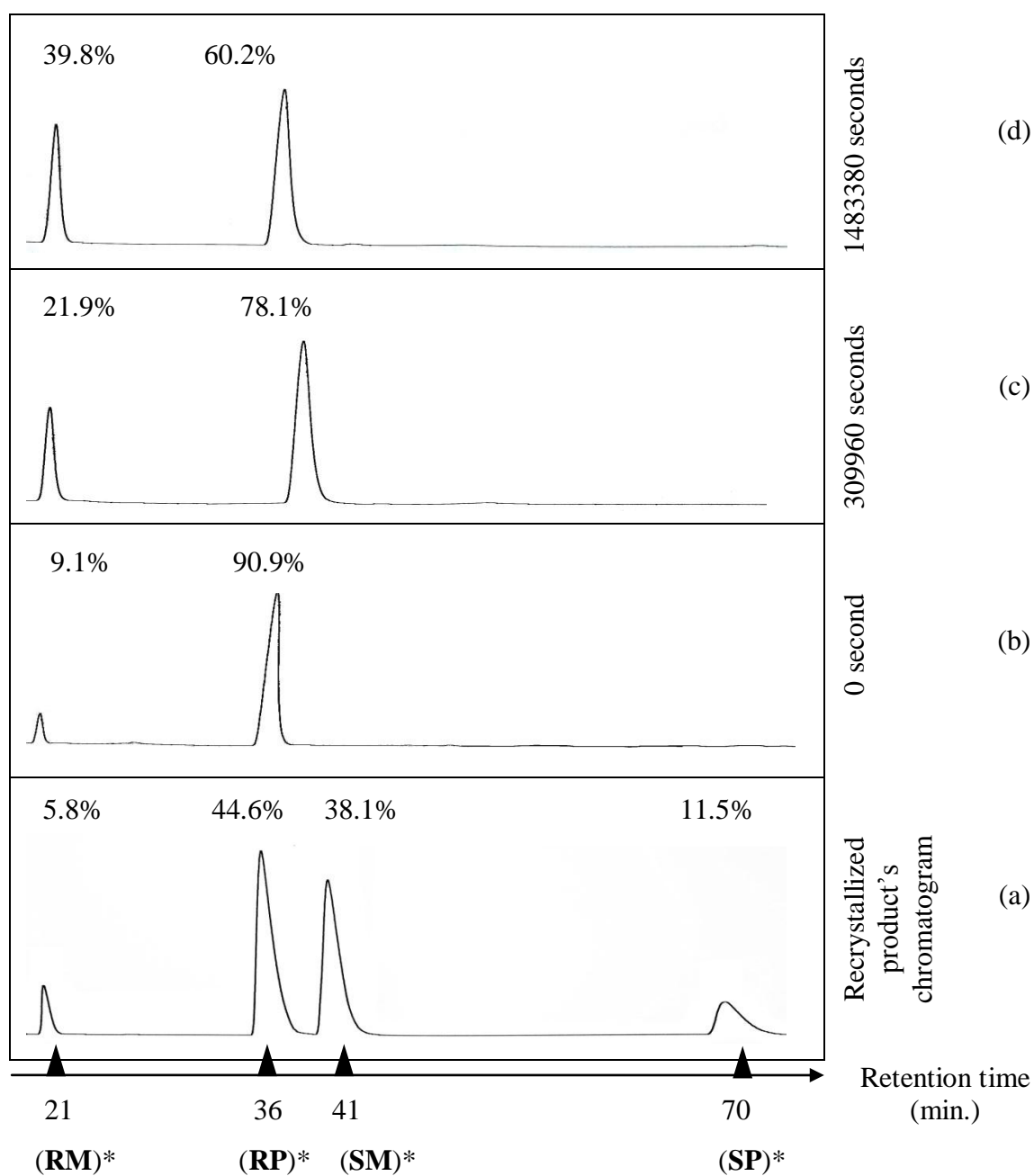


Figure 4.8. 5-Benzyl-3-(*o*-tolyl)-2-thiohydantoin HPLC chromatograms (ChiralPak IB as the stationary phase, 95:5 Hex:EtOH as the eluent, flow rate : 1.0 ml/min, column temperature : 7°C) for: (a) of the recrystallized product which shows the presence of four isomers, (b) the micropreparatively resolved **RP**, (c-d) conversion of **RP** to **RM** with time in **ethanol** at 298 K. (*) The assignments have been done with comparison by the ¹H-NMR spectrum.

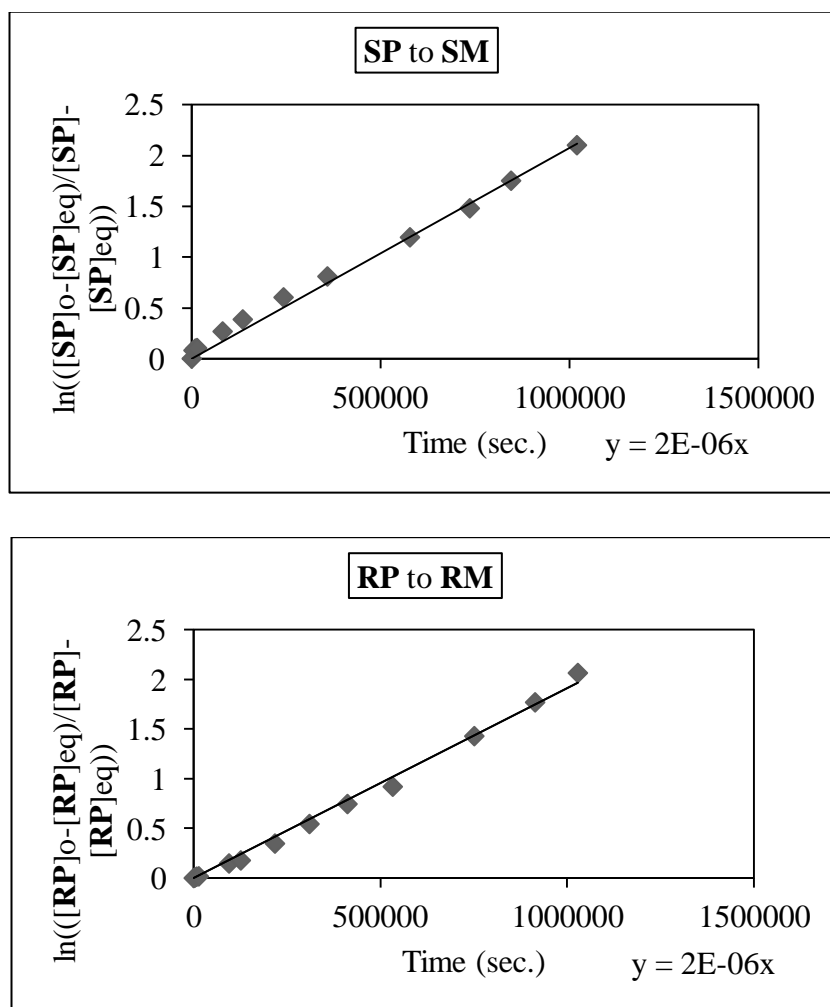


Figure 4.9. The plot of $\ln\left(\frac{[\text{SP}]_o - [\text{SP}]_{\text{eq}}}{[\text{SP}]_{\text{eq}}}\right)$ and $\ln\left(\frac{[\text{RP}]_o - [\text{RP}]_{\text{eq}}}{[\text{RP}]_{\text{eq}}}\right)$ versus time at 298 K for 5-benzyl-3-(*o*-tolyl)-2-thiohydantoin.

4.3.3. Determination of the Rotation around $\text{N3}_{(\text{sp}^2)}\text{-C}_{(\text{aryl})}$ bond ($\text{RP} \rightarrow \text{RM}$ Conversion) and Racemisation at C-5 Barrier ($\text{RM} \rightleftharpoons \text{SM}$ and $\text{RP} \rightleftharpoons \text{SP}$ Conversion) for 5-Benzyl-3-(*o*-bromophenyl)-2-thiohydantoin stereoisomers

For 5-Benzyl-3-(*o*-bromophenyl)-2-thiohydantoin stereoisomers at both 25°C 40°C, **RP** to **SP**, **RM** to **SM** and **SP** to **RP** conversions i.e. racemisation at C-5 have been observed. The corresponding ΔG^\ddagger racemisation energy barriers were calculated. For **SM**, the separation was not done due to its low concentration.

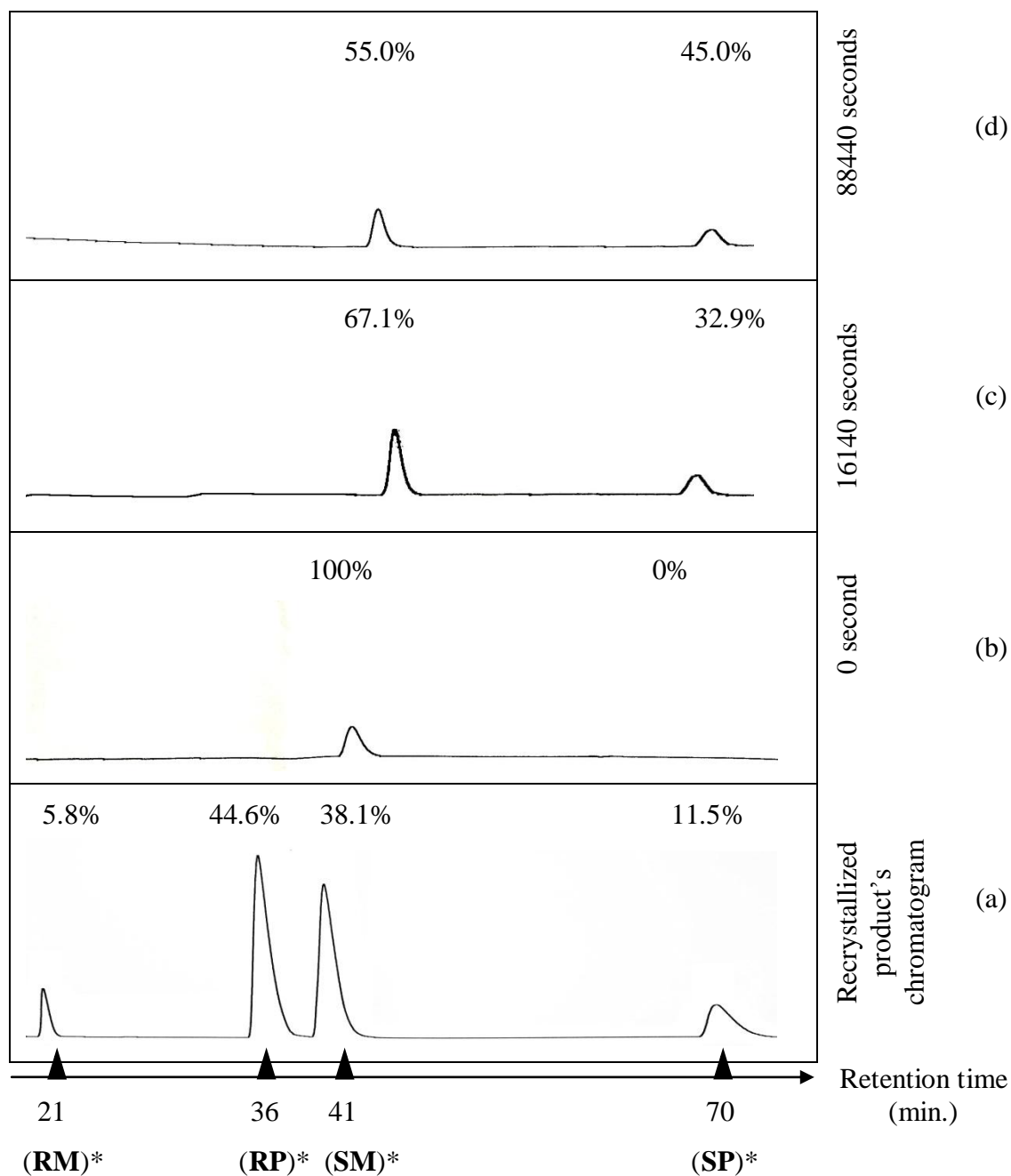


Figure 4.10. 5-Benzyl-3-(*o*-tolyl)-2-thiohydantoin HPLC chromatograms (ChiralPak IB as the stationary phase, 95:5 Hex:EtOH as the eluent, flow rate : 1.0 ml/min, column temperature : 7°C) for: (a) of the recrystallized product which shows the presence of four isomers, (b) the micropreparatively resolved **SM**, (c-d) conversion of **SM** to **SP** with time in **toluene** at 313 K. (*) The assignments have been done with comparison by the $^1\text{H-NMR}$ spectrum.

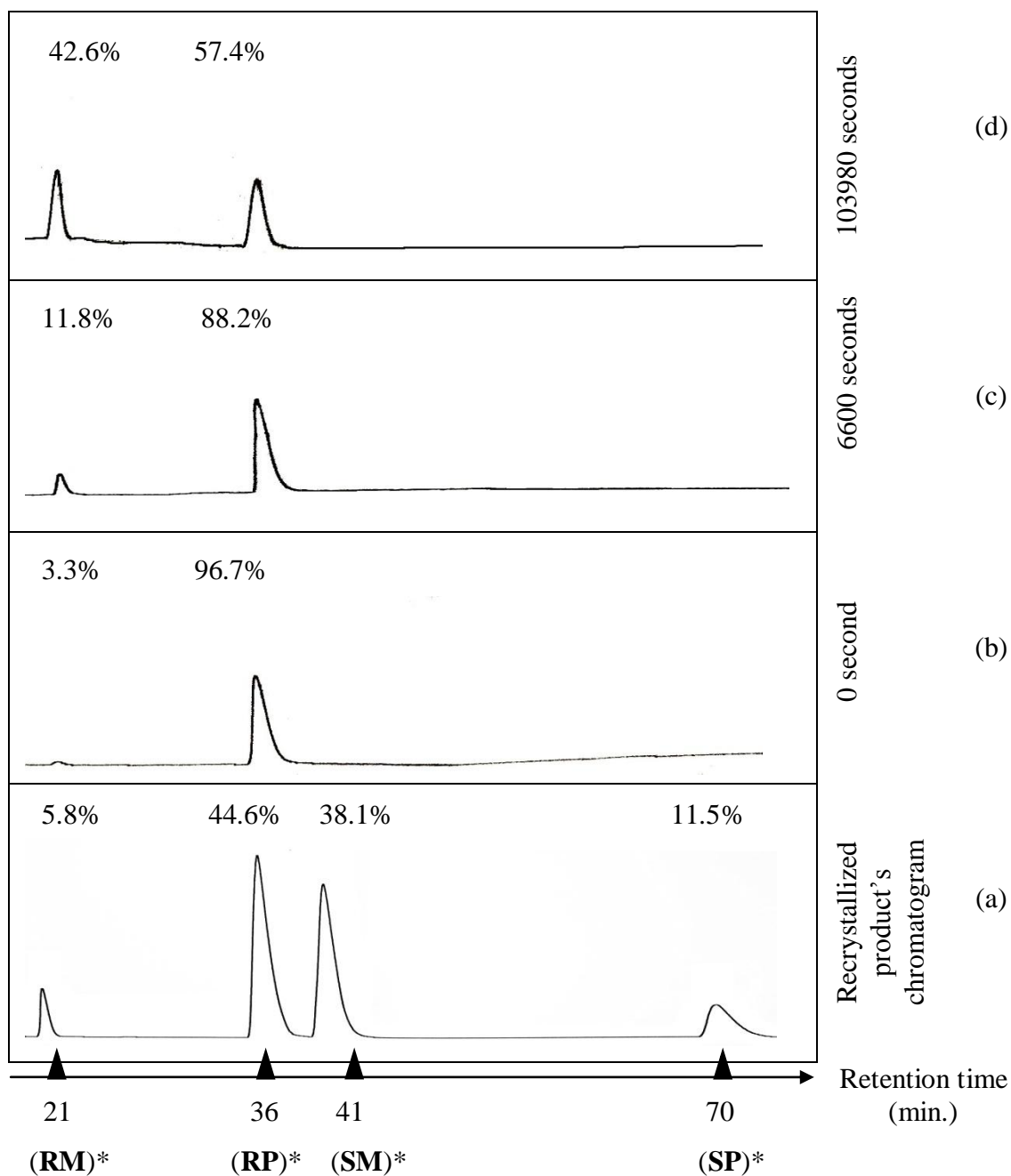


Figure 4.11. 5-Benzyl-3-(*o*-tolyl)-2-thiohydantoin HPLC chromatograms (ChiralPak IB as the stationary phase, 95:5 Hex:EtOH as the eluent, flow rate : 1.0 ml/min, column temperature : 7°C) for: (a) of the recrystallized product which shows the presence of four isomers, (b) the micropreparatively resolved **RP**, (c-d) conversion of **RP** to **RM** with time in **toluene** at 313 K. (*) The assignments have been done with comparison by the $^1\text{H-NMR}$ spectrum.

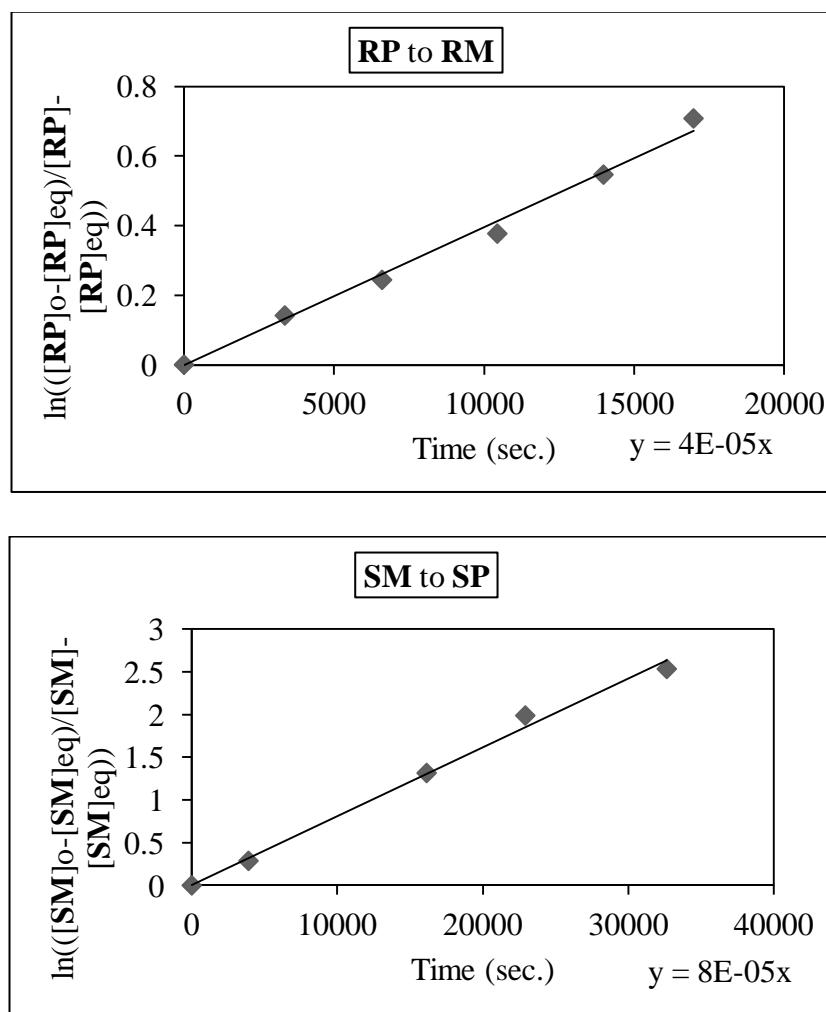


Figure 4.12. The plot of $\ln\left(\frac{[\text{RP}]_0 - [\text{RP}]_{\text{eq}}}{[\text{RP}] - [\text{RP}]_{\text{eq}}}\right)$ and $\ln\left(\frac{[\text{SM}]_0 - [\text{SM}]_{\text{eq}}}{[\text{SM}] - [\text{SM}]_{\text{eq}}}\right)$ versus time at 313 K for 5-benzyl-3-(*o*-tolyl)-2-thiohydantoin.

Stereoisomers were separated on Chiralpak IC column in hexane 95% and ethanol 5% mixture. **SP**, **RP** and **RM** resolved and kept in ethanol to follow the kinetics of conversion of the stereoisomers and to calculate the rate constants and ΔG^\ddagger energy barriers. At 25°C for conversions **SP** ⇌ **RP**, **RP** ⇌ **SP** and **RM** ⇌ **SM**, ΔG^\ddagger racemisation barriers and rate constants were calculated at 25°C and 40°C from the time versus $\ln\left(\frac{[\text{RP}] - [\text{RP}]_{\text{eq}}}{[\text{RP}]_0 - [\text{RP}]_{\text{eq}}}\right)$, $\ln\left(\frac{[\text{RM}] - [\text{RM}]_{\text{eq}}}{[\text{RM}]_0 - [\text{RM}]_{\text{eq}}}\right)$ and $\ln\left(\frac{[\text{SP}] - [\text{SP}]_{\text{eq}}}{[\text{SP}]_0 - [\text{SP}]_{\text{eq}}}\right)$ plots (Figure 4.13). The chromatograms for thermal racemisation of **SP** to **RP**, **RP** to **SP** and **RM** to **SM** at 25°C, are given in Figures 4.14, 4.15 and 4.16 respectively. The above experiment was also done to see the temperature effect on racemisation at 40°C in ethanol. Time versus $\ln\left(\frac{[\text{RP}] - [\text{RP}]_{\text{eq}}}{[\text{RP}]_0 - [\text{RP}]_{\text{eq}}}\right)$, $\ln\left(\frac{[\text{RM}] - [\text{RM}]_{\text{eq}}}{[\text{RM}]_0 - [\text{RM}]_{\text{eq}}}\right)$ and $\ln\left(\frac{[\text{SP}] - [\text{SP}]_{\text{eq}}}{[\text{SP}]_0 - [\text{SP}]_{\text{eq}}}\right)$ plots gave the racemisation barriers at 40 °C (Figure 4.17).

The corresponding HPLC chromatograms are given in Figures 4.18, 4.19 and 4.20 respectively. ΔG_r^\ddagger , ΔG_f^\ddagger , k_f and k_r were calculated for 25°C and 40°C are listed in Table 4.3. Increase in temperature increased the rates and the determined barriers. From the plot of $\ln K$ with $1/T$ (Figure 4.23) ΔH° was found as 13.58 kJ/mole and ΔS° was found as 49.55 J/K.mole. All the ΔG^\ddagger energy barriers of compound **3** were calculated from Eyring Equation (2.10).

4.3.3.1. Solvent Effect on the Interconversions Between the Stereoisomers of 5-Benzyl-3-(*o*-bromophenyl)-2-thiohydantoin. When the **RP** stereoisomer was separated and kept in toluene, it rotated to **RM**. At 40°C, the rotation was very slow, therefore the temperature was raised to 110°C. HPLC chromatograms for the rotation of **RP** to **RM** at 110°C in toluene are given in Figure 4.21. For **RP**, time versus $\ln ([\mathbf{RP}] - [\mathbf{RP}]_{\text{eq}}) / ([\mathbf{RP}]_0 - [\mathbf{RP}]_{\text{eq}})$ was plotted for 110°C (Figure 4.22). In toluene, no racemisation was observed even the temperature was 110 °C. However, at 25 and 40°C in ethanol, only racemisation was observed. The calculation of ΔG^\ddagger rotation energy barrier for 5-benzyl-3-(*o*-bromophenyl)-2-thiohydantoin in toluene, reversible reaction kinetic was used. All calculated ΔG^\ddagger values and rate constants for 5-benzyl-3-(*o*-bromophenyl)-2-thiohydantoin are given in Table 4.3.

Table 4.3. Calculated ΔG^\ddagger (kJ/mole) and k values for 5-benzyl-3-(*o*-bromophenyl)-2-thiohydantoin.

| Solvent | T (°C) | Stereoisomer conversion | ΔG_f^\ddagger (kJ/mole) | ΔG_r^\ddagger (kJ/mole) | k_f (s ⁻¹) | k_r (s ⁻¹) |
|---------|--------|-------------------------|---------------------------------|---------------------------------|--------------------------|--------------------------|
| Ethanol | 25 | RP to SP | 97.9±3.2 | 99.1±3.2 | 4.31 x 10 ⁻⁵ | 2.69 x 10 ⁻⁵ |
| Ethanol | 25 | SP to RP | 102.3±3.2 | 100.9±3.2 | 7.34 x 10 ⁻⁶ | 1.26 x 10 ⁻⁵ |
| Ethanol | 25 | RM to SM | 104.1±3.2 | 102.6±3.2 | 3.54 x 10 ⁻⁶ | 6.46 x 10 ⁻⁶ |
| Ethanol | 40 | RP to SP | 100.0±3.2 | 101.9±3.2 | 1.36 x 10 ⁻⁴ | 6.43 x 10 ⁻⁵ |
| Ethanol | 40 | SP to RP | 104.6±3.2 | 102.7±3.2 | 2.26 x 10 ⁻⁵ | 4.74 x 10 ⁻⁵ |
| Ethanol | 40 | RM to SM | 105.7±3.2 | 104.3±3.2 | 1.48 x 10 ⁻⁵ | 2.52 x 10 ⁻⁵ |
| Toluene | 110 | RP to RM | 118.7±3.2 | 118.9±3.2 | 5.18 x 10 ⁻⁴ | 4.82 x 10 ⁻⁴ |

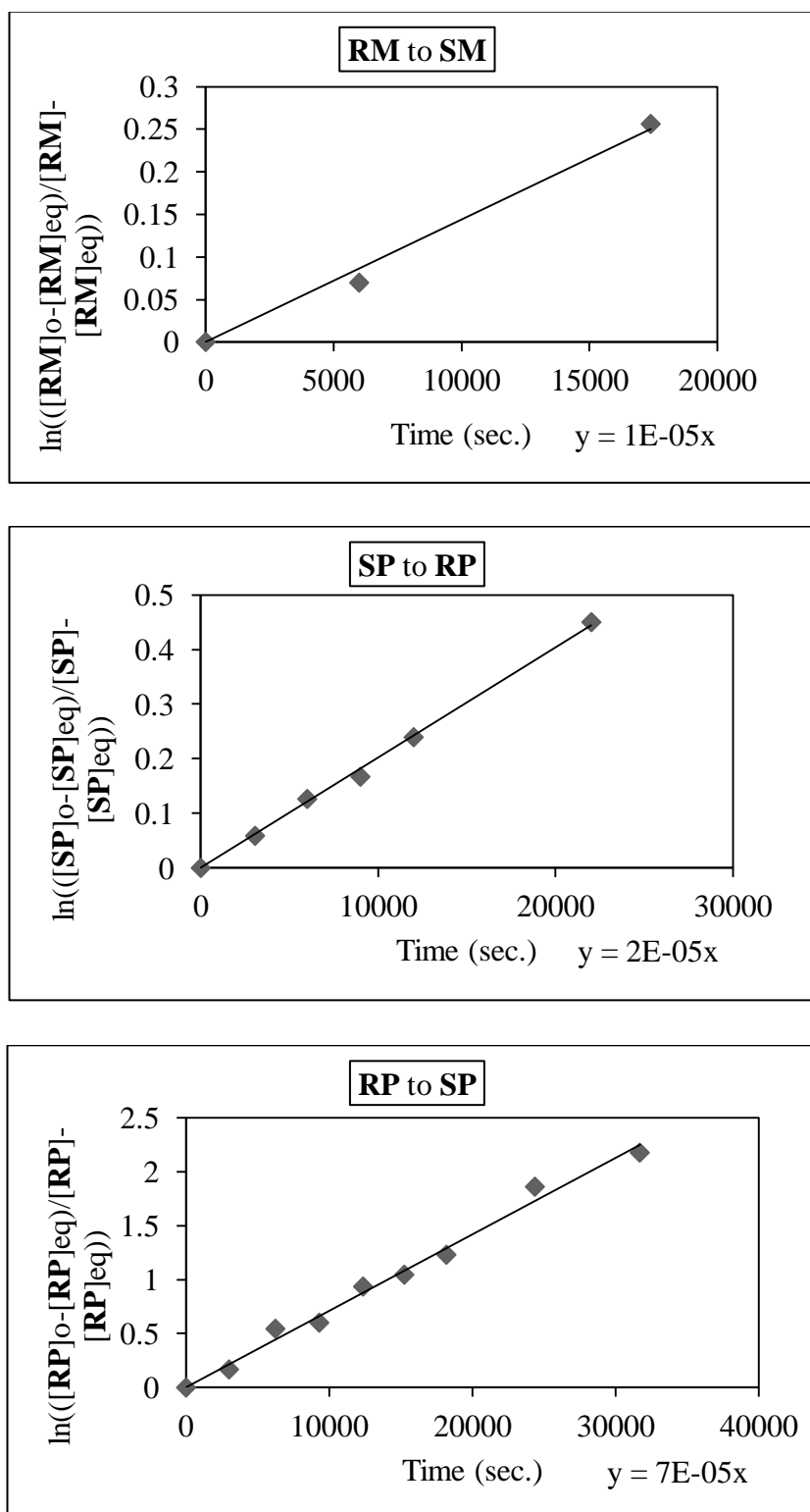


Figure 4.13. The plot of $\ln\left(\frac{[\text{RM}]_0 - [\text{RM}]_{\text{eq}}}{[\text{RM}]_{\text{eq}}}\right)$, $\ln\left(\frac{[\text{SP}]_0 - [\text{SP}]_{\text{eq}}}{[\text{SP}]_{\text{eq}}}\right)$, $\ln\left(\frac{[\text{RP}]_0 - [\text{RP}]_{\text{eq}}}{[\text{RP}]_{\text{eq}}}\right)$, versus time at 298 K for 5-benzyl-3-(*o*-bromophenyl)-2-thiohydantoin.

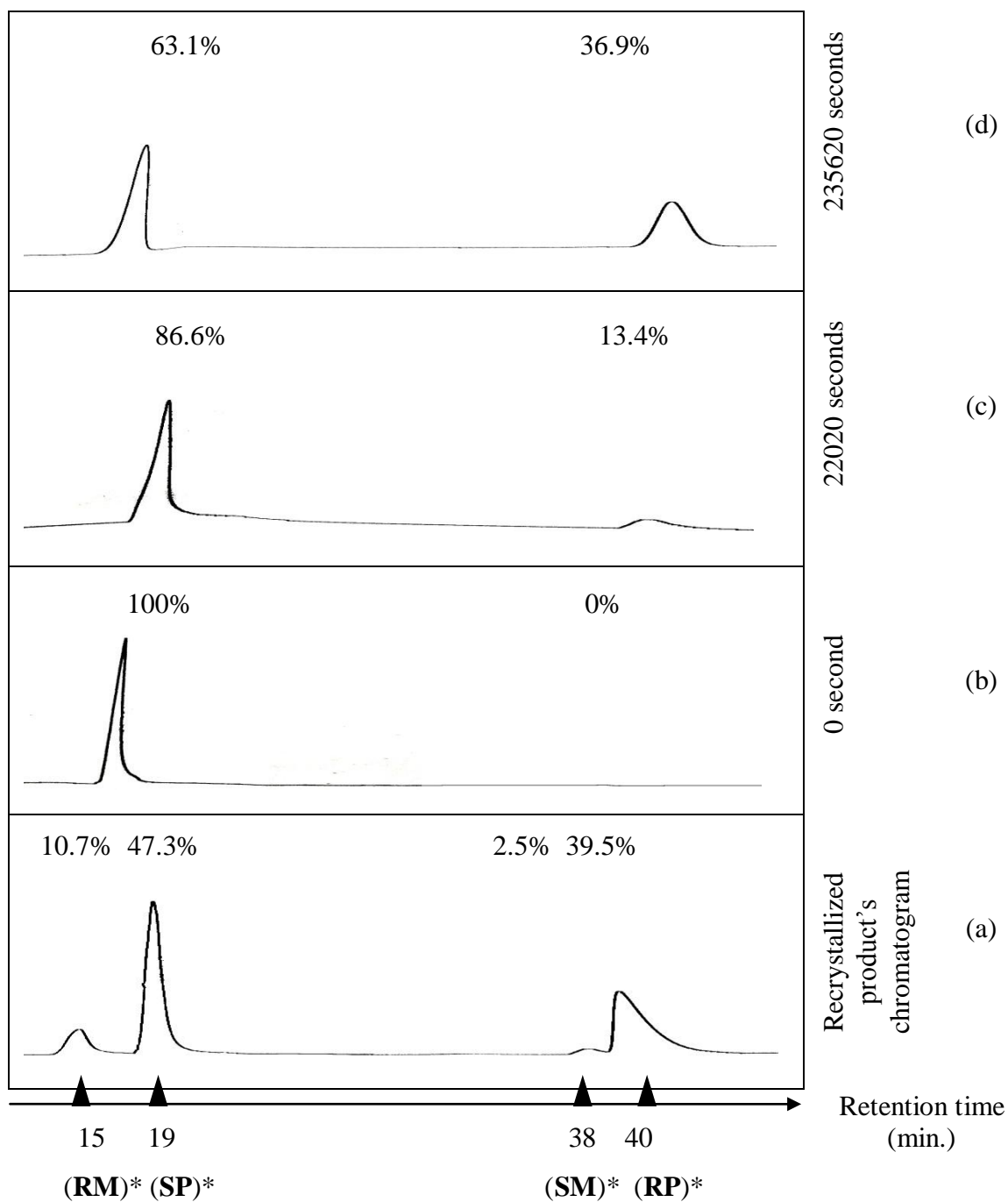


Figure 4.14. 5-Benzyl-3-(*o*-bromophenyl)-2-thiohydantoin HPLC chromatograms (ChiralPak IC as the stationary phase, 95:5 Hex:EtOH as the eluent, flow rate : 0.8 ml/min, column temperature : 7°C) for: (a) of the recrystallized product which shows the presence of four isomers, (b) the micropreparatively resolved **SP**, (c-d) conversion of **SP** to **RP** with time in **ethanol** at 298 K. (*) The assignments have been done with comparison by the $^1\text{H-NMR}$ spectrum.

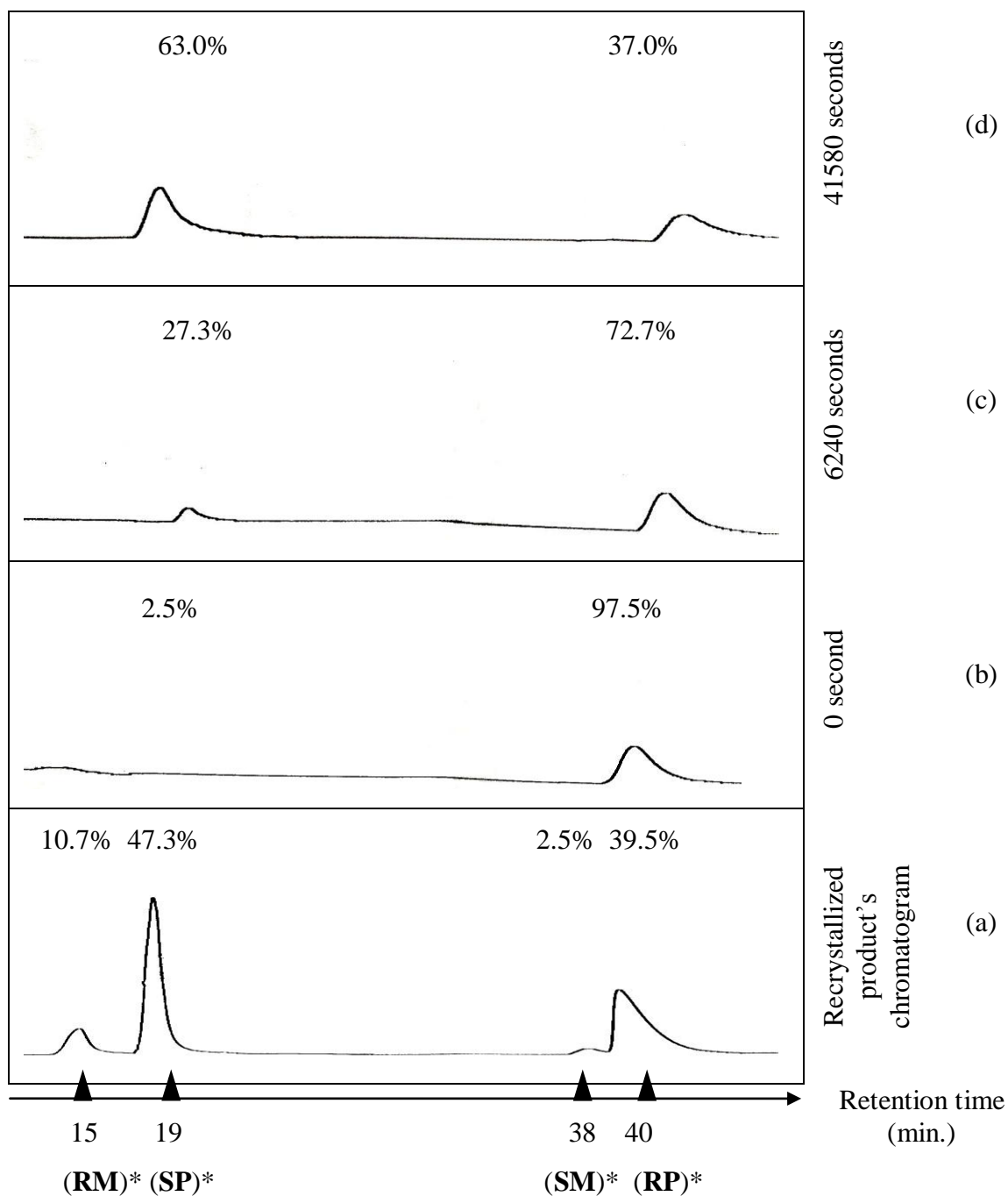


Figure 4.15. 5-Benzyl-3-(*o*-bromophenyl)-2-thiohydantoin HPLC chromatograms (ChiralPak IC as the stationary phase, 95:5 Hex:EtOH as the eluent, flow rate : 0.8 ml/min, column temperature : 7°C) for: (a) of the recrystallized product which shows the presence of four isomers, (b) the micropreparatively resolved **RP**, (c-d) conversion of **RP** to **SP** with time in **ethanol** at 298 K. (*) The assignments have been done with comparison by the ¹H-NMR spectrum.

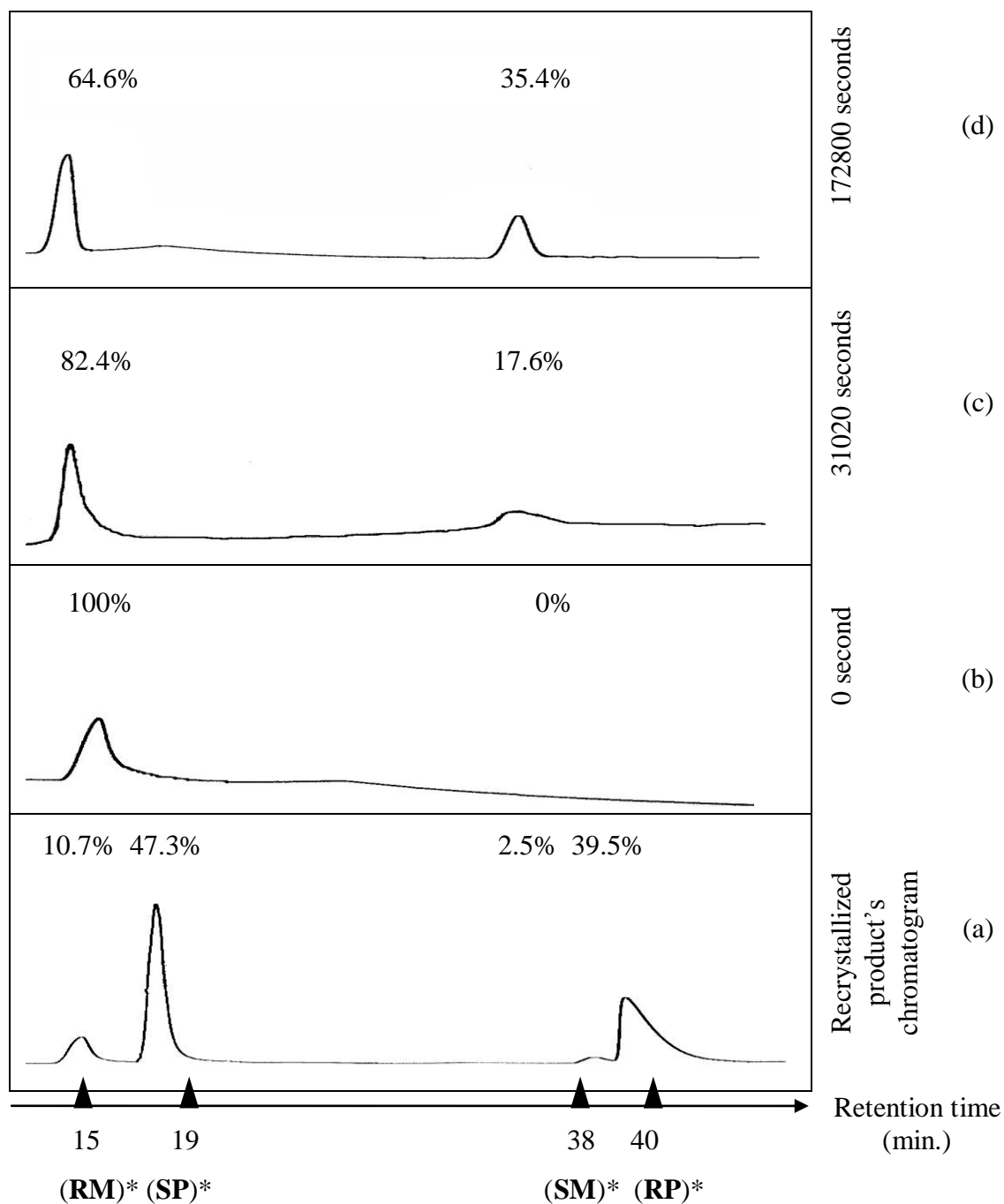


Figure 4.16. 5-Benzyl-3-(*o*-bromophenyl)-2-thiohydantoin HPLC chromatograms (ChiralPak IC as the stationary phase, 95:5 Hex:EtOH as the eluent, flow rate : 0.8 ml/min, column temperature : 7°C) for: (a) of the recrystallized product which shows the presence of four isomers, (b) the micropreparatively resolved **RM**, (c-d) conversion of **RM** to **SM** with time in **ethanol** at 298 K. (*) The assignments have been done with comparison by the $^1\text{H-NMR}$ spectrum.

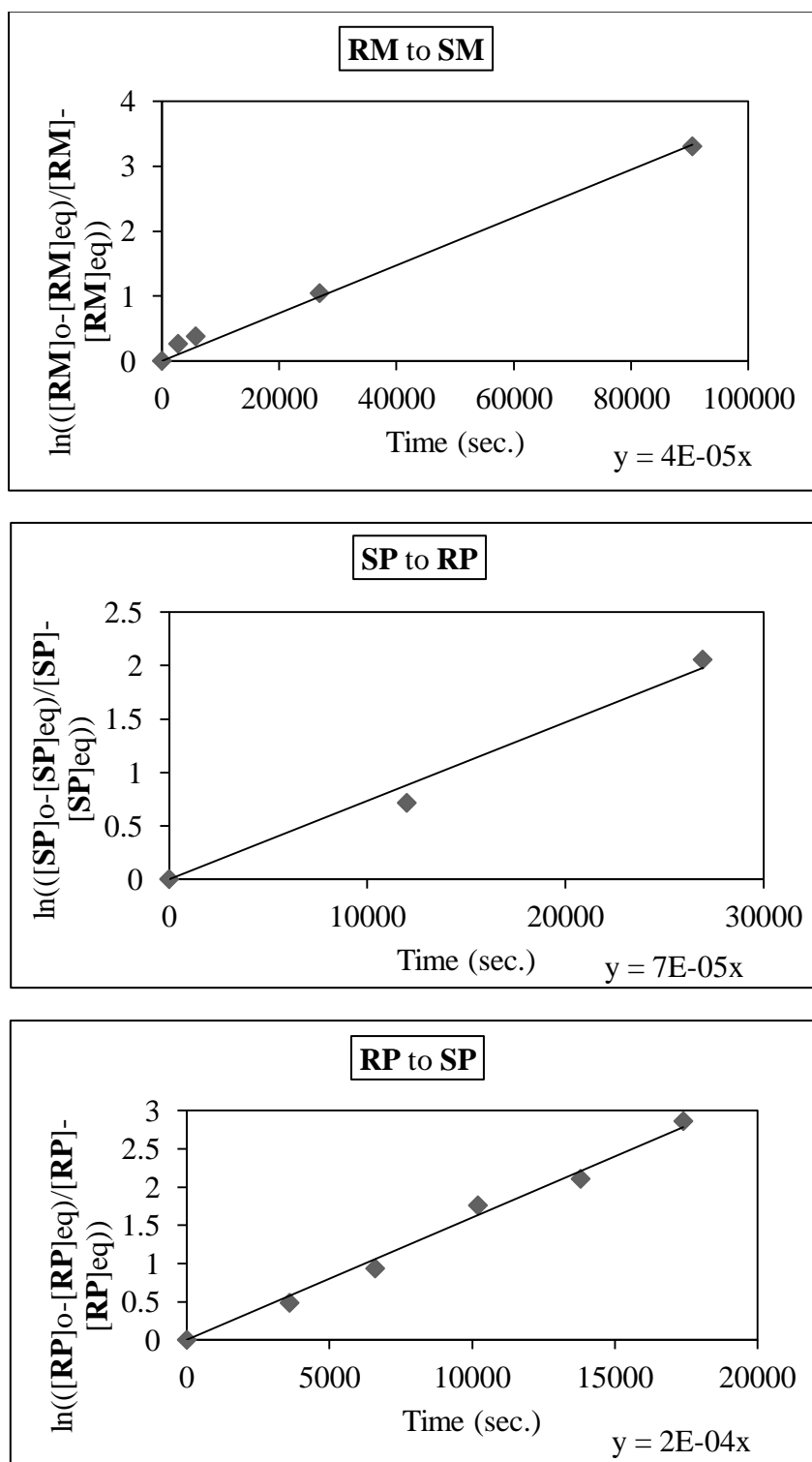


Figure 4.17. The plot of $\ln\left(\frac{[\text{RM}]_0 - [\text{RM}]_{\text{eq}}}{[\text{RM}] - [\text{RM}]_{\text{eq}}}\right)$, $\ln\left(\frac{[\text{SP}]_0 - [\text{SP}]_{\text{eq}}}{[\text{SP}] - [\text{SP}]_{\text{eq}}}\right)$, $\ln\left(\frac{[\text{RP}]_0 - [\text{RP}]_{\text{eq}}}{[\text{RP}] - [\text{RP}]_{\text{eq}}}\right)$, versus time at 313 K for 5-benzyl-3-(*o*-bromophenyl)-2-thiohydantoin.

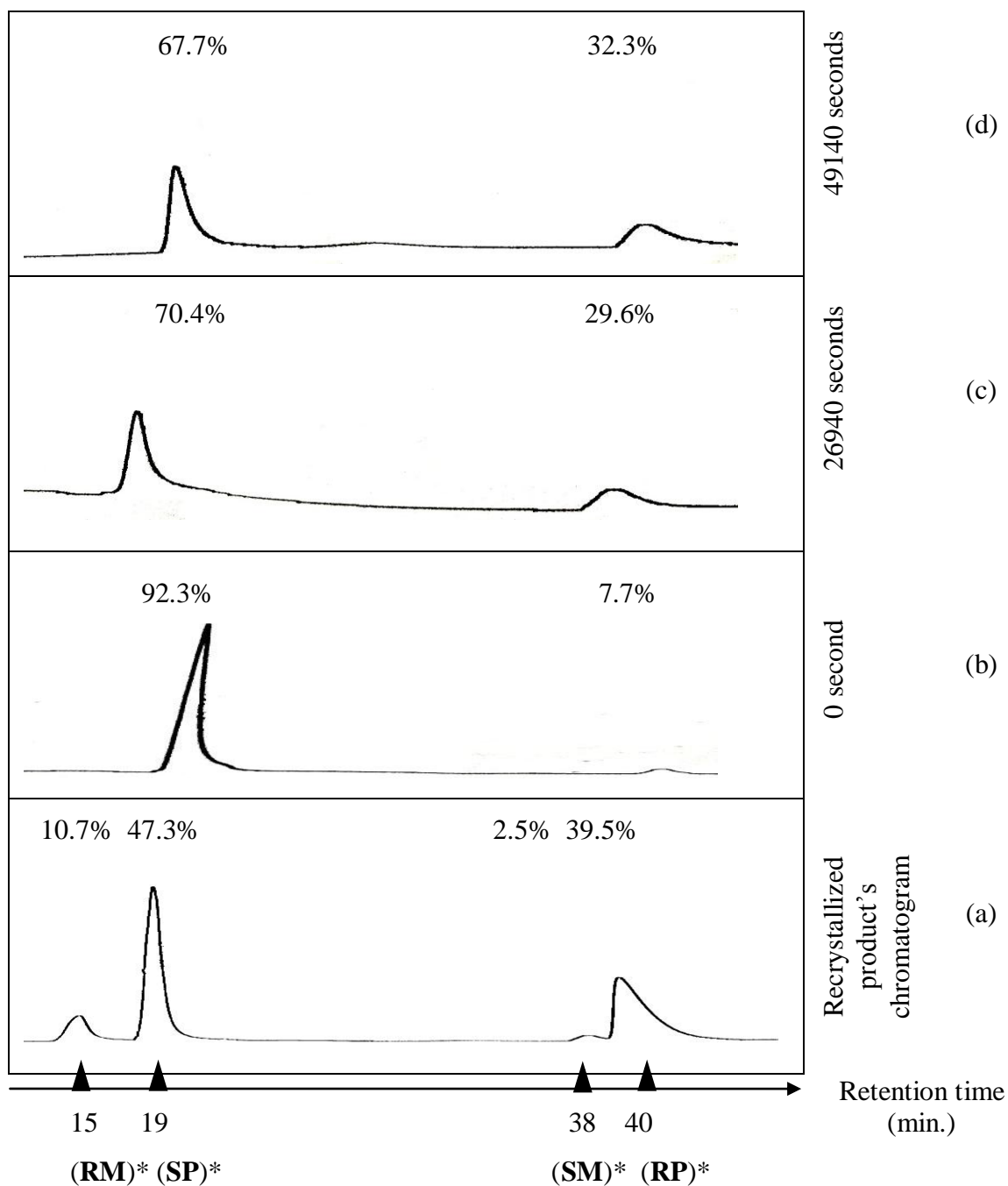


Figure 4.18. 5-Benzyl-3-(*o*-bromophenyl)-2-thiohydantoin HPLC chromatograms (ChiralPak IC as the stationary phase, 95:5 Hex:EtOH as the eluent, flow rate: 0.8 ml/min, column temperature : 7°C) for: (a) of the recrystallized product which shows the presence of four isomers, (b) the micropreparatively resolved **SP**, (c-d) conversion of **SP** to **RP** with time in **ethanol** at 313 K. (*) The assignments have been done with comparison by the ^1H -NMR spectrum.

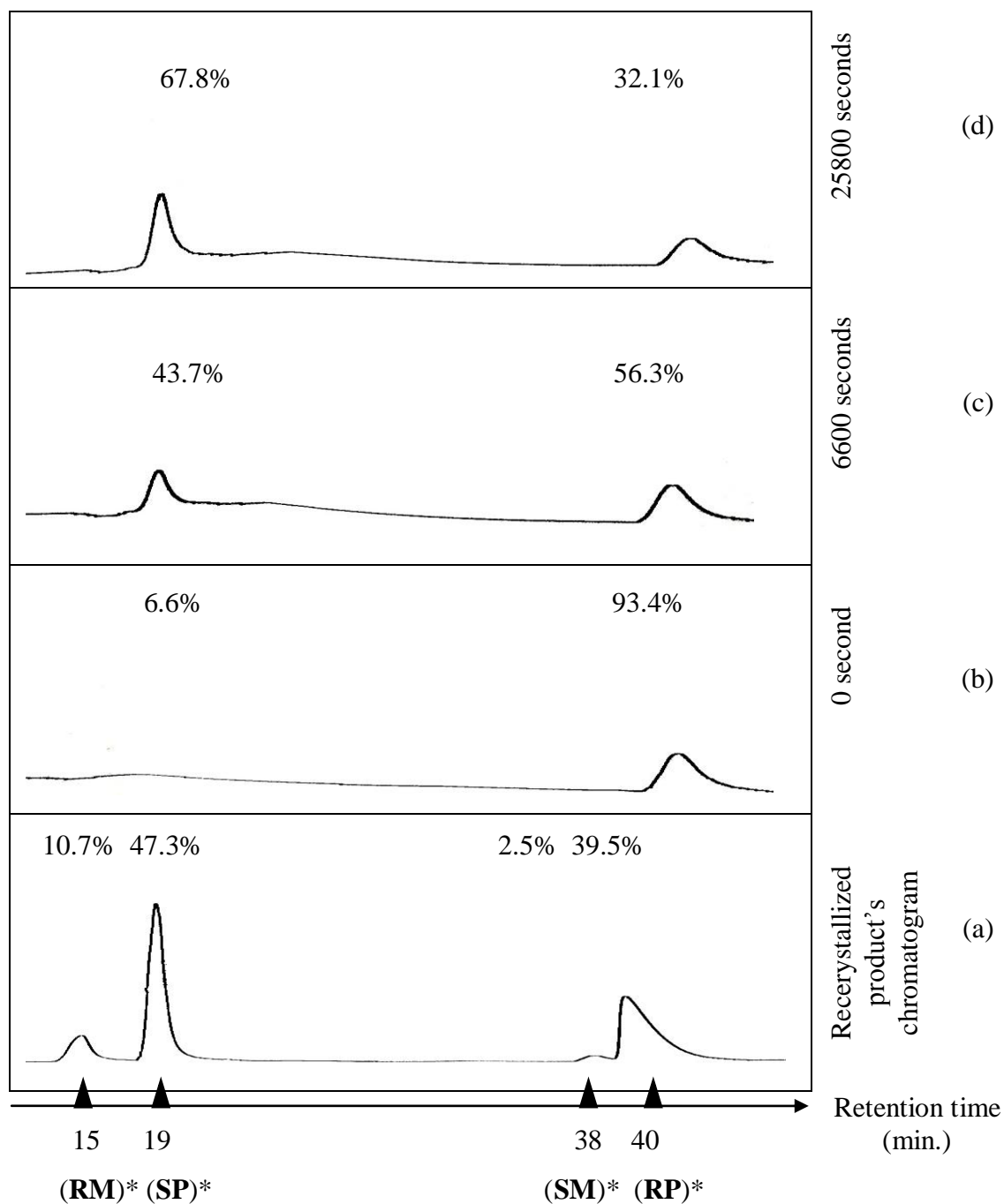


Figure 4.19. 5-Benzyl-3-(*o*-bromophenyl)-2-thiohydantoin HPLC chromatograms (ChiralPak IC as the stationary phase, 95:5 Hex:EtOH as the eluent, flow rate : 0.8 ml/min, column temperature : 7°C) for: (a) of the recrystallized product which shows the presence of four isomers, (b) the micropreparatively resolved **RP**, (c-d) conversion of **RP** to **SP** with time in **ethanol** at 313 K. (*) The assignments have been done with comparison by the $^1\text{H-NMR}$ spectrum.

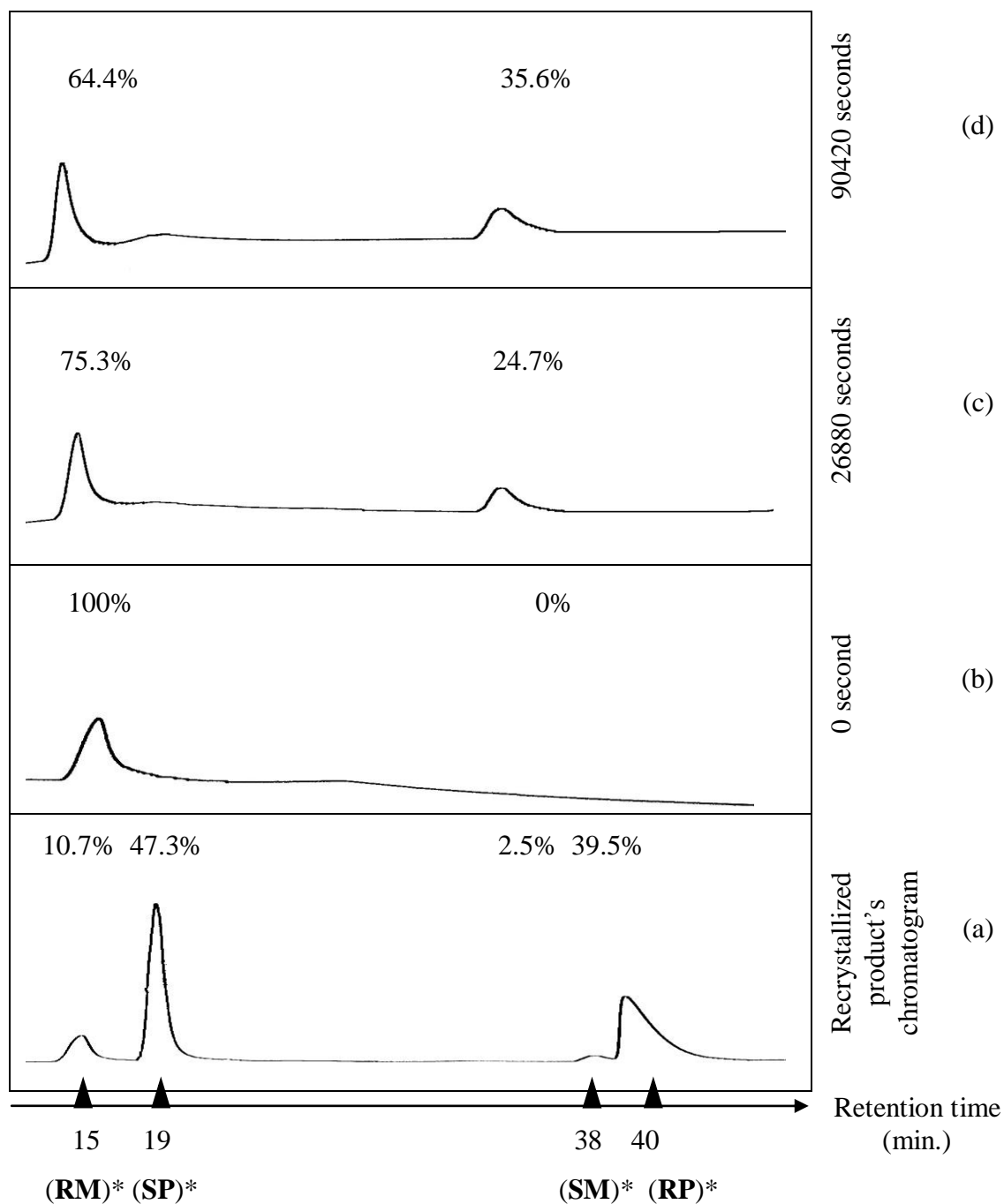


Figure 4.20. 5-Benzyl-3-(*o*-bromophenyl)-2-thiohydantoin HPLC chromatograms (ChiralPak IC as the stationary phase, 95:5 Hex:EtOH as the eluent, flow rate : 0.8 ml/min, column temperature : 7°C) for: (a) of the recrystallized product which shows the presence of four isomers, (b) the micropreparatively resolved **RM**, (c-d) conversion of **RM** to **SM** with time in **ethanol** at 313 K. (*) The assignments have been done with comparison by the $^1\text{H-NMR}$ spectrum.

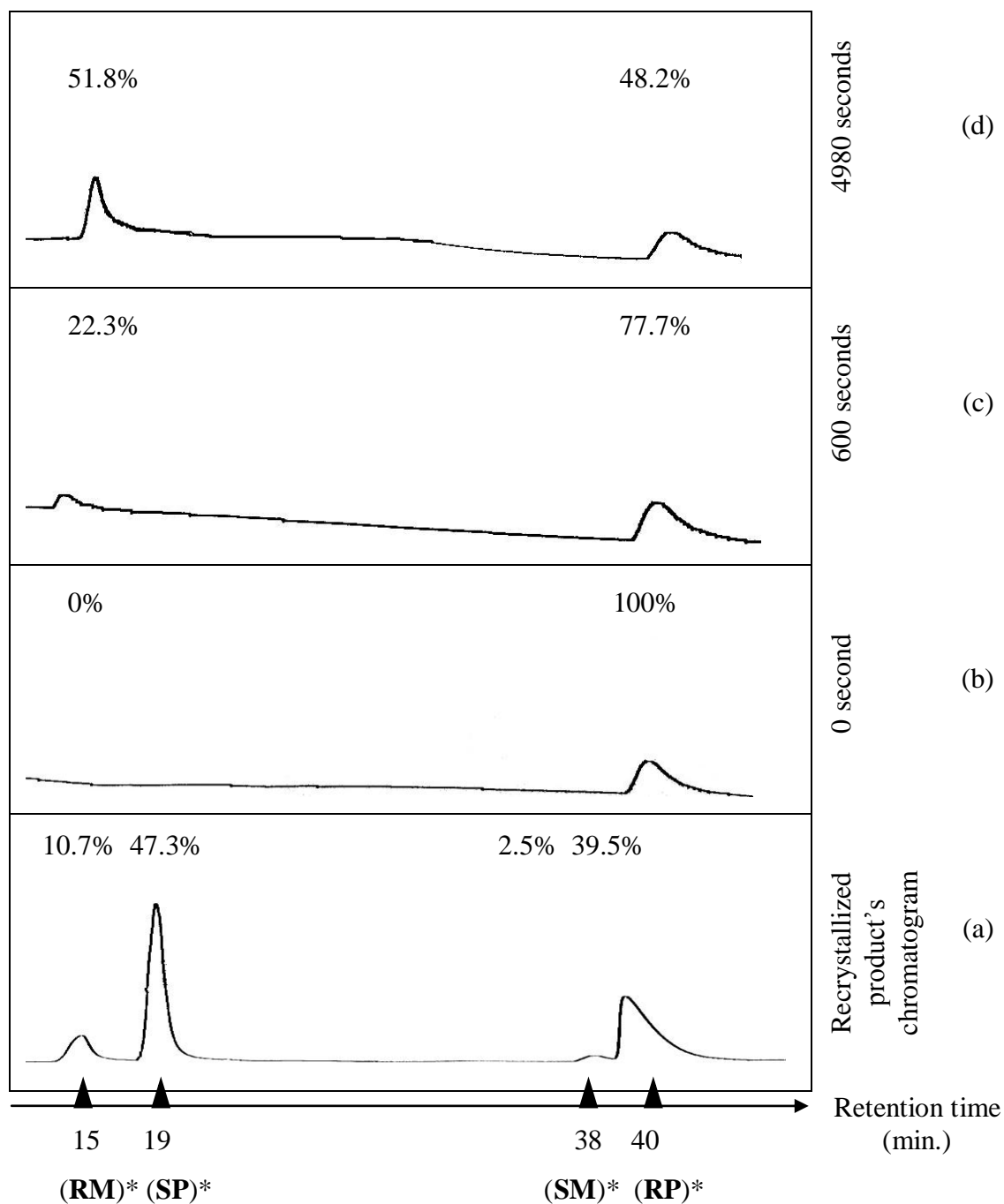


Figure 4.21. 5-Benzyl-3-(*o*-bromophenyl)-2-thiohydantoin HPLC chromatograms (ChiralPak IC as the stationary phase, 95:5 Hex:EtOH as the eluent, flow rate : 0.8 ml/min, column temperature : 7°C) for: (a) of the recrystallized product which shows the presence of four isomers, (b) the micropreparatively resolved **RP**, (c-d) conversion of **RP** to **RM** with time in **toluene** at 383 K. (*) The assignments have been done with comparison by the $^1\text{H-NMR}$ spectrum.

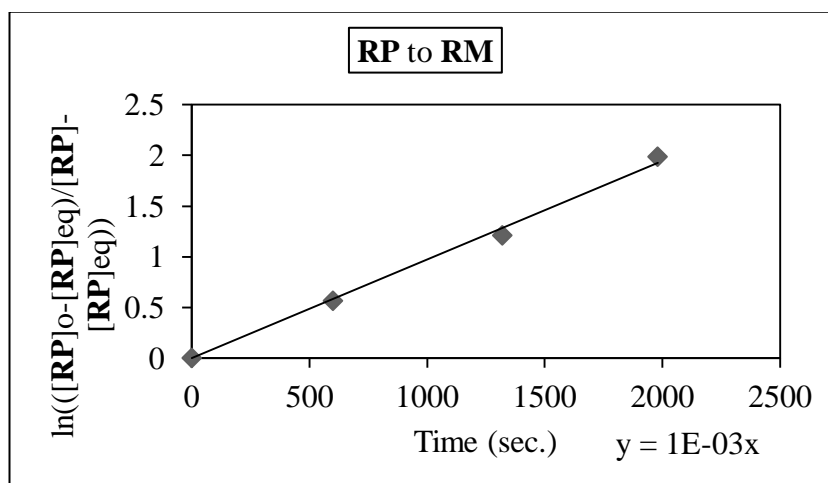


Figure 4.22. The plot of $\ln\left(\frac{[\text{RP}]_0 - [\text{RP}]_{\text{eq}}}{[\text{RP}]_{\text{eq}}}\right)$ versus time at 383 K for 5-benzyl-3-(*o*-bromophenyl)-2-thiohydantoin.

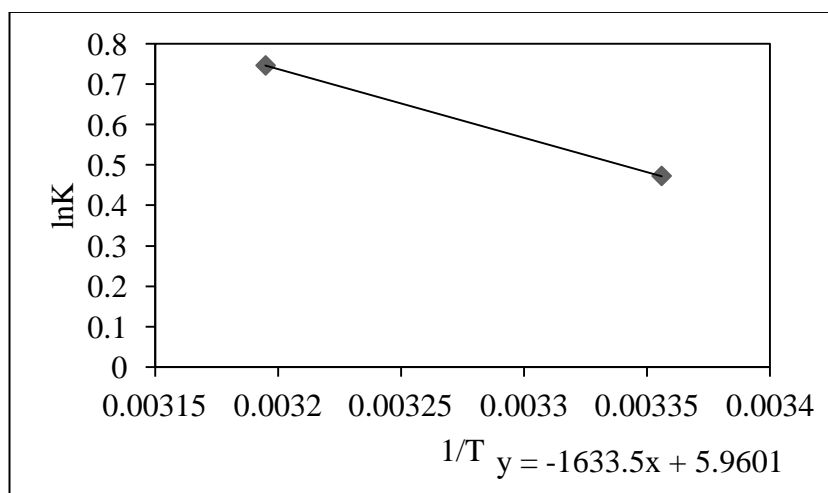


Figure 4.23. The plot of $\ln K$ versus $1/T$ for 5-benzyl-3-(*o*-bromophenyl)-2-thiohydantoin.

4.3.4. Determination of Racemisation at C-5 Barrier (S→R Conversion) for 5-Isobutyl-3-phenyl-2-thiohydantoin Enantiomers

5-Isobutyl-3-phenyl-2-thiohydantoin, was separated on Chiralpak IC column in hexane 95% + ethanol 5% mixture. **R** and **S** enantiomers were separated from each other via chiral HPLC. To calculate the ΔG^\ddagger energy barrier of **R** or **S** enantiomer, one of the enantiomers was selected. Due to non-axially chiral structure of 5-isobutyl-3-phenyl-2-thiohydantoin, **R** and **S** enantiomers signals were not differentiated in $^1\text{H-NMR}$. Therefore, the selected stereoisomers conformation was unknown. To simplify the calculations it was named as **S**. The **S** enantiomer was resolved and kept in ethanol and at 40°C the racemisation was observed via HPLC with time until equilibrium. Time versus $\ln\left(\frac{[\text{S}]_0 - [\text{S}]_{\text{eq}}}{[\text{S}] - [\text{S}]_{\text{eq}}}\right)$ was plotted (Figure 4.24). From the slope, k was found as $1 \times 10^{-4} \text{ s}^{-1}$. From HPLC chromatograms it was proved that there was racemisation for 5-isobutyl-3-phenyl-2-thiohydantoin in ethanol at 40°C (Figure 4.25). The ΔG^\ddagger energy barrier was found as; $\Delta G^\ddagger = 100.8 \text{ kJ/mole}$ for 40°C in ethanol from the Eyring Equation (2.10) by using reversible reaction kinetics.

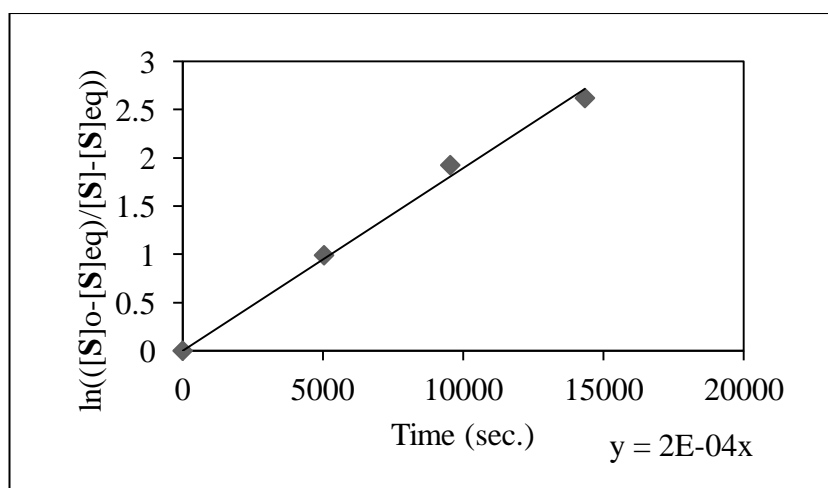


Figure 4.24. The plot of $\ln\left(\frac{[\text{S}]_0 - [\text{S}]_{\text{eq}}}{[\text{S}] - [\text{S}]_{\text{eq}}}\right)$ versus time at 313 K for 5-isobutyl-3-phenyl-2-thiohydantoin.

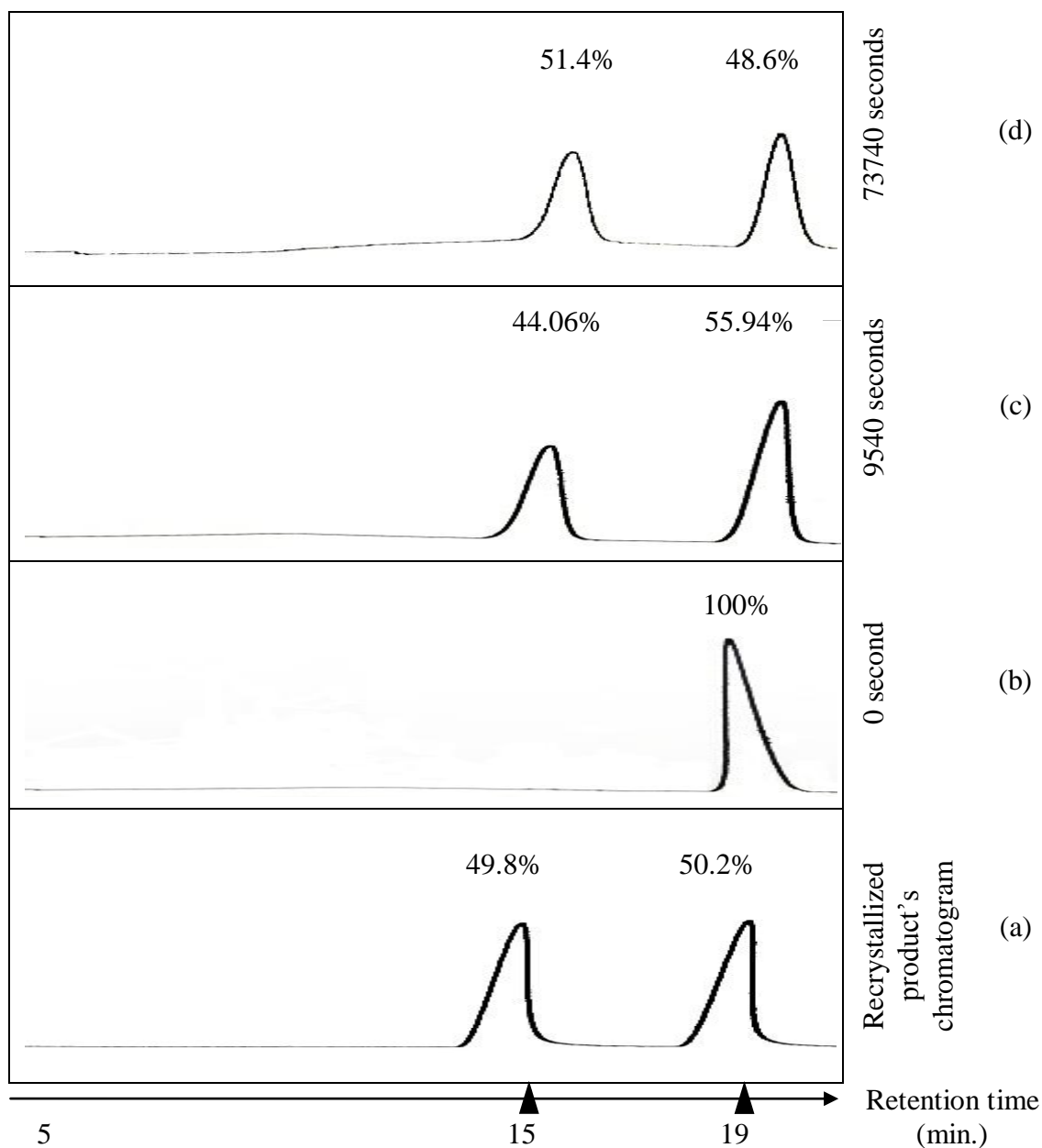


Figure 4.25. 5-Isobutyl-3-phenyl-2-thiohydantoin HPLC chromatograms (ChiralPak IC as the stationary phase, 95:5 Hex:EtOH as the eluent, flow rate : 0.8 ml/min, column temperature : 7°C) for: (a) the racemic recrystallised product, (b) the micropreparatively resolved second eluted enantiomer, (c-d) the thermal racemisation experiment; the conversion of the resolved enantiomer to its counterpart in **ethanol** with time at 313 K.

4.3.5. Determination of the Rotation around N3_(sp²)-C_(aryl) bond (RM→RP Conversion) and Racemisation at C-5 Barrier (RM⇌SM and RP⇌SP Conversion) for 5-Isobutyl-3-(*o*-tolyl)-2-thiohydantoin stereoisomers

5-Isobutyl-3-*o*-tolyl-2-thiohydantoin stereoisomers **SP**, **SM**, **RM** and **RP** were separated in Chiralpak IB column on hexane 95% and ethanol 5% mixture. ΔG^\ddagger energy barriers tried to be determined at 40°C in ethanol however both racemisation and rotation was observed. Therefore, the experiments have been done at 25°C ΔG^\ddagger and barriers were calculated for 4 stereoisomers.

After separation of **RM**, **SM**, **RP** and **SP**, each stereoisomer was dissolved in ethanol at 25°C. For all stereoisomers only racemisation was observed with time until equilibrium in ethanol at 25°C. The reaction kinetics were calculated with reversible reaction kinetics due to **SM**⇌**RM** and **RP**⇌**SP**. Time versus $\ln ([\text{SM}] - [\text{SM}]_{\text{eq}} / [\text{SM}]_0 - [\text{SM}]_{\text{eq}})$, $\ln ([\text{SP}] - [\text{SP}]_{\text{eq}} / [\text{SP}]_0 - [\text{SP}]_{\text{eq}})$, $\ln ([\text{RM}] - [\text{RM}]_{\text{eq}} / [\text{RM}]_0 - [\text{RM}]_{\text{eq}})$, $\ln ([\text{RP}] - [\text{RP}]_{\text{eq}} / [\text{RP}]_0 - [\text{RP}]_{\text{eq}})$, was plotted for **SM**, **SP**, **RM** and **RP** respectively (Figure 4.26). From the slopes, k_f and k_r values were determined (Table 4.4). With k_f and k_r values for each stereoisomer, the racemisation ΔG^\ddagger energy barriers were calculated (Table 4.4). The corresponding HPLC chromatograms have been shown for **SM** to **RM** (Figure 4.27), **RM** to **SM** (Figure 4.28), **SP** to **RP** (Figure 4.29) and **RP** to **SP** (Figure 4.30) were determined.

When 5-benzyl-3-(*o*-tolyl)-2-thiohydantoin and 5-isobutyl-3-(*o*-tolyl)-2-thiohydantoin at 25°C in ethanol reactions were compared, it was observed that, for 5-benzyl-3-(*o*-tolyl)-2-thiohydantoin, **SM** and **RM** gave racemisation however **SP** and **RP** gave rotation. For 5-isobutyl-3-(*o*-tolyl)-2-thiohydantoin however, at 25°C in ethanol, all 4 stereoisomers gave racemisation. At 40 °C for both compounds **2** and **5**, rotation and racemisation was observed together.

4.3.5.1. Solvent Effect on the Interconversions Between the Stereoisomers of 5-Isobutyl-3-(*o*-tolyl)-2-thiohydantoin. The thermal interconversion experiment was done in toluene. **RM** stereoisomer was separated and kept in toluene in order to observe the solvent effect on racemisation. **RM** rotated to **RP** in toluene at 40°C (Figure 4.31). No racemisation was detected in this experiment. However, at 40°C in ethanol, both racemisation and rotation

had been observed. For rotation of **RM** to **RP**, time versus $\ln ([\mathbf{RM}] - [\mathbf{RM}]_{\text{eq}} / [\mathbf{RM}]_0 - [\mathbf{RM}]_{\text{eq}})$ was plotted for **RM** (Figure 4.32). From the slope, k_f and k_r were determined to calculate the rotational ΔG^\ddagger energy barrier from Eyring Equation (2.10). All calculated ΔG^\ddagger and k values for 5-isobutyl-3-*o*-tolyl-2-thiohydantoin are given in Table 4.4.

For 5- isobutyl-3-*o*-tolyl-2-thiohydantoin at 25°C in ethanol, only racemisation was observed. At 40°C both racemisation and rotation were observed in ethanol. In toluene at 40°C, only rotation was observed.

Table 4.4. Calculated ΔG^\ddagger (kJ/mole) and k values for 5-isobutyl-3-*o*-tolyl-2-thiohydantoin.

| Solvent | T (°C) | Stereoisomer conversion | ΔG^\ddagger_f (kJ/mole) | ΔG^\ddagger_r (kJ/mole) | k_f (s ⁻¹) | k_r (s ⁻¹) |
|---------|--------|-------------------------|---------------------------------|---------------------------------|--------------------------|--------------------------|
| Ethanol | 25 | RP to SP | 99.4±1.8 | 100.2±1.8 | 2.30 x 10 ⁻⁵ | 1.70 x 10 ⁻⁵ |
| Ethanol | 25 | SP to RP | 102.0±1.8 | 101.1±1.8 | 8.25 x 10 ⁻⁶ | 1.18 x 10 ⁻⁶ |
| Ethanol | 25 | RM to SM | 102.0±1.8 | 101.1±1.8 | 8.28 x 10 ⁻⁶ | 1.17 x 10 ⁻⁶ |
| Ethanol | 25 | SM to RM | 100.5±1.8 | 100.6±1.8 | 1.53 x 10 ⁻⁵ | 1.47 x 10 ⁻⁵ |
| Toluene | 40 | RM to RP | 103.8±1.8 | 103.2±1.8 | 3.13 x 10 ⁻⁵ | 3.87 x 10 ⁻⁵ |

4.3.6 Determination of the Rotation around N3(sp²)-C(aryl) bond (SP→SM Conversion) and Racemisation at C-5 Barrier (RM⇌SM and RP⇌SP Conversion) for 5-Isobutyl-3-(*o*-bromophenyl)-2-thiohydantoin stereoisomers

5-Isobutyl-3-(*o*-bromophenyl)-2-thiohydantoin stereoisomers were separated on Chiralpak IA column in hexane 95% and ethanol 5% mixture. **SP**, **RP** and **RM** stereoisomers were successfully separated from each other however for **SM** the separation could not be done due to its low concentration. **SP**, **RP** and **RM** have been dissolved in ethanol at 40 °C in order to observe the type of conversion and to calculate k and ΔG^\ddagger energy barriers. For these 3 stereoisomers, there was racemisation in ethanol at 40°C.

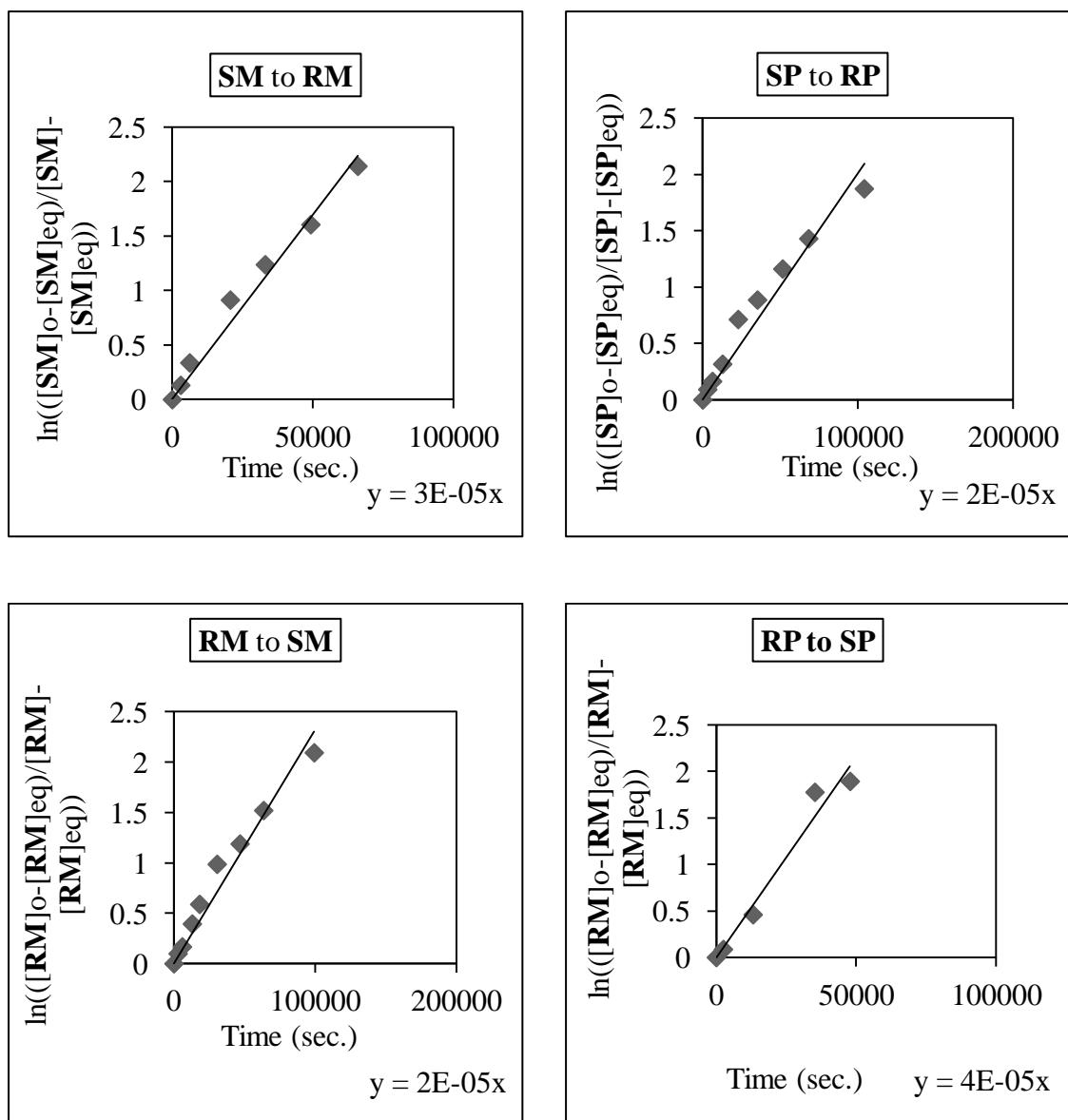


Figure 4.26. The plot of $\ln\left(\frac{[\text{SM}]_o - [\text{SM}]_{\text{eq}}}{[\text{SM}] - [\text{SM}]_{\text{eq}}}\right)$, $\ln\left(\frac{[\text{SP}]_o - [\text{SP}]_{\text{eq}}}{[\text{SP}] - [\text{SP}]_{\text{eq}}}\right)$, $\ln\left(\frac{[\text{RM}]_o - [\text{RM}]_{\text{eq}}}{[\text{RM}] - [\text{RM}]_{\text{eq}}}\right)$, $\ln\left(\frac{[\text{RP}]_o - [\text{RP}]_{\text{eq}}}{[\text{RP}] - [\text{RP}]_{\text{eq}}}\right)$, versus time at 298 K for 5-isobutyl-3-(*o*-tolyl)-2-thiohydantoin.

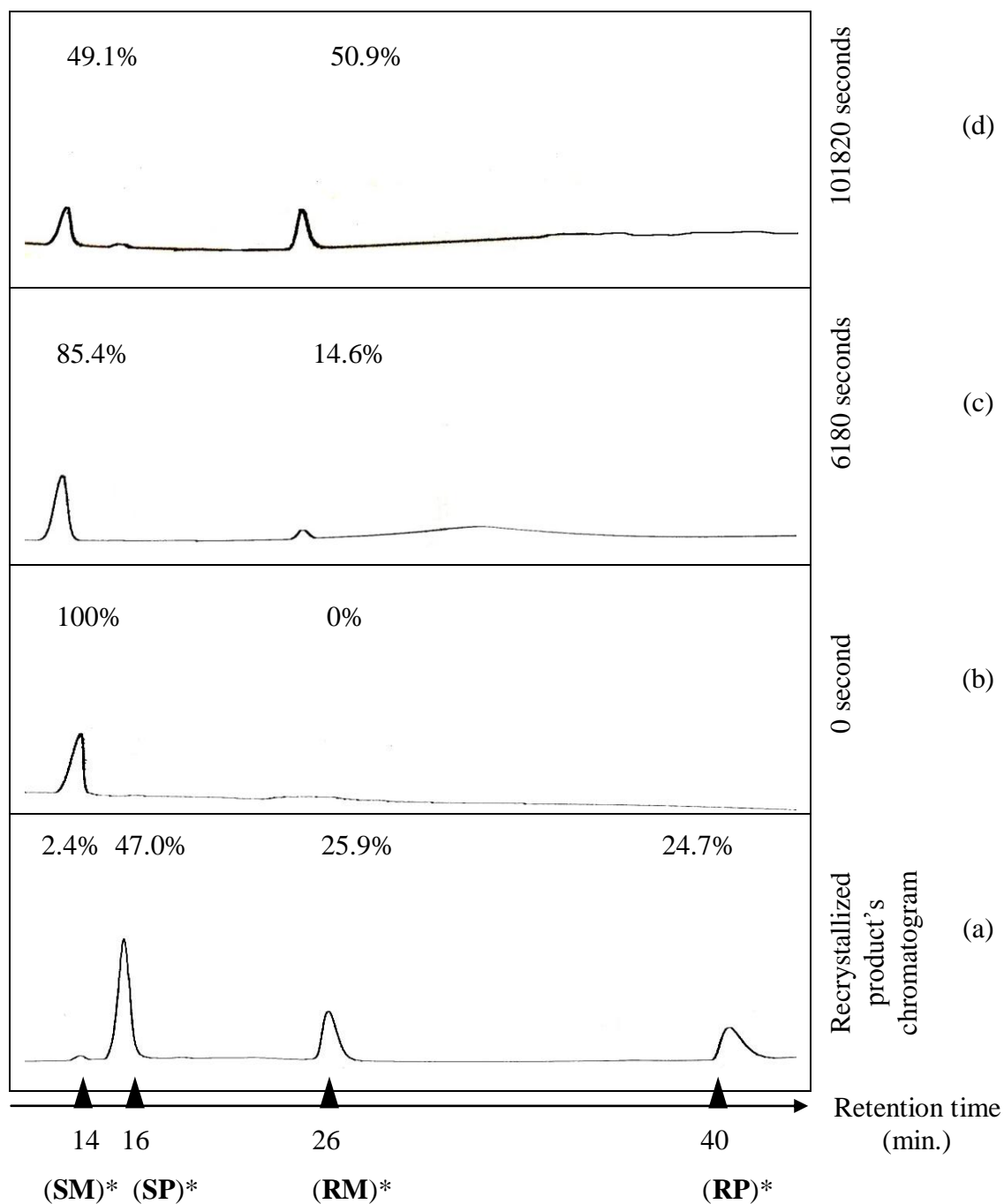


Figure 4.27. 5-Isobutyl-3-(*o*-tolyl)-2-thiohydantoin HPLC chromatograms (ChiralPak IB as the stationary phase, 95:5 Hex:EtOH as the eluent, flow rate : 0.8 ml/min, column temperature : 7°C) for: (a) of the recrystallized product which shows the presence of four isomers, (b) the micropreparatively resolved **SM**, (c-d) conversion of **SM** to **RM** with time in **ethanol** at 298 K. (*) The assignments have been done with comparison by the $^1\text{H-NMR}$ spectrum.

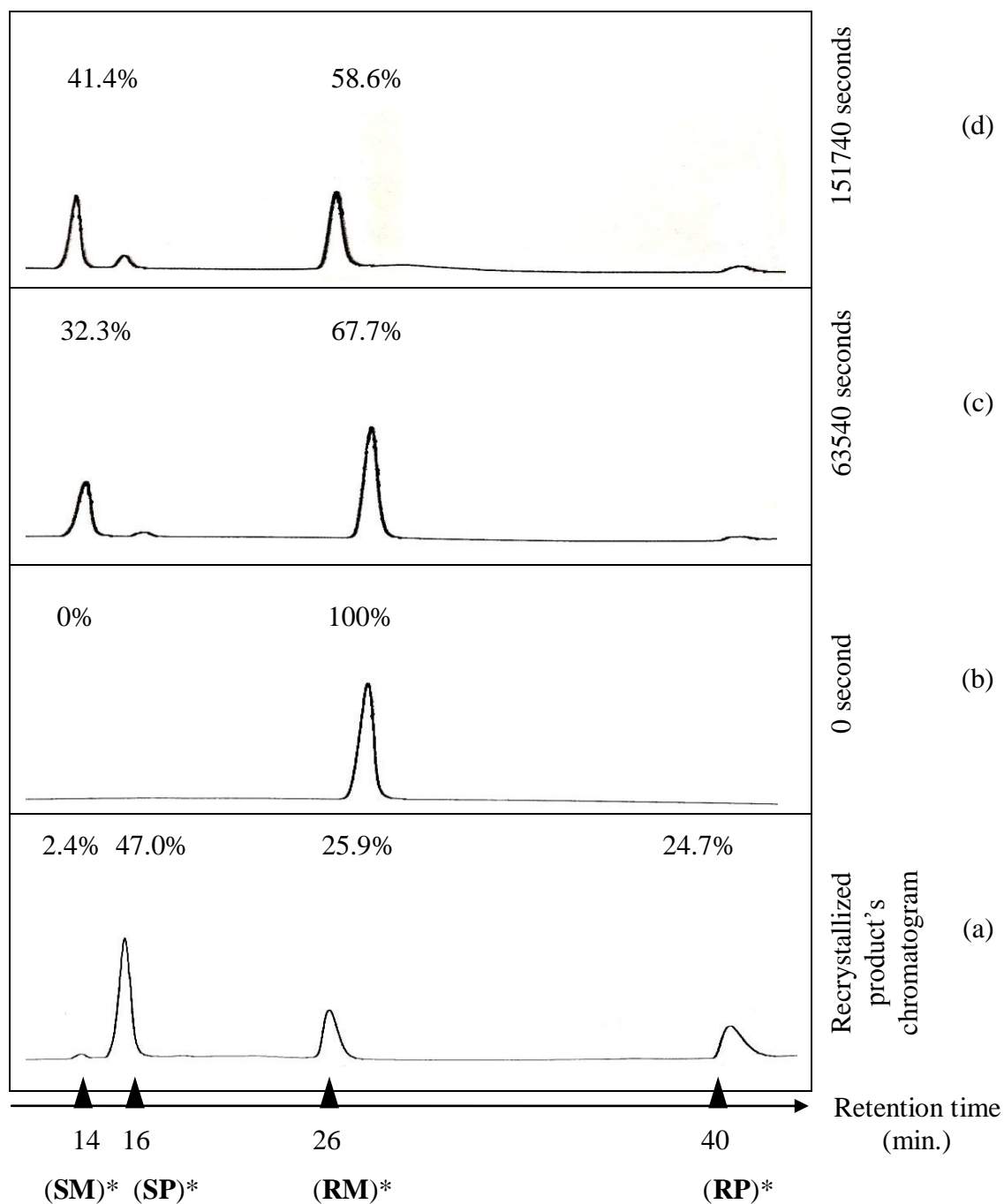


Figure 4.28. 5-Isobutyl-3-(*o*-tolyl)-2-thiohydantoin HPLC chromatograms (ChiralPak IB as the stationary phase, 95:5 Hex:EtOH as the eluent, flow rate: 0.8 ml/min, column temperature : 7°C) for: (a) of the recrystallized product which shows the presence of four isomers, (b) the micropreparatively resolved **RM**, (c-d) conversion of **RM** to **SM** with time in **ethanol** at 298 K. (*) The assignments have been done with comparison by the ¹H-NMR spectrum.

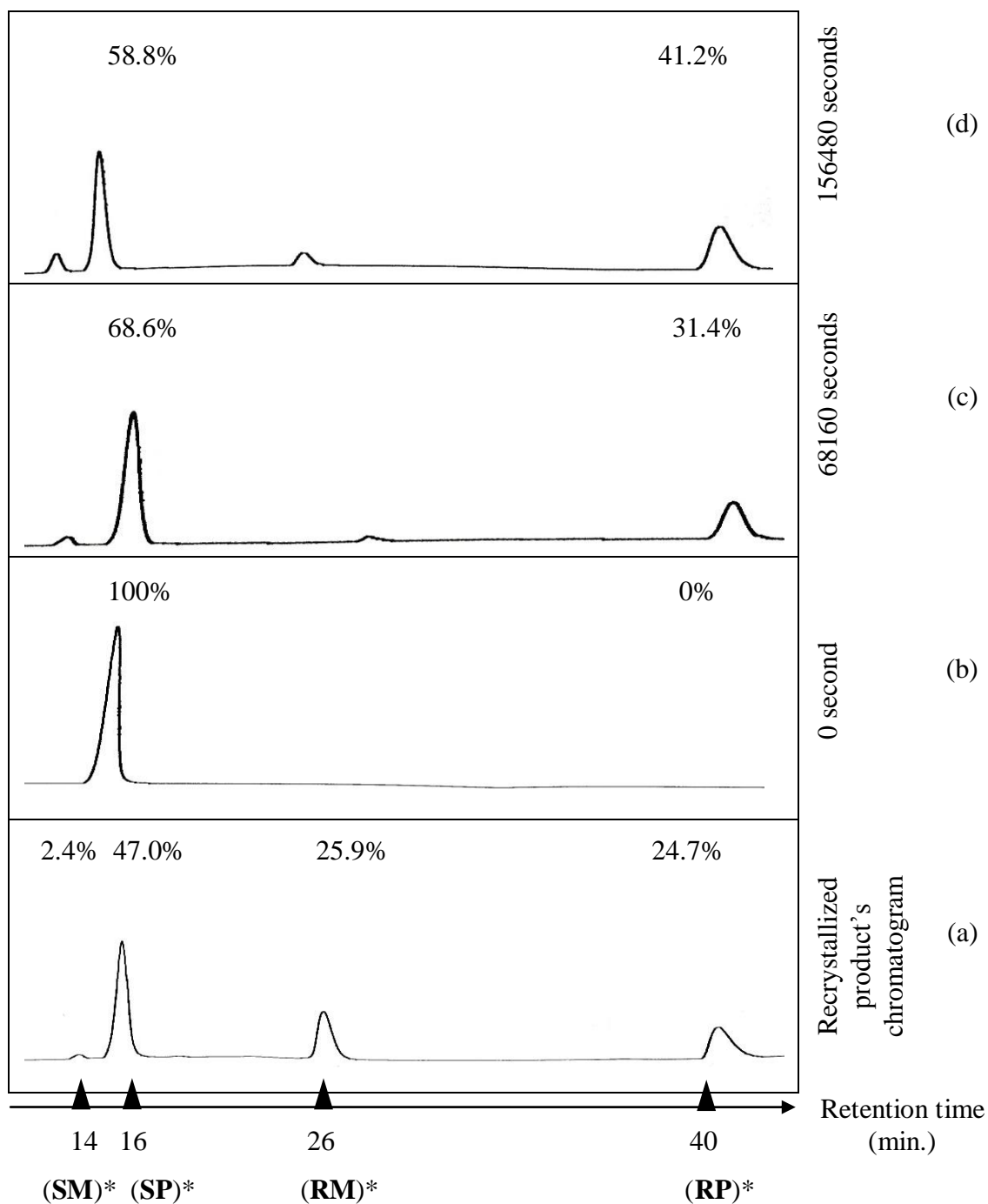


Figure 4.29. 5-Isobutyl-3-(*o*-tolyl)-2-thiohydantoin HPLC chromatograms (ChiralPak IB as the stationary phase, 95:5 Hex:EtOH as the eluent, flow rate : 0.8 ml/min, column temperature : 7°C) for: (a) of the recrystallized product which shows the presence of four isomers, (b) the micropreparatively resolved **SP**, (c-d) conversion of **SP** to **RP** with time in **ethanol** at 298 K. (*) The assignments have been done with comparison by the $^1\text{H-NMR}$ spectrum.

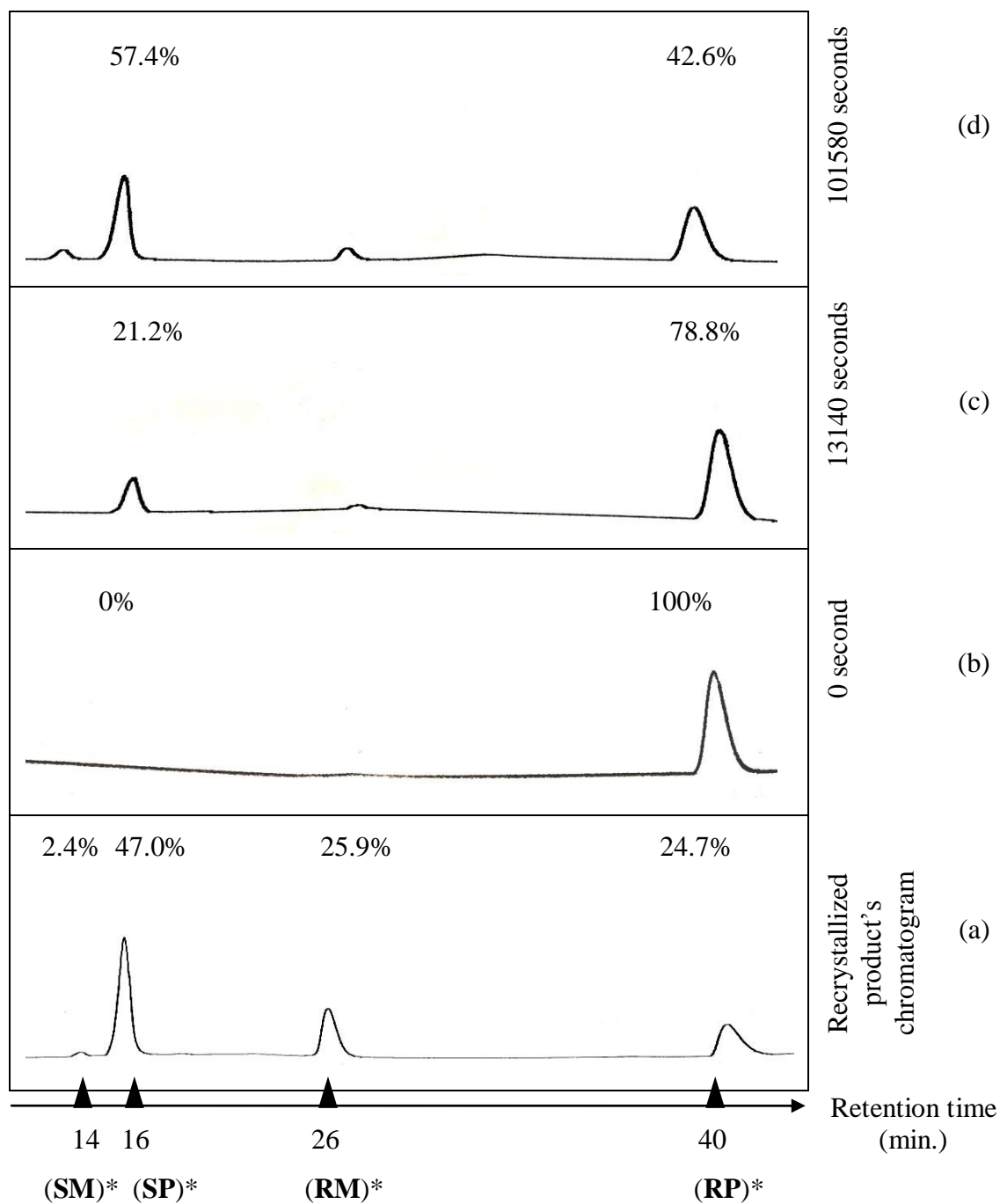


Figure 4.30. 5-Isobutyl-3-(*o*-tolyl)-2-thiohydantoin HPLC chromatograms (ChiralPak IB as the stationary phase, 95:5 Hex:EtOH as the eluent, flow rate : 0.8 ml/min, column temperature : 7°C) for: (a) of the recrystallized product which shows the presence of four isomers, (b) the micropreparatively resolved **RP**, (c-d) conversion of **RP** to **SP** with time in **ethanol** at 298 K. (*) The assignments have been done with comparison by the $^1\text{H-NMR}$ spectrum.

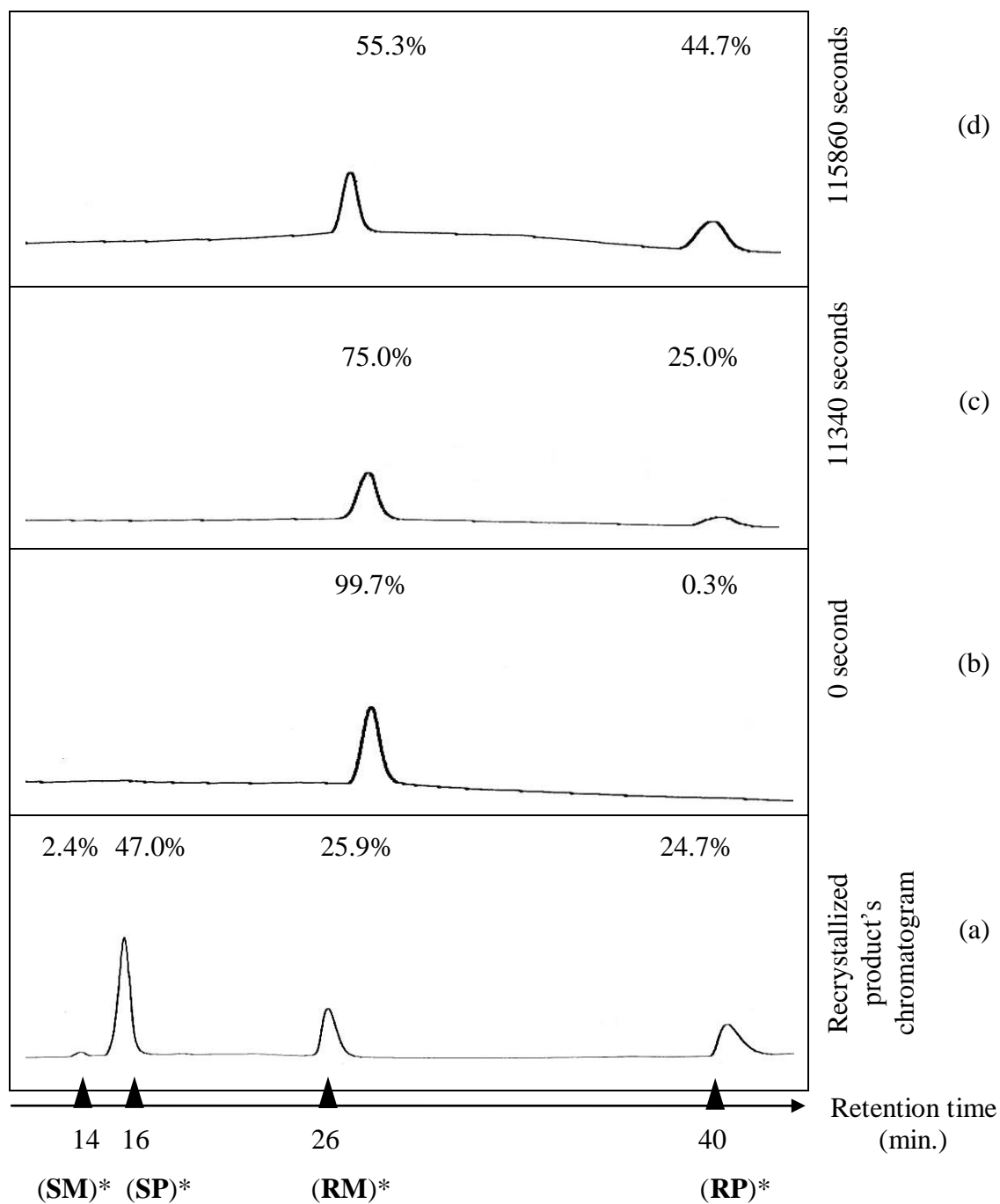


Figure 4.31. 5-Isobutyl-3-(*o*-tolyl)-2-thiohydantoin HPLC chromatograms (ChiralPak IB as the stationary phase, 95:5 Hex:EtOH as the eluent, flow rate : 0.8 ml/min, column temperature : 7°C) for: (a) of the recrystallized product which shows the presence of four isomers, (b) the micropreparatively resolved **RM**, (c-d) conversion of **RM** to **RP** with time in **toluene** at 313 K. (*) The assignments have been done with comparison by the $^1\text{H-NMR}$ spectrum.

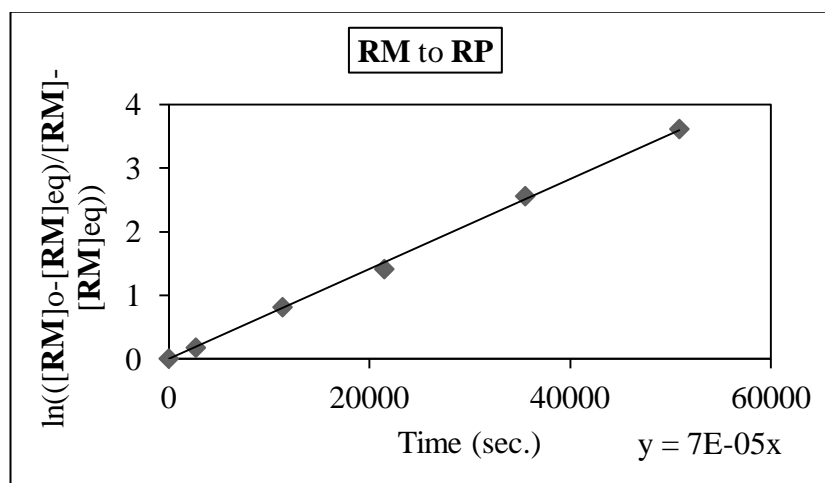


Figure 4.32. The plot of $\ln\left(\frac{[RM]_0 - [RM]_{eq}}{[RM] - [RM]_{eq}}\right)$ versus time at 313 K for 5-isobutyl-3-(*o*-tolyl)-2-thiohydantoin.

Time versus $\ln\left(\frac{[RP] - [RP]_{eq}}{[RP]_0 - [RP]_{eq}}\right)$, $\ln\left(\frac{[SP] - [SP]_{eq}}{[SP]_0 - [SP]_{eq}}\right)$, $\ln\left(\frac{[RM] - [RM]_{eq}}{[RM]_0 - [RM]_{eq}}\right)$ was plotted to calculate k_f and k_r for **RP**, **SP** and **RM** respectively (Figure 4.33). Due to $RP \rightleftharpoons SP$, $SP \rightleftharpoons RP$ and $RM \rightleftharpoons SM$ the ΔG^\ddagger energy barriers were calculated from reversible reaction kinetics using Eyring Equation (2.10). Change of concentration at 40°C in ethanol for **RP** to **SP** (Figure 4.34), **SP** to **RP** (Figure 4.35) and **RM** to **SM** (Figure 4.36) were measured.

4.3.6.1. Solvent Effect on the Interconversions Between the Stereoisomers of 5-Isobutyl-3-(*o*-bromophenyl)-2-thiohydantoin. **SP** stereoisomer was separated and it kept in toluene to determine the ΔG^\ddagger energy barrier using HPLC at a constant temperature. It rotated to **SM** at 110°C in toluene. The rotation of **SP** to **SM** at 110°C in toluene and HPLC chromatograms are given in Figure 4.37. For **SP**, time versus $\ln\left(\frac{[SP] - [SP]_{eq}}{[SP]_0 - [SP]_{eq}}\right)$ was plotted for 110°C (Figure 4.38). From the slope, k_f and k_r were determined and for rotation, the reversible reaction kinetics were used. From the k_f and k_r the rotational ΔG^\ddagger was calculated by using Eyring Equation (2.10) In toluene, no racemisation was observed even the temperature is 110 °C. However, at 40°C in ethanol, only racemisation was observed. All calculated ΔG^\ddagger and k values for 5-isobutyl-3-(*o*-bromophenyl)-2-thiohydantoin are given in Table 4.5.

Table 4.5. Calculated ΔG^\ddagger (kJ/mole) and k values for 5-isobutyl-3-(*o*-bromophenyl)-2-thiohydantoin.

| Solvent | T (°C) | Stereoisomer conversion | ΔG_f^\ddagger (kJ/mole) | ΔG_r^\ddagger (kJ/mole) | k_f (s ⁻¹) | k_r (s ⁻¹) |
|---------|--------|-------------------------|---------------------------------|---------------------------------|--------------------------|--------------------------|
| Ethanol | 40 | RP to SP | 102.1±0.1 | 103.1±0.1 | 5.97 x 10 ⁻⁵ | 4.04 x 10 ⁻⁵ |
| Ethanol | 40 | SP to RP | 103.2±0.1 | 102.1±0.1 | 3.98 x 10 ⁻⁵ | 6.02 x 10 ⁻⁵ |
| Ethanol | 40 | RM to SM | 103.0±0.1 | 102.2±0.1 | 4.27 x 10 ⁻⁵ | 5.73 x 10 ⁻⁵ |
| Toluene | 110 | SP to SM | 118.4±0.1 | 118.0±0.1 | 5.65 x 10 ⁻⁴ | 6.35 x 10 ⁻⁴ |

4.4. Deuteration of 5-Benzyl-3-aryl-2-thiohydantoins and 5-Isobutyl-3-aryl 2-thiohydantoins

In order to investigate the kinetics of rotation and racemisation mechanism of 5-benzyl-3-(*o*-tolyl)-2-thiohydantoin derivative, both HPLC and NMR was used during the study. The enolisation was observed from the deuterium exchange at C-5 of compound **2** in the presence of deuterio-methanol by ¹H-NMR. Deuterium-exchange with C-5 hydrogen showed that, with the enolisation of the synthesized derivative, the racemisation can be observed (Figure 2.5).

For 5-benzyl-3-(*o*-tolyl)-2-thiohydantoin derivative, the exchange of deuterium was calculated with time until the C-5 hydrogen signal completely disappeared in the spectrum (Figure 4.40). The CH₃ signals are unaffected by hydrogen/deuterium exchange whereas the intensity of the NMR signal of C-5 hydrogen decreased with hydrogen/deuterium exchange. Since the deuteration rate was equal to racemisation rate from the enolisation mechanism, the ln(C-5/CH₃) versus time was plotted to calculate the racemisation energy barrier of 5-benzyl-3-(*o*-tolyl)-2-thiohydantoin (Figure 4.39). From the Eyring equation, ΔG^\ddagger was found as 97.1 kJ/mole.

For the compounds **2**, **3**, **4** and **6** hydrogen/deuterium exchange was observed in CD₃OD by NMR (Figures 4.42, 4.43, 4.44 and 4.45) but not for **5** (Figure 4.41).

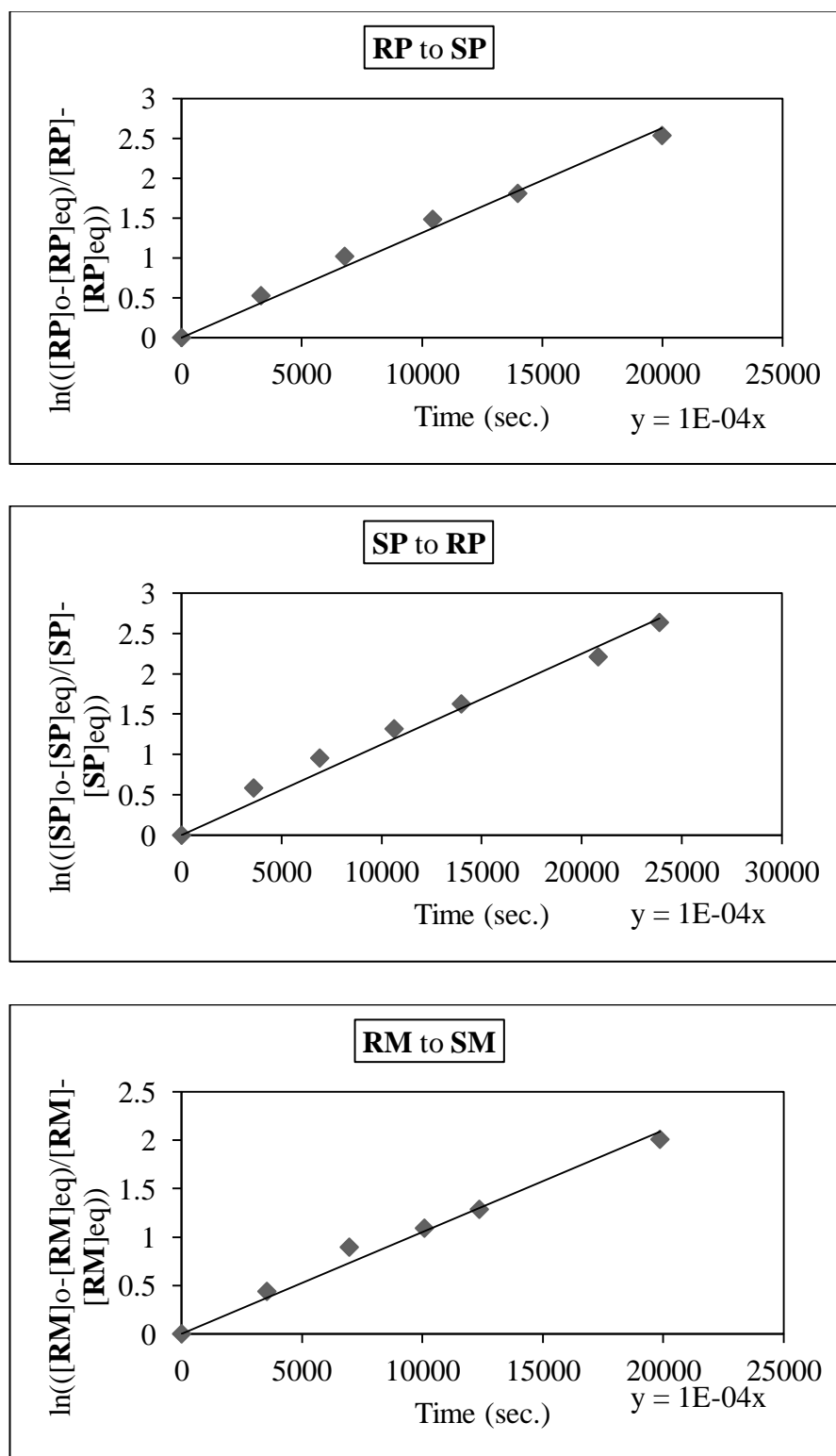


Figure 4.33. The plot of $\ln\left(\frac{[\text{RP}]_o - [\text{RP}]_{\text{eq}}}{[\text{RP}]_{\text{eq}}}\right)$, $\ln\left(\frac{[\text{SP}]_o - [\text{SP}]_{\text{eq}}}{[\text{SP}]_{\text{eq}}}\right)$, $\ln\left(\frac{[\text{RM}]_o - [\text{RM}]_{\text{eq}}}{[\text{RM}]_{\text{eq}}}\right)$, versus time at 313 K for 5-isobutyl-3-(*o*-bromophenyl)-2-thiohydantoin.

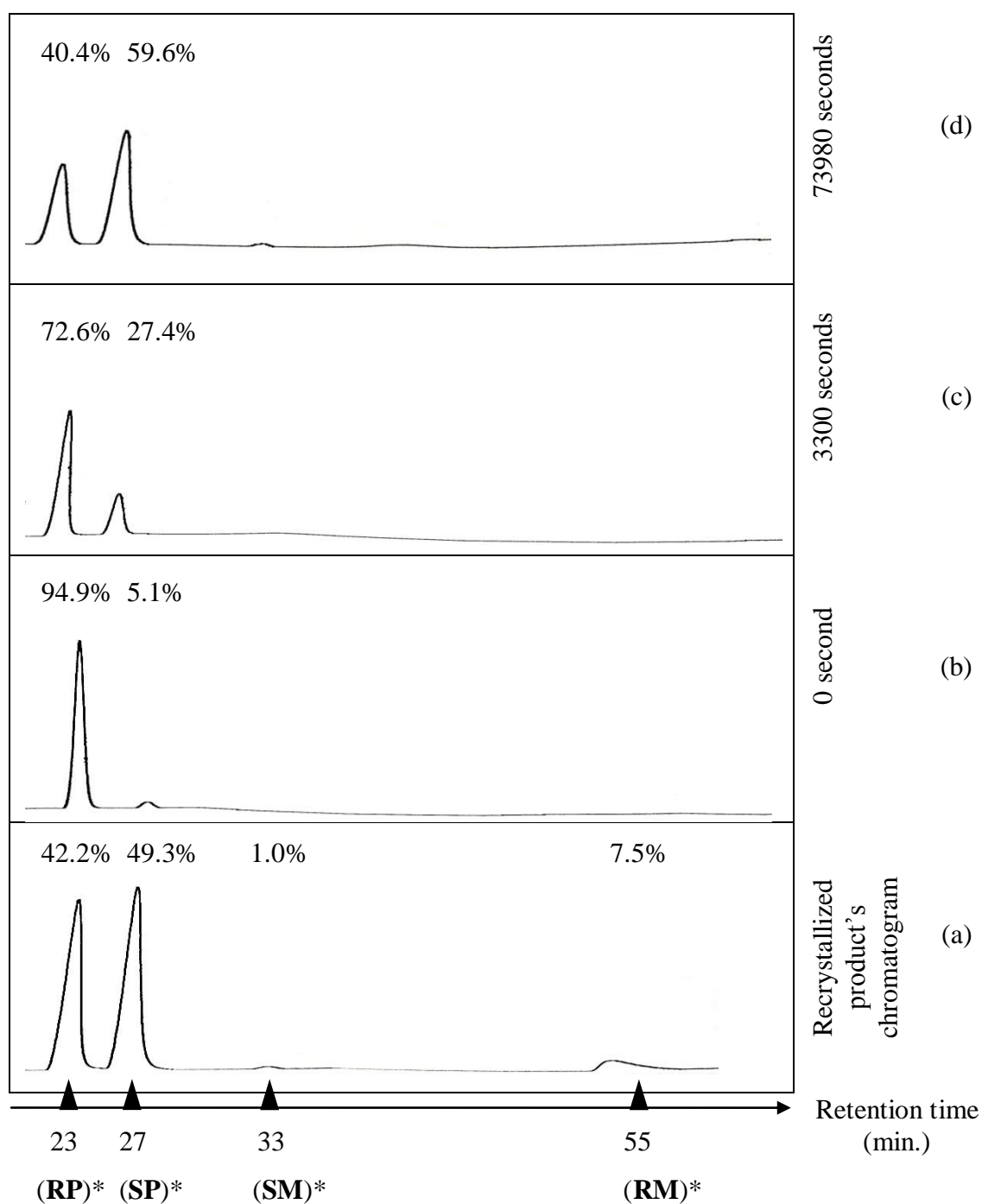


Figure 4.34. 5-Isobutyl-3-(*o*-bromophenyl)-2-thiohydantoin HPLC chromatograms (ChiralPak IA as the stationary phase, 95:5 Hex:EtOH as the eluent, flow rate : 0.8 ml/min, column temperature : 7°C) for: (a) of the recrystallized product which shows the presence of four isomers, (b) the micropreparatively resolved **RP**, (c-d) conversion of **RP** to **SP** with time in **ethanol** at 313 K. (*) The assignments have been done with comparison by the ¹H-NMR spectrum.

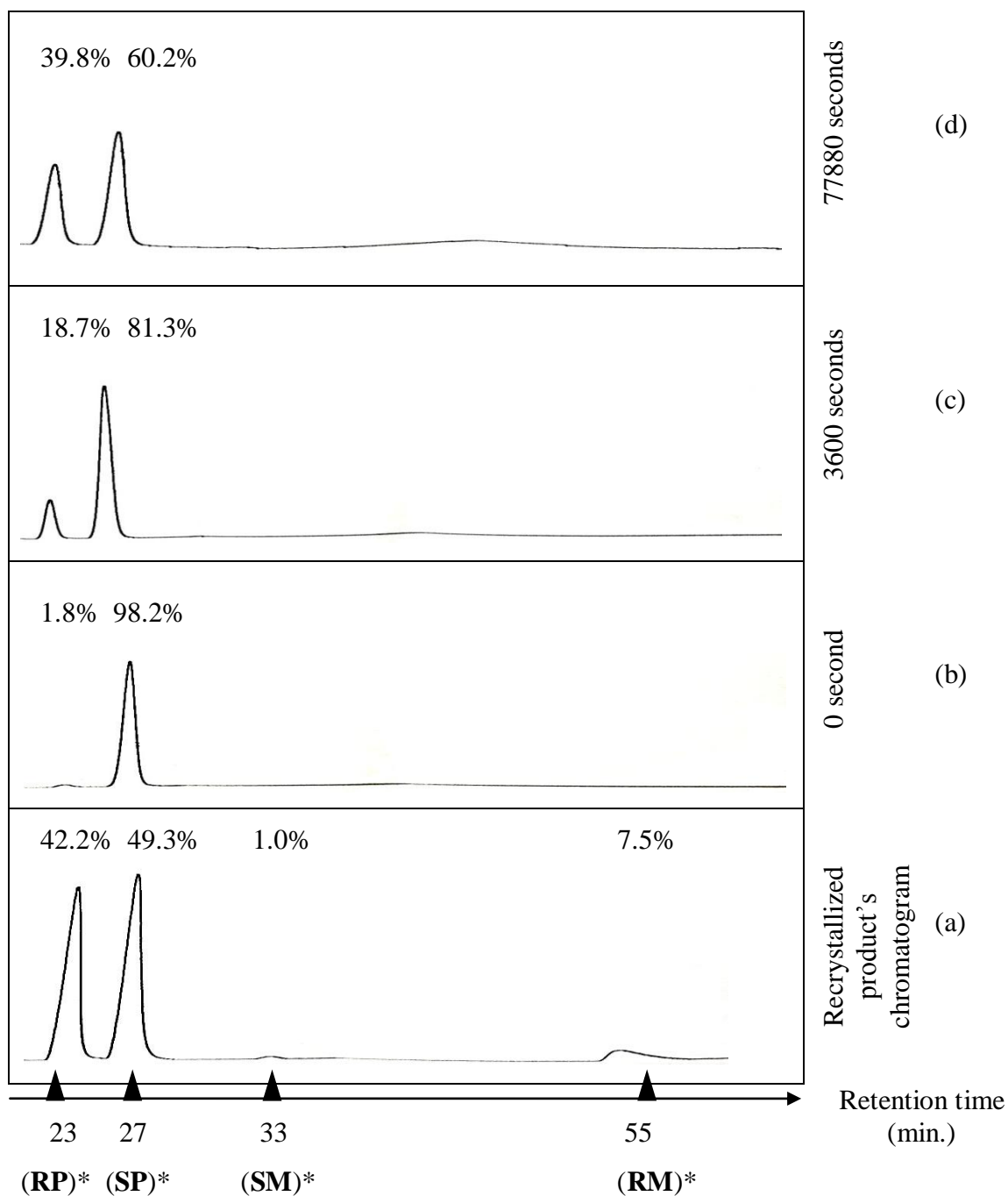


Figure 4.35. 5-Isobutyl-3-(*o*-bromophenyl)-2-thiohydantoin HPLC chromatograms (ChiralPak IA as the stationary phase, 95:5 Hex:EtOH as the eluent, flow rate : 0.8 ml/min, column temperature : 7°C) for: (a) of the recrystallized product which shows the presence of four isomers, (b) the micropreparatively resolved **SP**, (c-d) conversion of **SP** to **RP** with time in **ethanol** at 313 K. (*) The assignments have been done with comparison by the ^1H -NMR spectrum.

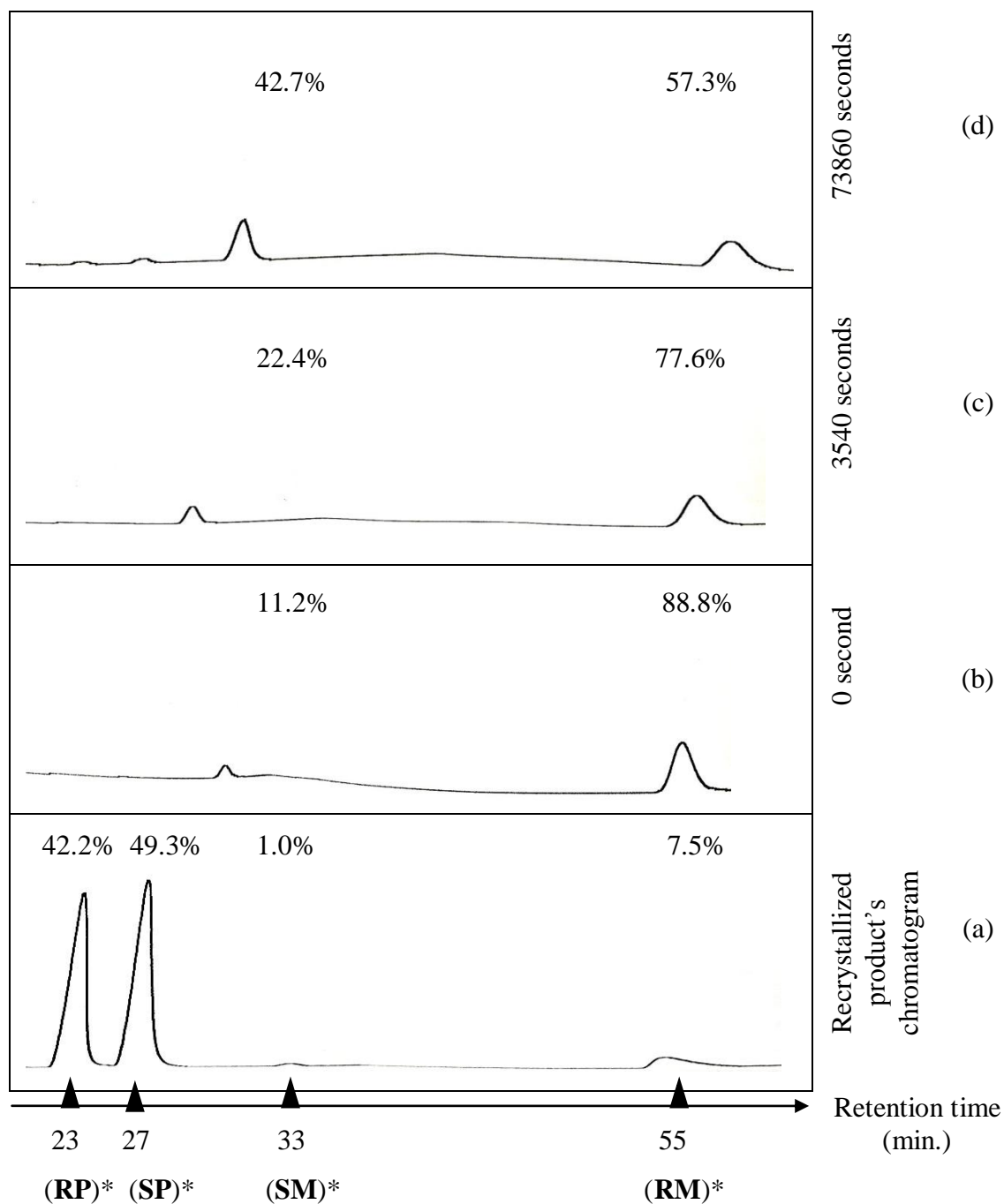


Figure 4.36. 5-Isobutyl-3-(*o*-bromophenyl)-2-thiohydantoin HPLC chromatograms (ChiralPak IA as the stationary phase, 95:5 Hex:EtOH as the eluent, flow rate : 0.8 ml/min, column temperature : 7°C) for: (a) of the recrystallized product which shows the presence of four isomers, (b) the micropreparatively resolved **RM**, (c-d) conversion of **RM** to **SM** with time in **ethanol** at 313 K. (*) The assignments have been done with comparison by the $^1\text{H-NMR}$ spectrum.

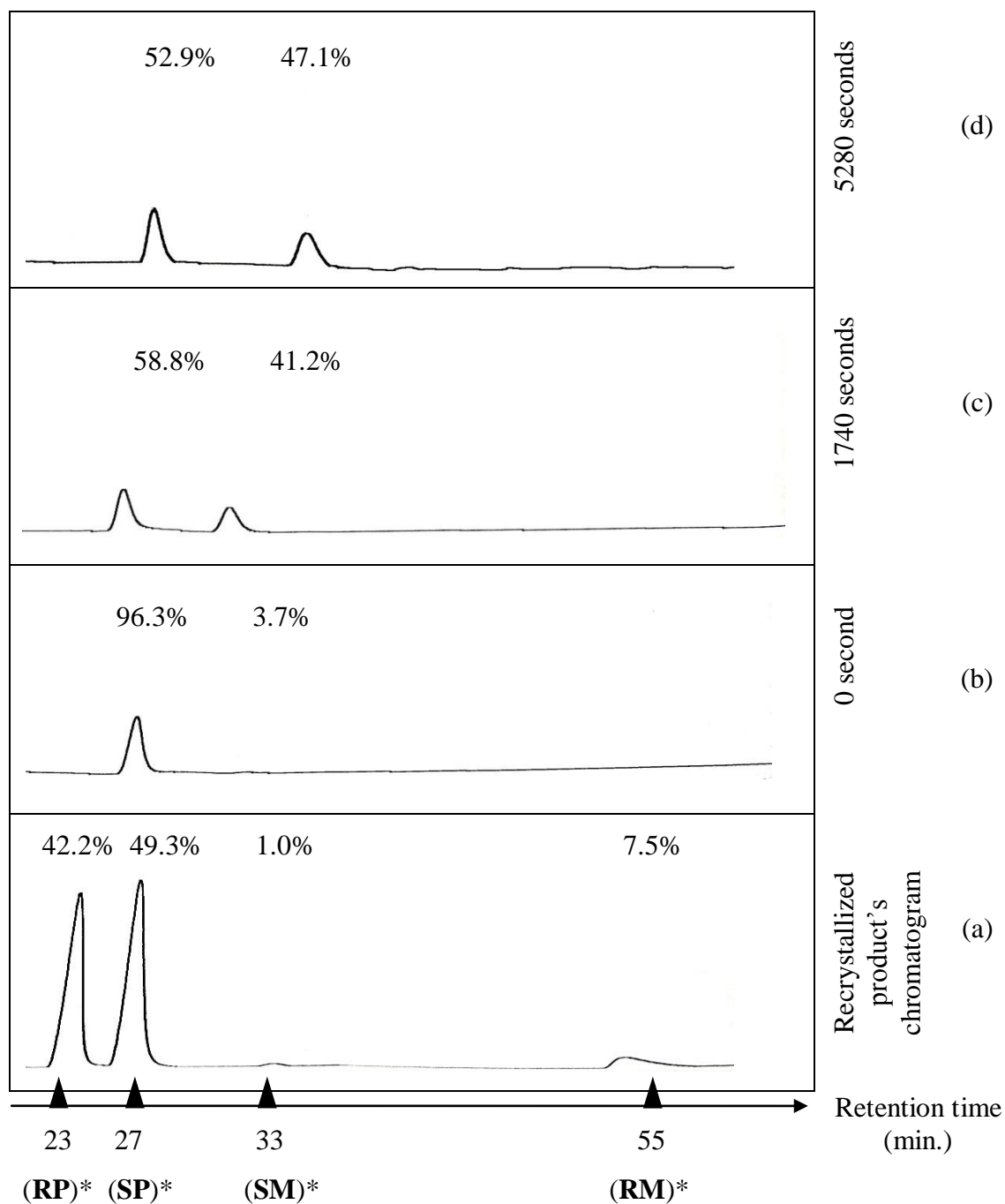


Figure 4.37. 5-Isobutyl-3-(*o*-bromophenyl)-2-thiohydantoin HPLC chromatograms (ChiralPak IA as the stationary phase, 95:5 Hex:EtOH as the eluent, flow rate : 0.8 ml/min, column temperature : 7°C) for: (a) of the recrystallized product which shows the presence of four isomers, (b) the micropreparatively resolved **SP**, (c-d) conversion of **SP** to **SM** with time in **toluene** at 383 K. (*) The assignments have been done with comparison by the ^1H -NMR spectrum.

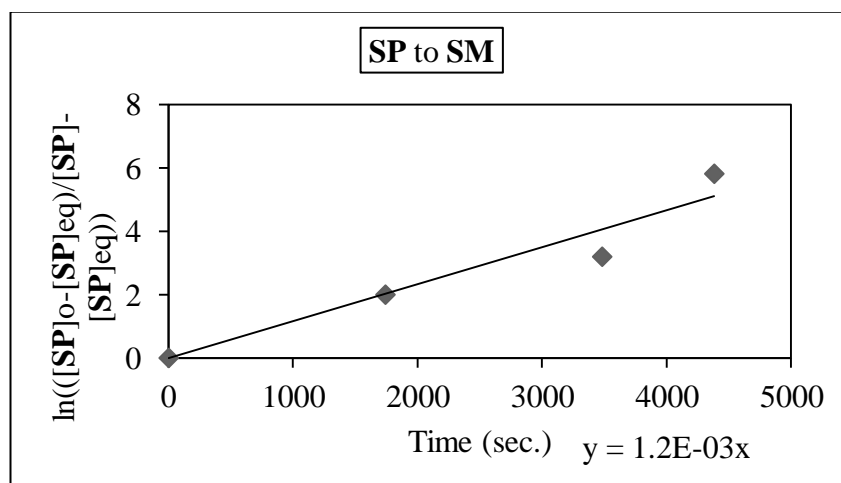


Figure 4.38. The plot of $\ln\left(\frac{[\text{SP}]_0 - [\text{SP}]_{\text{eq}}}{[\text{SP}]_{\text{eq}}}\right)$ versus time at 383 K for 5-isobutyl-3-(*o*-bromophenyl)-2-thiohydantoin.

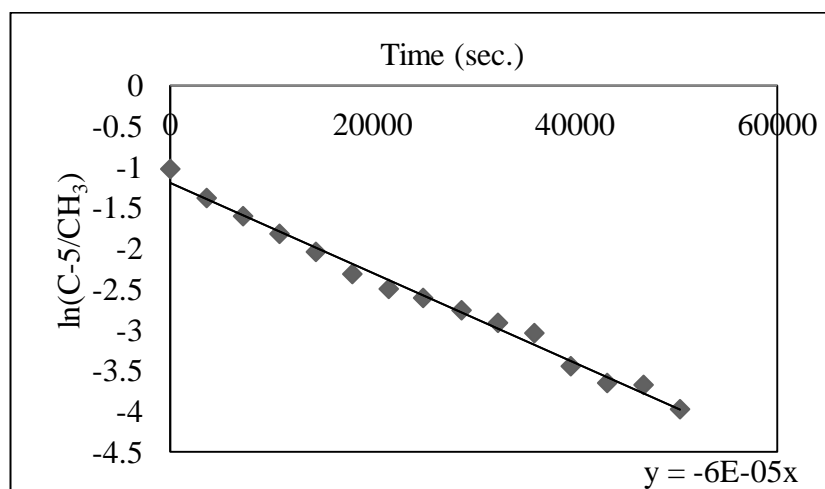


Figure 4.39. $\ln(C-5/CH_3)$ versus time graphic for calculation of racemisation barrier of 5-benzyl-3-(*o*-tolyl)-2-thiohydantoin by $^1\text{H-NMR}$.

4.5. Separation Factors (α) for the Synthesized Derivatives

Separation factor (α) for the synthesized derivatives determined from Equation (2.4) where V_0 equals to 2.9 and calculations are given in Table 4.6.

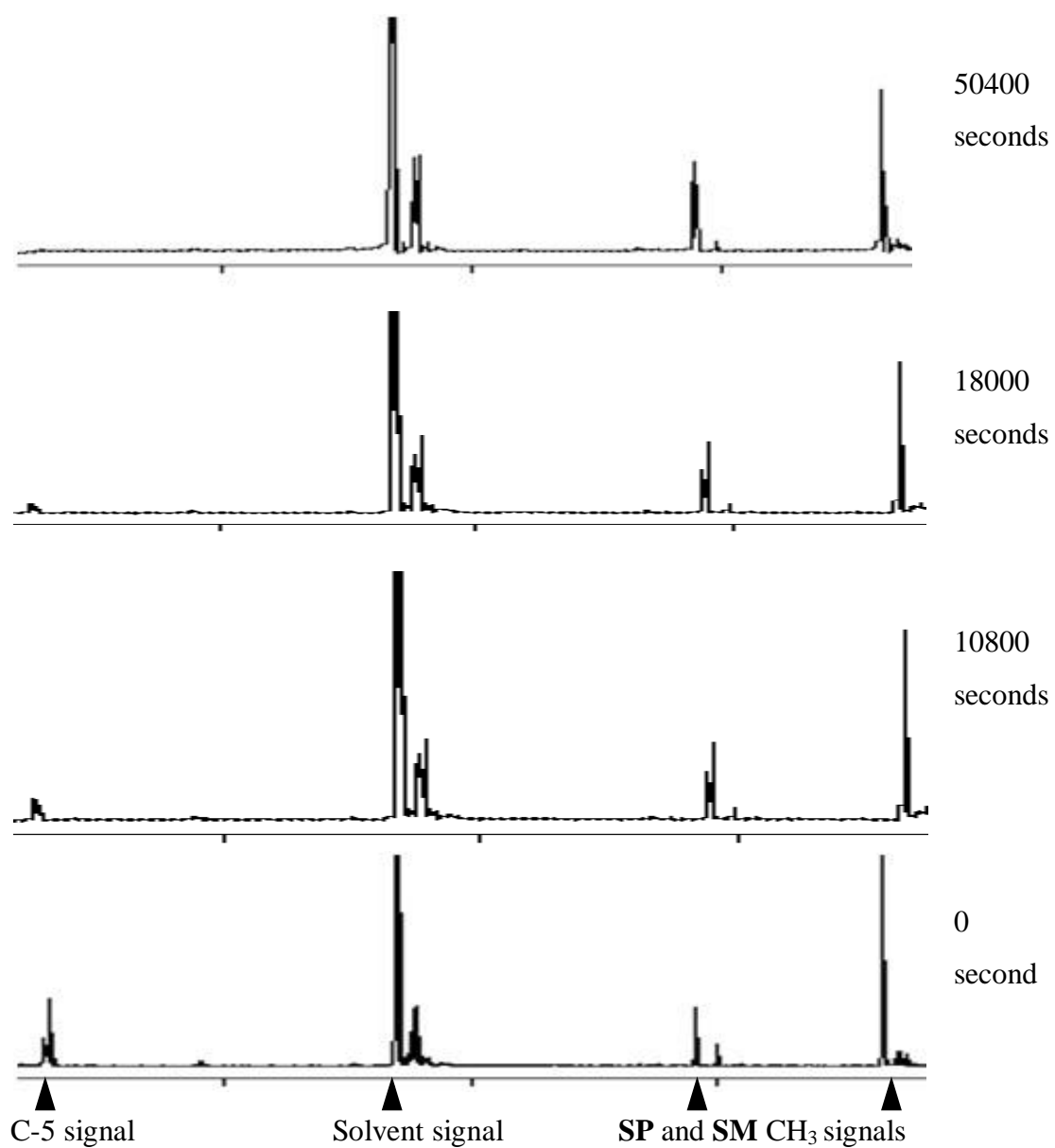


Figure 4.40. Exchange of deuterium with hydrogen atom at C-5 of the 5-benzyl-3-(*o*-tolyl)-2-thiohydantoin in time by $^1\text{H-NMR}$.

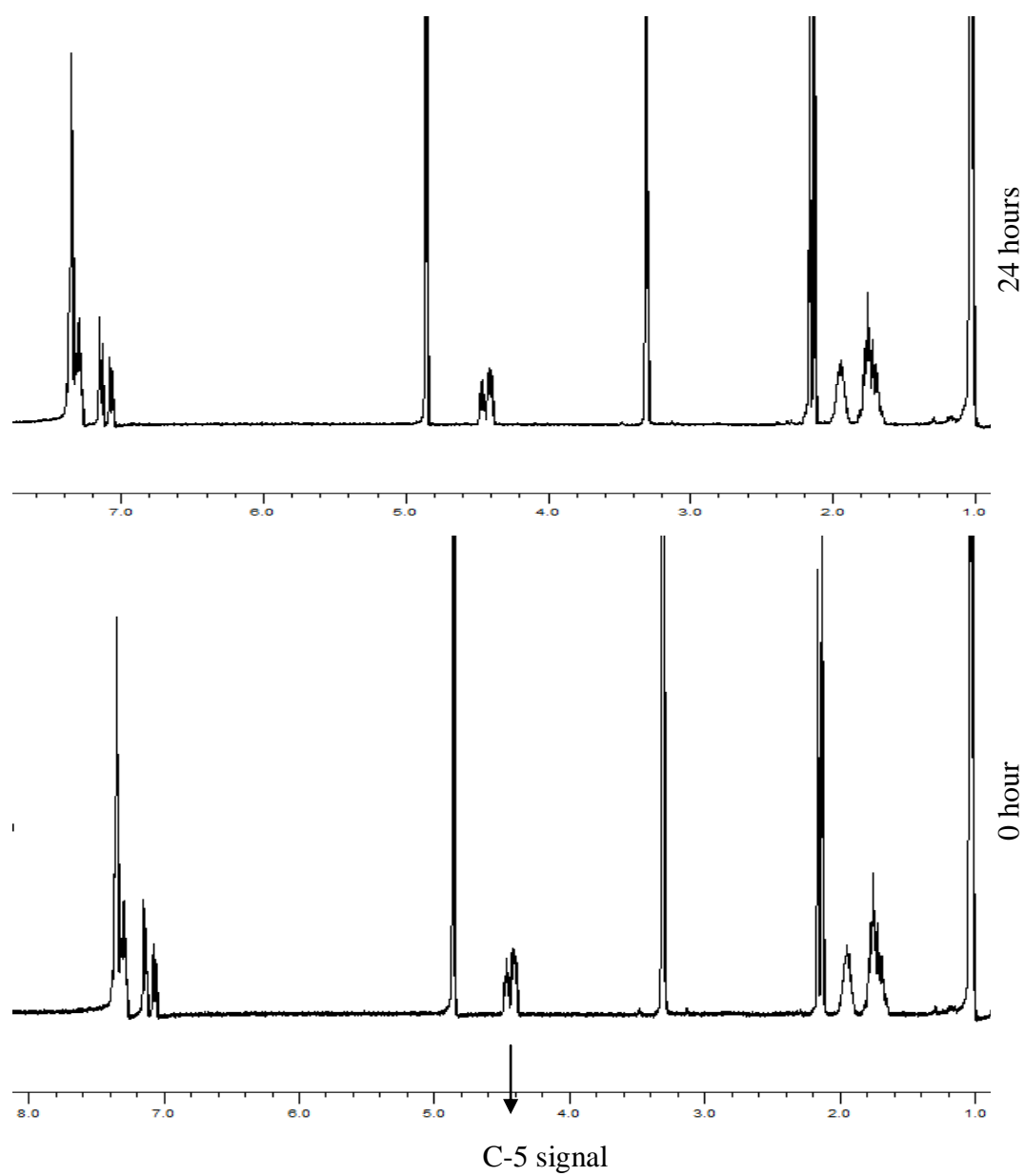


Figure 4.41. 5-isobutyl-3-(*o*-tolyl)-2-thiohydantoin C-5 hydrogen signal change with time in CD₃OD.

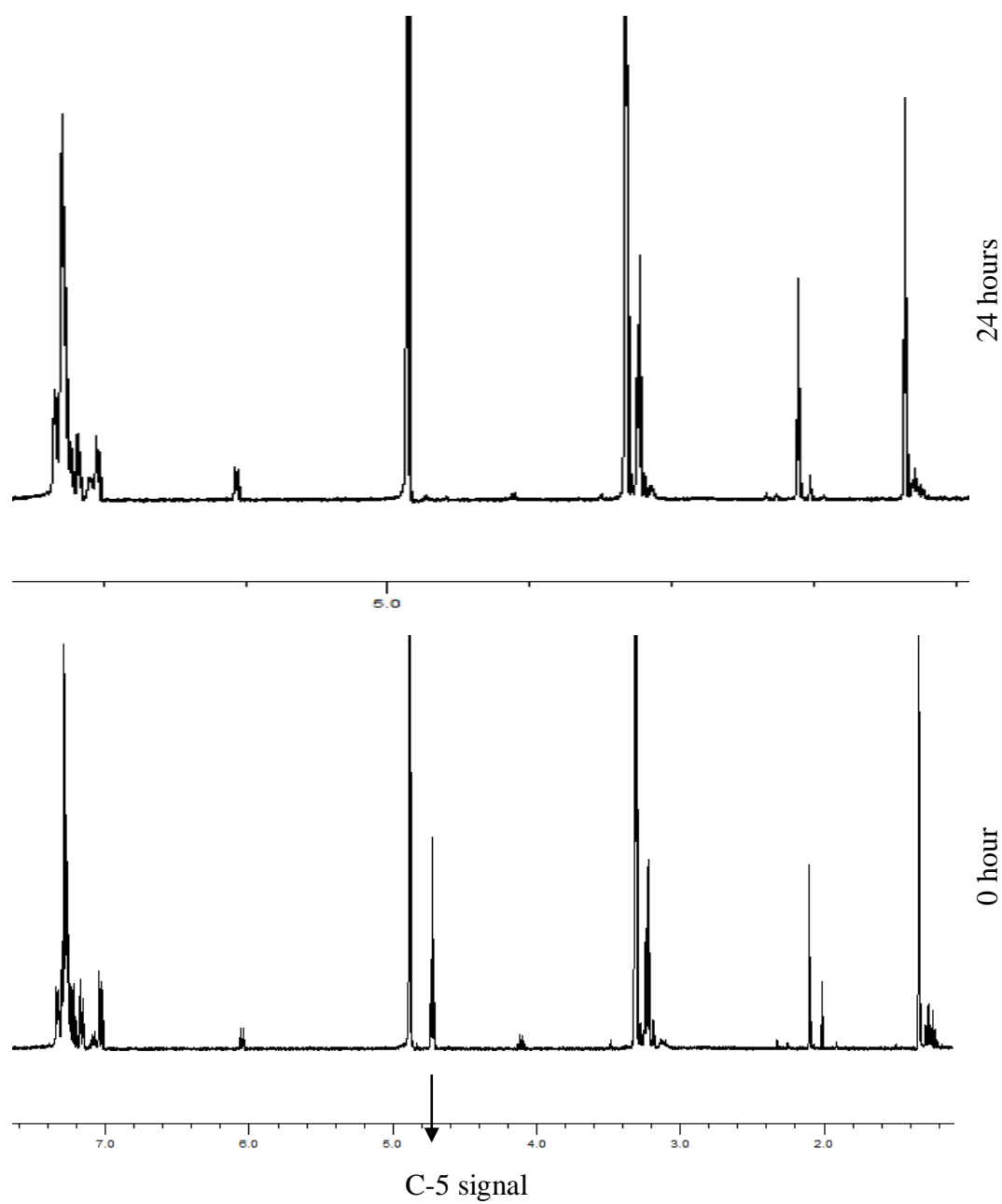


Figure 4.42. 5-benzyl-3-(*o*-tolyl)-2-thiohydantoin C-5 hydrogen signal change with time in CD₃OD.

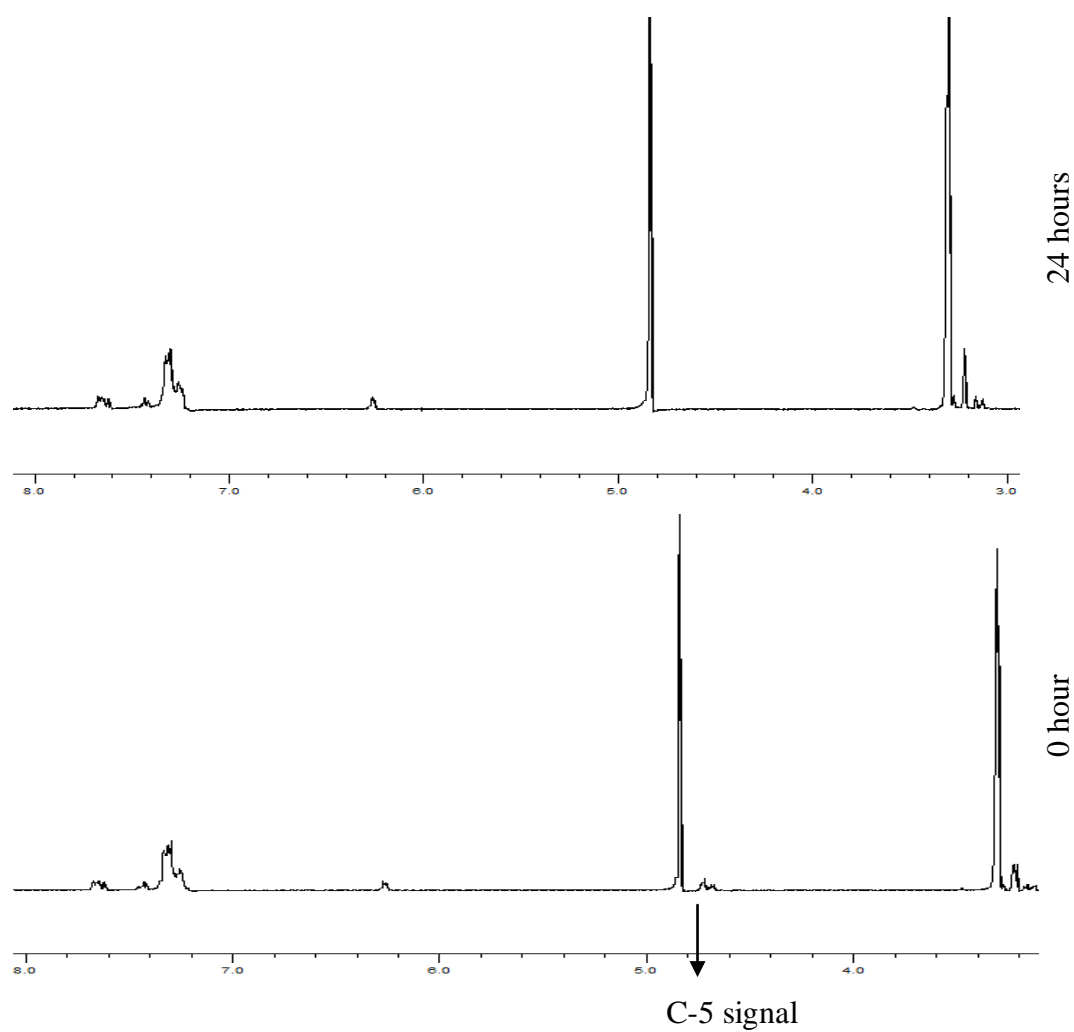


Figure 4.43. 5-benzyl-3-(*o*-bromophenyl)-2-thiohydantoin C-5 hydrogen signal change with time in CD₃OD.

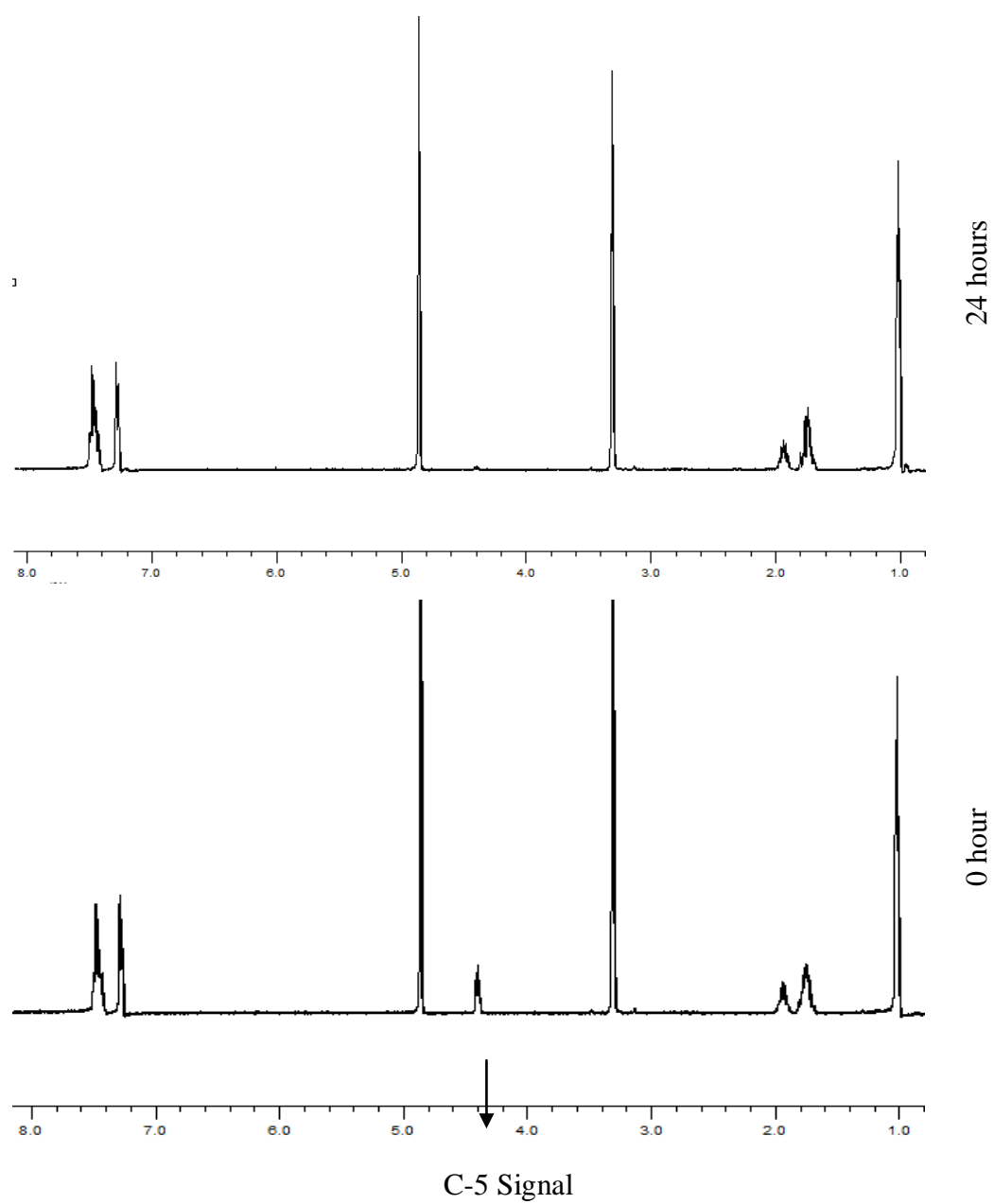


Figure 4.44. 5-isobutyl-3-phenyl-2-thiohydantoin C-5 hydrogen signal change with time in CD₃OD.

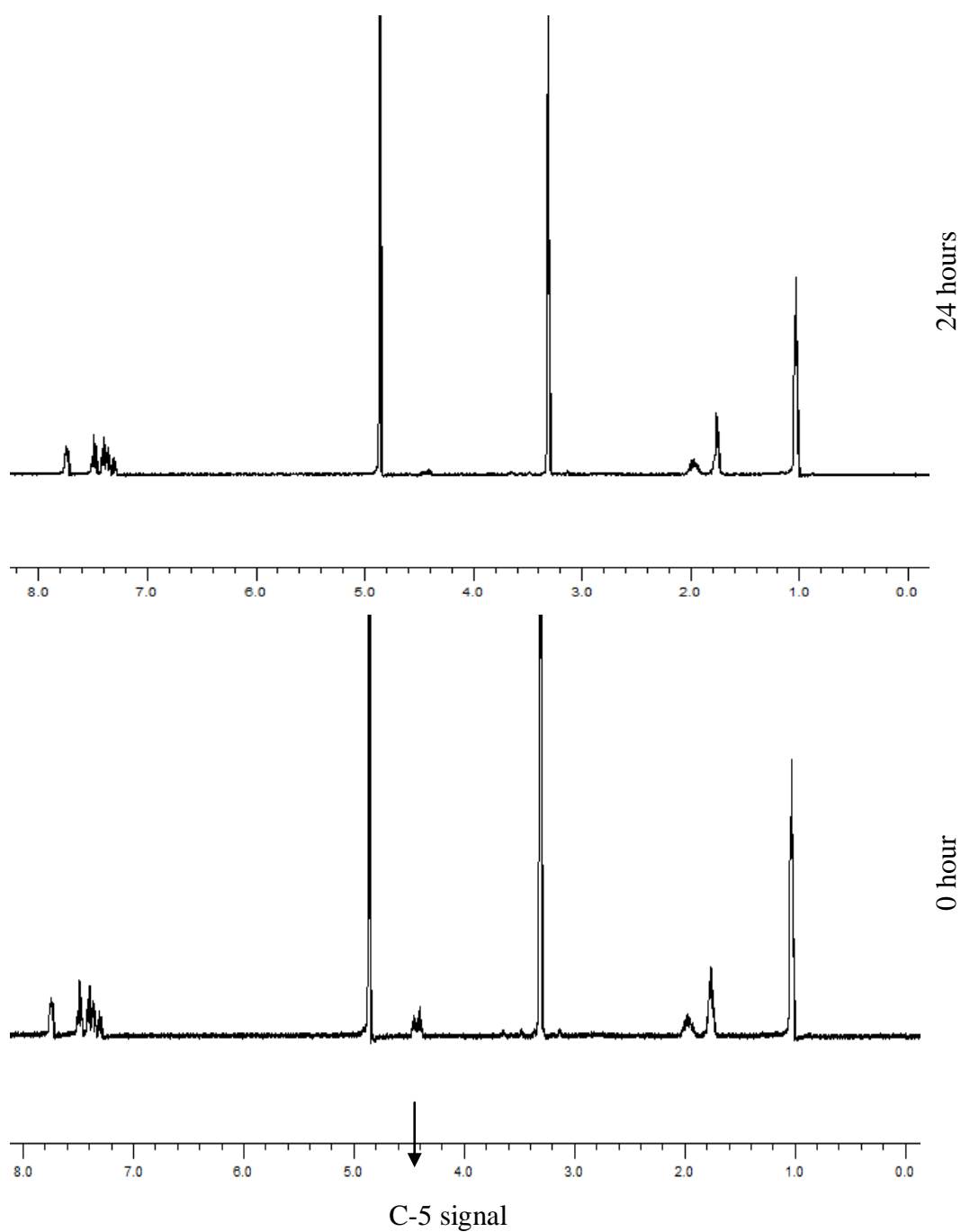


Figure 4.45. 5-isobutyl-3-(*o*-bromophenyl)-2-thiohydantoin C-5 hydrogen signal change with time in CD₃OD.

Table 4.6. Calculated separation factors (α) for the synthesized derivatives for HPLC.

| Compound | Separation Factors (α) ^a | | | | Separation Factors (α) ^b | | | |
|--|--|------------------------|------------------------|------------------------|--|------------------------|------------------------|------------------------|
| | SM \rightarrow RM | SP \rightarrow RP | RM \rightarrow SM | RP \rightarrow SP | SM \rightarrow SP | SP \rightarrow SM | RM \rightarrow RP | RP \rightarrow RM |
| (2) ^c | 0.475 | 0.493 | 2.105 | 2.027 | 1.761 | 0.568 | 1.829 | 0.547 |
| (3) ^d | 0.331 | 2.366 | 3.022 | 0.423 | 0.447 | 2.236 | 3.198 | 0.313 |
| (5) ^e | 2.157 | 2.939 | 0.464 | 0.340 | 1.193 | 0.838 | 1.626 | 0.615 |
| (6) ^f | 1.749 | 0.829 | 0.572 | 1.206 | 0.796 | 1.257 | 0.377 | 2.652 |
| | S to R | | R to S | | - | | - | |
| (1) ^d | 1.468 | | 0.681 | | - | | - | |
| (4) ^d | 1.352 | | 0.740 | | - | | - | |
| ^a Racemisation was observed between these stereoisomers. ^b Rotation was observed between these stereoisomers. ^c ChiralPak IB as the stationary phase, 95:5 Hex:EtOH as eluent, flow rate : 1.0 ml/min ^d ChiralPak IC as the stationary phase, 95:5 Hex:EtOH as eluent, flow rate : 0.8 ml/min ^e ChiralPak IB as the stationary phase, 95:5 Hex:EtOH as eluent, flow rate : 0.8 ml/min. ^f ChiralPak IA as the stationary phase, 95:5 Hex:EtOH as eluent, flow rate : 0.8 ml/min. | | | | | | | | |

5. CONCLUSION

In this study, synthesized derivatives of 5-benzyl-3-aryl-2-thiohydantoins and 5-isobutyl-3-phenyl-2-thiohydantoins stereoisomers were separated from each other and the ΔG^\ddagger racemisation or rotation barrier energies were calculated.

For compound **2**, **P** stereoisomers gave predominantly rotation however **M** stereoisomers gave exclusively racemisation in ethanol at 25 °C. For the separated stereoisomers of compounds **3** and **5**, both **P** and **M** gave racemisation in ethanol at 25 °C. For compound **1** no racemisation was observed at 25 °C in ethanol, but racemisation occurred at 40°C. When the racemisations were tried to be proved with hydrogen-deuterium exchange, the C5-Hydrogen's ¹H-NMR signals of compounds **2**, **3**, **4** and **6** C-5 disappeared, that is H/D exchange took place for these compounds. For compound **5** although racemisation was observed in HPLC experiments, the hydrogen-deuterium exchange was not observed in deuterio-methanol by ¹H-NMR.

For compound **3**, ΔG^\ddagger racemisation barriers in ethanol showed that when the temperature was increased from 25°C to 40°C, ΔG^\ddagger energy barriers slightly increased for the resolved stereoisomers. For compounds **2** and **5**, both racemisation and rotation were observed at 40 °C for separated stereoisomers, however in toluene they gave only rotation. In addition, the ΔG^\ddagger racemisation energy barrier of compound **1** was found higher than compound **4**.

The HPLC experiments done on chiral stationary phases showed that, in toluene the only dynamic process occurring among the stereoisomers was rotation. Racemisation did not take place at all. However, in ethanol both racemisation and rotation were observed due to enolisation of 2-thiohydantoins with the assistance of the hydroxyl group of ethanol and methanol. However, in toluene, there is no environment to capture a proton for synthesized 2-thiohydantoins for racemisation.

Table 5.1. Summary of the results of racemisations and rotations observed within the stereoisomers of the compounds studied.

| Comp. No | Solvent | T (°C) | Isomer conversion | ΔG_r^\ddagger (kJ/mole) | ΔG_r^\ddagger (kJ/mole) | k_f (s ⁻¹) | k_r (s ⁻¹) |
|----------|---------|--------|-------------------|---------------------------------|---------------------------------|--------------------------|--------------------------|
| (1) | Ethanol | 40 | S to R | 111.7±1.2 | 111.7±1.2 | 1.5 x 10 ⁻⁶ | 1.5 x 10 ⁻⁶ |
| (2) | Ethanol | 25 | SP to SM | 105.5±1.2 | - | 2 x 10 ⁻⁶ | - |
| (2) | Ethanol | 25 | RP to RM | 105.5±1.2 | - | 2 x 10 ⁻⁶ | - |
| (2) | Ethanol | 25 | SM to RM | 100.4±1.2 | 99.3± 1.2 | 1.59 x 10 ⁻⁵ | 2.41 x 10 ⁻⁵ |
| (2) | Ethanol | 25 | RM to SM | 100.5±1.2 | 100.5±1.2 | 1.51 x 10 ⁻⁵ | 1.49 x 10 ⁻⁵ |
| (2) | Toluene | 40 | SM to SP | 103.4±1.2 | 102.9±1.2 | 3.59 x 10 ⁻⁵ | 4.4 x 10 ⁻⁵ |
| (2) | Toluene | 40 | RP to RM | 105.4±1.2 | 104.6±1.2 | 1.7 x 10 ⁻⁵ | 2.3 x 10 ⁻⁵ |
| (3) | Ethanol | 25 | RP to SP | 97.9±3.2 | 99.1± 3.2 | 4.31 x 10 ⁻⁵ | 2.69 x 10 ⁻⁵ |
| (3) | Ethanol | 25 | SP to RP | 102.3±3.2 | 100.9±3.2 | 7.34 x 10 ⁻⁶ | 1.26 x 10 ⁻⁵ |
| (3) | Ethanol | 25 | RM to SM | 104.1±3.2 | 102.6±3.2 | 3.54 x 10 ⁻⁶ | 6.46 x 10 ⁻⁶ |
| (3) | Ethanol | 40 | RP to SP | 100.0±3.2 | 101.9±3.2 | 1.36 x 10 ⁻⁴ | 6.43 x 10 ⁻⁵ |
| (3) | Ethanol | 40 | SP to RP | 104.6±3.2 | 102.7±3.2 | 2.26 x 10 ⁻⁵ | 4.74 x 10 ⁻⁵ |
| (3) | Ethanol | 40 | RM to SM | 105.7±3.2 | 104.3±3.2 | 1.48 x 10 ⁻⁵ | 2.52 x 10 ⁻⁵ |
| (3) | Toluene | 110 | RP to RM | 118.7±3.2 | 118.9±3.2 | 5.18 x 10 ⁻⁴ | 4.82 x 10 ⁻⁴ |
| (4) | Ethanol | 40 | S to R | 100.8±1.2 | 100.8±1.2 | 1 x 10 ⁻⁴ | 1 x 10 ⁻⁴ |
| (5) | Ethanol | 25 | RP to SP | 99.4±1.8 | 100.2±1.8 | 2.3 x 10 ⁻⁵ | 1.7 x 10 ⁻⁵ |
| (5) | Ethanol | 25 | SP to RP | 102.0±1.8 | 101.1±1.8 | 8.25 x 10 ⁻⁶ | 1.18 x 10 ⁻⁶ |
| (5) | Ethanol | 25 | RM to SM | 102.0±1.8 | 101.1±1.8 | 8.28 x 10 ⁻⁶ | 1.17 x 10 ⁻⁶ |
| (5) | Ethanol | 25 | SM to RM | 100.5±1.8 | 100.6±1.8 | 1.53 x 10 ⁻⁵ | 1.47 x 10 ⁻⁵ |

Table 5.1. Summary of the results of racemisations and rotations observed within the stereoisomers of the compounds studied (continued).

| | | | | | | | |
|-----|---------|-----|-----------------|-----------|-----------|----------------------------|----------------------------|
| (5) | Toluene | 40 | RM to RP | 103.8±1.8 | 103.2±1.8 | 3.13 x 10 ⁻⁵ | 3.87 x 10 ⁻⁵ |
| (6) | Ethanol | 40 | RP to SP | 102.1±0.1 | 103.1±0.1 | 5.97 x 10 ⁻⁵ | 4.04 x 10 ⁻⁵ |
| (6) | Ethanol | 40 | SP to RP | 103.2±0.1 | 102.1±0.1 | 3.98 x 10 ⁻⁵ | 6.02 x 10 ⁻⁵ |
| (6) | Ethanol | 40 | RM to SM | 103.0±0.1 | 102.2±0.1 | 4.27 x 10 ⁻⁵ | 5.73 x 10 ⁻⁵ |
| (6) | Toluene | 110 | SP to SM | 118.4±0.1 | 118.0±0.1 | 5.65 x 10 ⁻⁴ | 6.35 x 10 ⁻⁴ |

REFERENCES

1. Doğan, İ., S. İçli, "Conformational and Spectral Investigations of Thiazolidinone Derivatives by ^1H and ^{13}C NMR Spectroscopy", *Spectroscopy Letters*, Vol. 16, No. 7, pp. 499, 1983.
2. Doğan, İ., T. Burgermeister, S. İçli and A. Mannschreck, "Synthesis and NMR of Chiral 4-Oxazolinones and Rhodanines", *Tetrahadron*, Vol. 48, No. 35, pp. 7157, 1992.
3. Doğan, İ., N. Pustet and A. Mannschreck, "The Enantiomers of N-Aryl-2-thioxo-4-oxazolidinones and N-Arylrhodanines. Investigation by Liquid Chromatography, Circular Dichroism and Thermal Racemization", *Journal of the Chemical Society, Perkin Transactions 2*, Vol. 8, pp. 1557, 1993.
4. Karataş, M., S. Koni and İ. Doğan, "Chiral N-(*o*-Aryl)-thiazolidinediones; Synthesis from Rhodanines and Investigation on Rotational Enantiomers by NMR", *Canadian Journal of Chemistry*, Vol 76, pp. 254, 1998.
5. Stoughton, R. W., R. Adams, "Stereochemistry of Biphenyl Compounds (XI) Prepn. And Resolution of 2-Methyl-6-nitro-2' Carboxybiphenyl", *Journal of the American Chemical Society*, Vol. 52, pp. 5263-5267, 1930.
6. Adams, R., H. C. Yuan, "Stereochemistry of Biphenyls and Analogous Compounds", *Chemical Reviews*, Vol. 12, pp. 161, 1933.
7. Westheimer, F. H., *Steric Effects in Organic Chemistry*, John Wiley, New York, 1956.
8. Eliel. E. L., *Stereochemistry of Carbon Compounds*, McGRAW Hill, New York, 1962.

9. Hall, D. M., "Stereochemistry of 2, 2'-Bridged Biphenyls", *Progress in Stereochemistry*, Vol. 4, pp. 1-42, 1969.
10. Bentz, W. E., L. D. Colebrook, J. R. Fehlner and A. Rosowsky, "Hindered Rotation About C-N Bonds: Equilibrium of Diastereomeric Rotational Isomer", *Chemical Communications*, Vol. 1, pp. 974, 1970.
11. Colebrook, L. D., Giles H. G., "Restricted Internal Rotation in 1-Arylhydantoin 3-Arylhydantoins and 3-Aryl-2-thiohydantoins: Reversal of the Effective Sizes of Methyl and Chlorine", *Canadian Journal of Chemistry*, Vol. 51, pp. 3635-3639, 1973.
12. Colebrook, L. D., S. Içli, and F. H. Hund, "NMR Studies of Enantiomeric Internal Rotational Isomers of 1-and 3-Arylhydantoins in Achiral and Chiral Solvents", *Canadian Journal of Chemistry*, Vol. 53, pp. 1556-1562, 1975.
13. Ayada, D., C. Roussel, J. Sandström, "Conformational Analysis of Trigonal and Planar Rotors attached to Δ^4 -Azoline-2-thiones. The effect of Ring Geometry", *Journal of the Chemical Society, Perkin Transactions 2*, Vol. 2, pp. 273-277, 1985.
14. Vorkopic-Furac, J., M. F. Mintas, F. Kestmer, and A. Mannschreck, "Enantiomers and Barriers to Racemisation of Sterically Hindered N-aryl and N-heteroarylpyrroles", *Journal of Heterocyclic Chemistry*, Vol 29, pp. 327-333, 1992.
15. Link, A., C. Sparr, "Organocatalytic Atroposelective Aldol Condensation: Synthesis of Axially Chiral Biaryls by Arene Formation", *Angewandte Chemie International Edition*, Vol. 53, pp. 5458-5461, 2014.
16. Lopez, C. A., G. G. Trigo, "The Chemistry of Hydantoins", *Advances in Heterocyclic Chemistry*. Vol. 38, pp. 177-228, 1985.

17. Mo, B., J. Li, and S. Liang, “ A Method for Preparation of Amino Acid Thiohydantoins from Free Amino Acids Activated by Acetyl Chloride for Development of Protein C-Terminal Sequencing”, *Analytical Biochemistry*, Vol. 249, pp. 207-211, 1997.
18. Kandil, S. S., G. B. El-Hefnawy, and E. A. Baker, “Thermal and spectral studies of 5-(phenylazo)-2-thiohydantoin and 5-(2-hydroxyphenylazo)-2-thiohydantoin complexes of cobalt(II), nickel (II) and copper (II)” *Thermochimica Acta*, Vol. 414, pp. 105-113, 2004.
19. Burgess, K., S. Reyes, “On Formation of Thiohydantoins from Amino Acids under Acylation Conditions”, *Journal of Organic. Chemistry.*, Vol. 71, pp. 2507-2509, 2006.
20. Oki, M., “Recent Advances in Atropisomerism”, *Topics in Stereochemistry*, Vol.1 pp.14, 1983.
21. Cahn, R. S., C. Ingold, and V. Prelog, “Specification of Molecular Chirality”, *Angewandte Chemie International Edition in English*, Vol. 5, No. 4, pp. 385-415, 1966.

APPENDIX A: ^1H -NMR SPECTRA OF THE COMPOUNDS

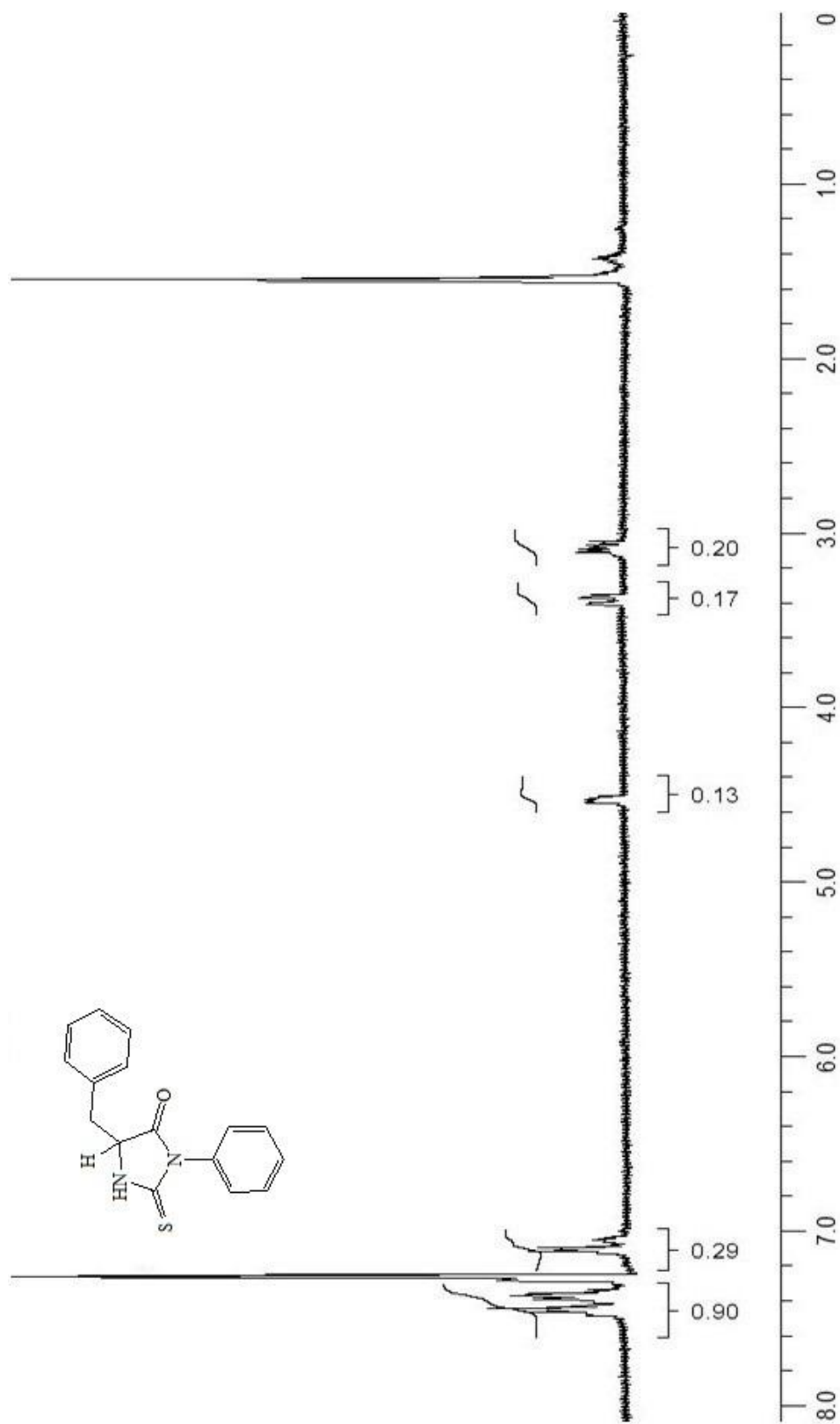


Figure A.1. The 400 MHz ^1H NMR spectrum of recrystallized 5-benzyl-3-phenyl-2-thiohydantoin in CDCl_3 .

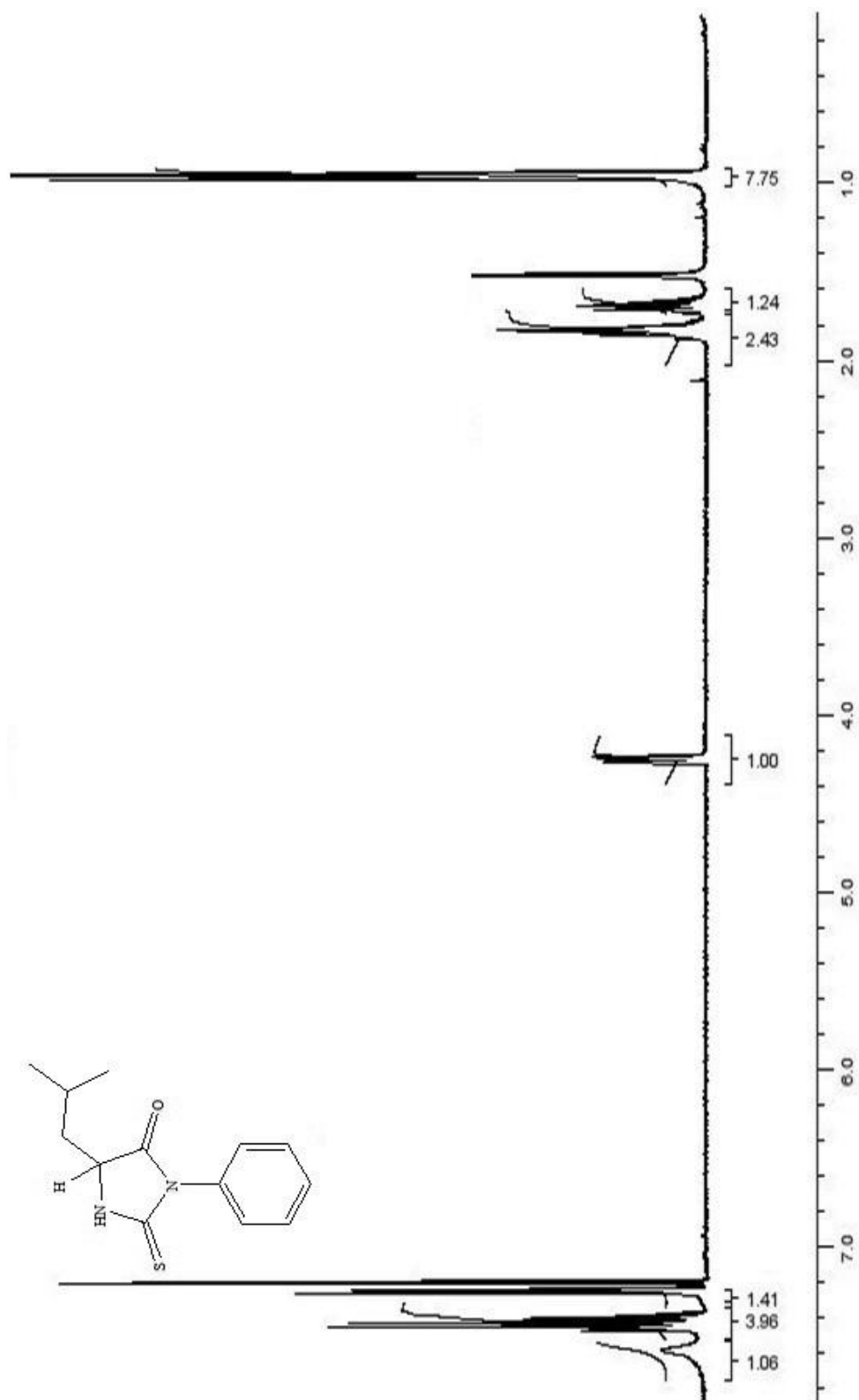


Figure A.3. The 400 MHz ¹H NMR spectrum of recrystallized 5-isobutyl-3-phenyl-2-thiohydantoin in CDCl₃.

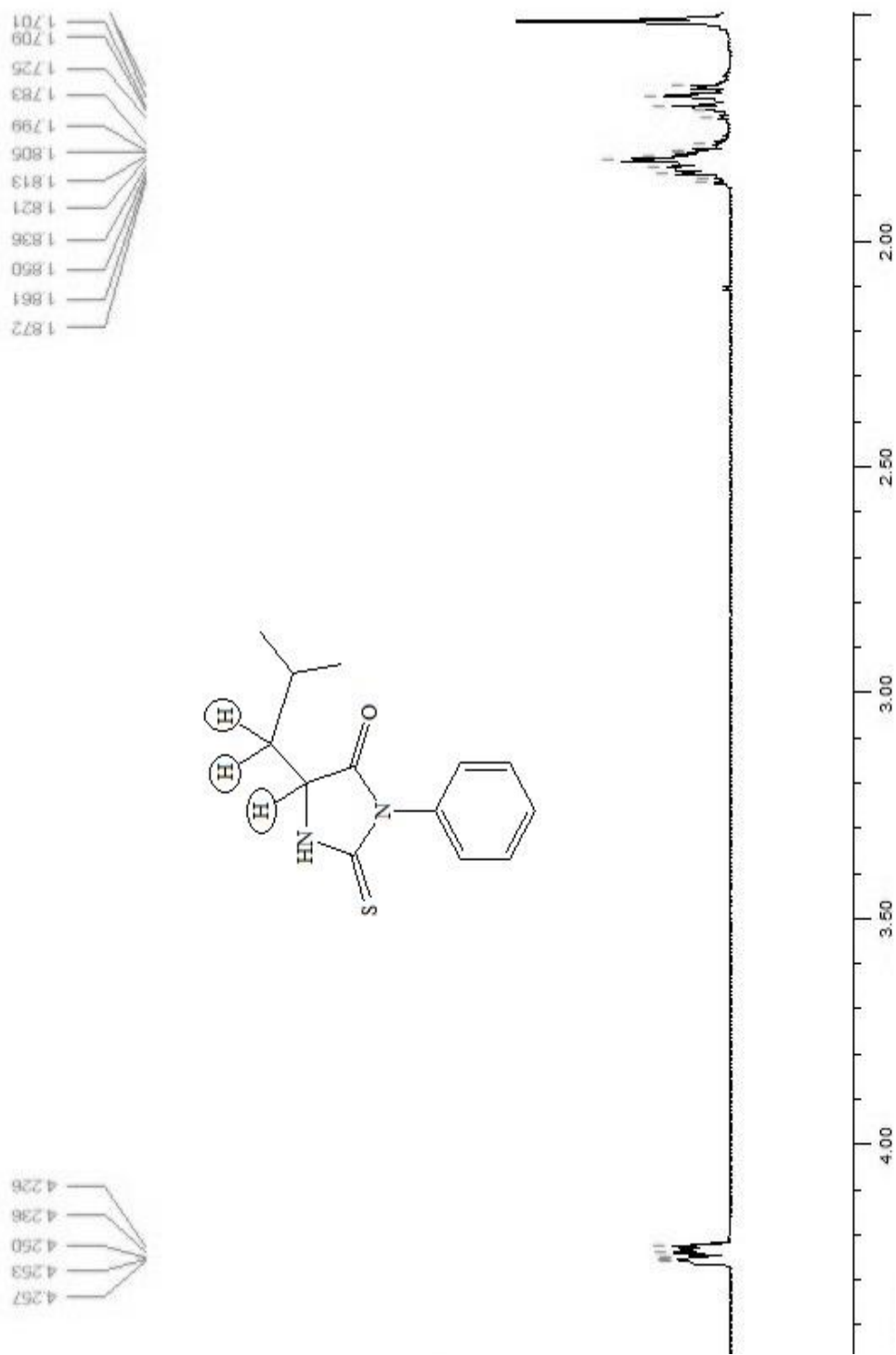


Figure A.4. The coupling constants of recrystallized 5-isobutyl-3-phenyl-2-thiohydantoin in CDCl₃.

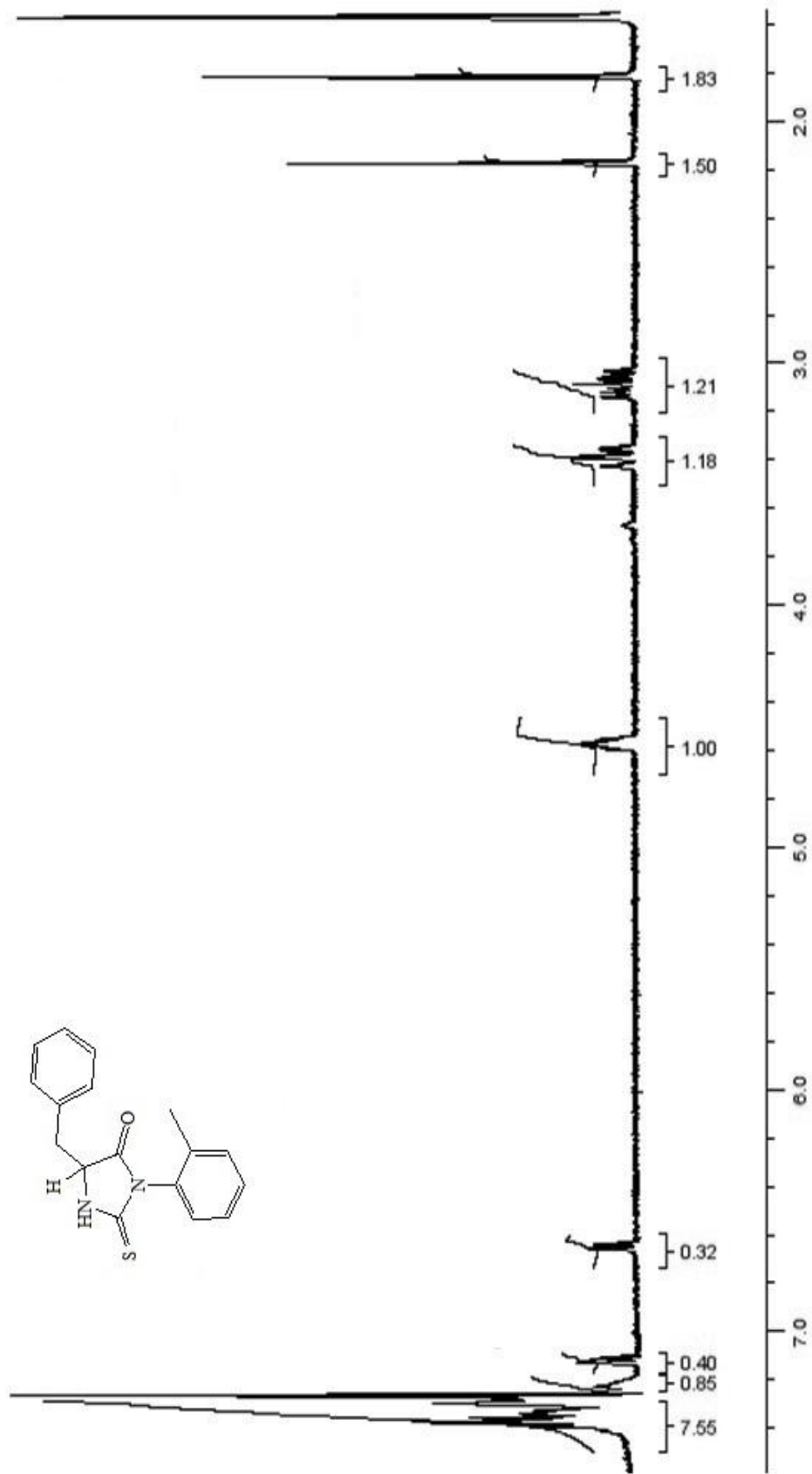


Figure A.5. The 400 MHz ¹H NMR spectrum of 5-benzyl-3-(*o*-tolyl)-2-thiohydantoin in CDCl₃, not used for assignment.

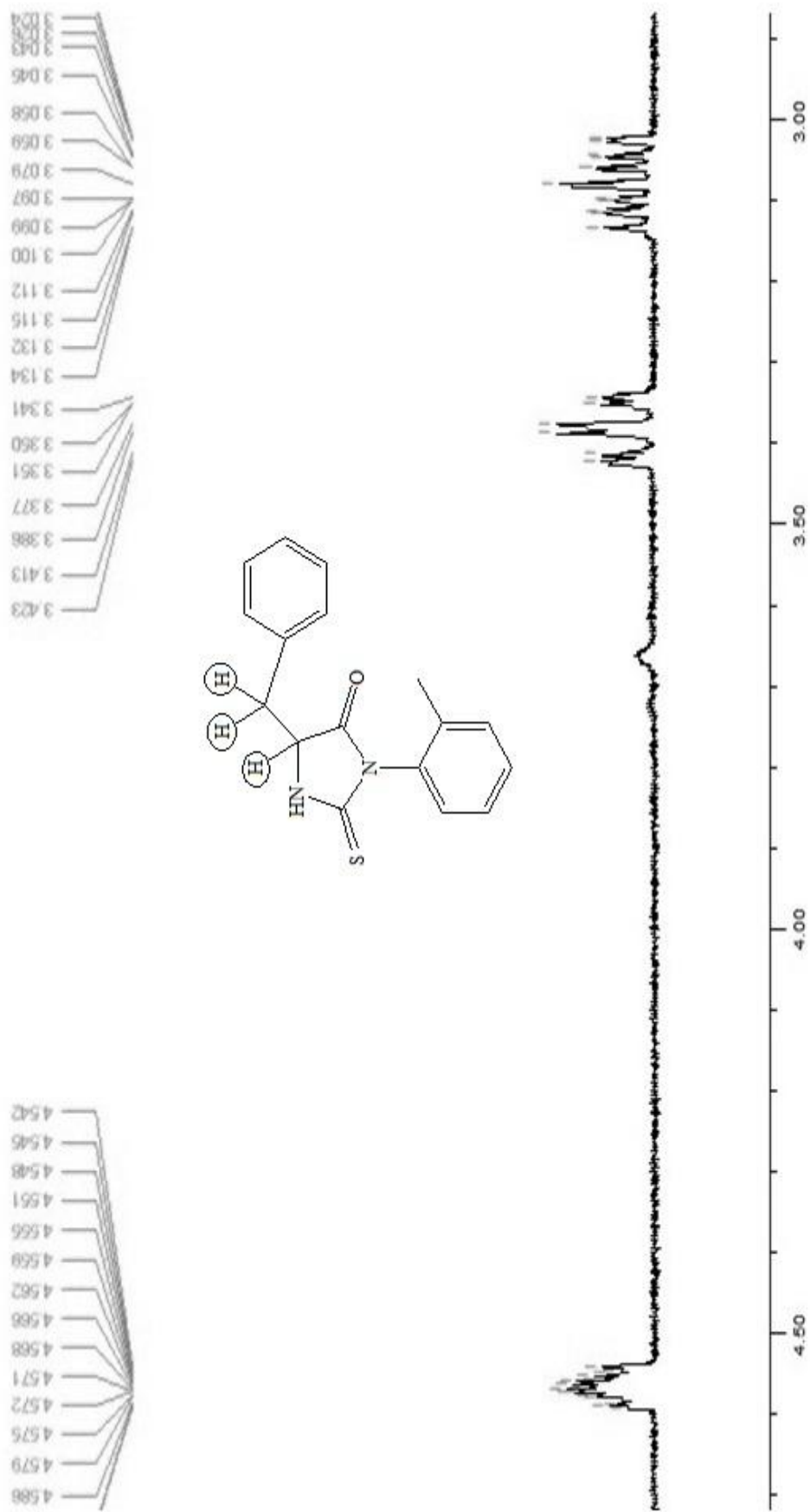


Figure A.6. The coupling constants of 5-benzyl-3-(*o*-tolyl)-2-thiohydantoin in CDCl₃, not used for assignment.

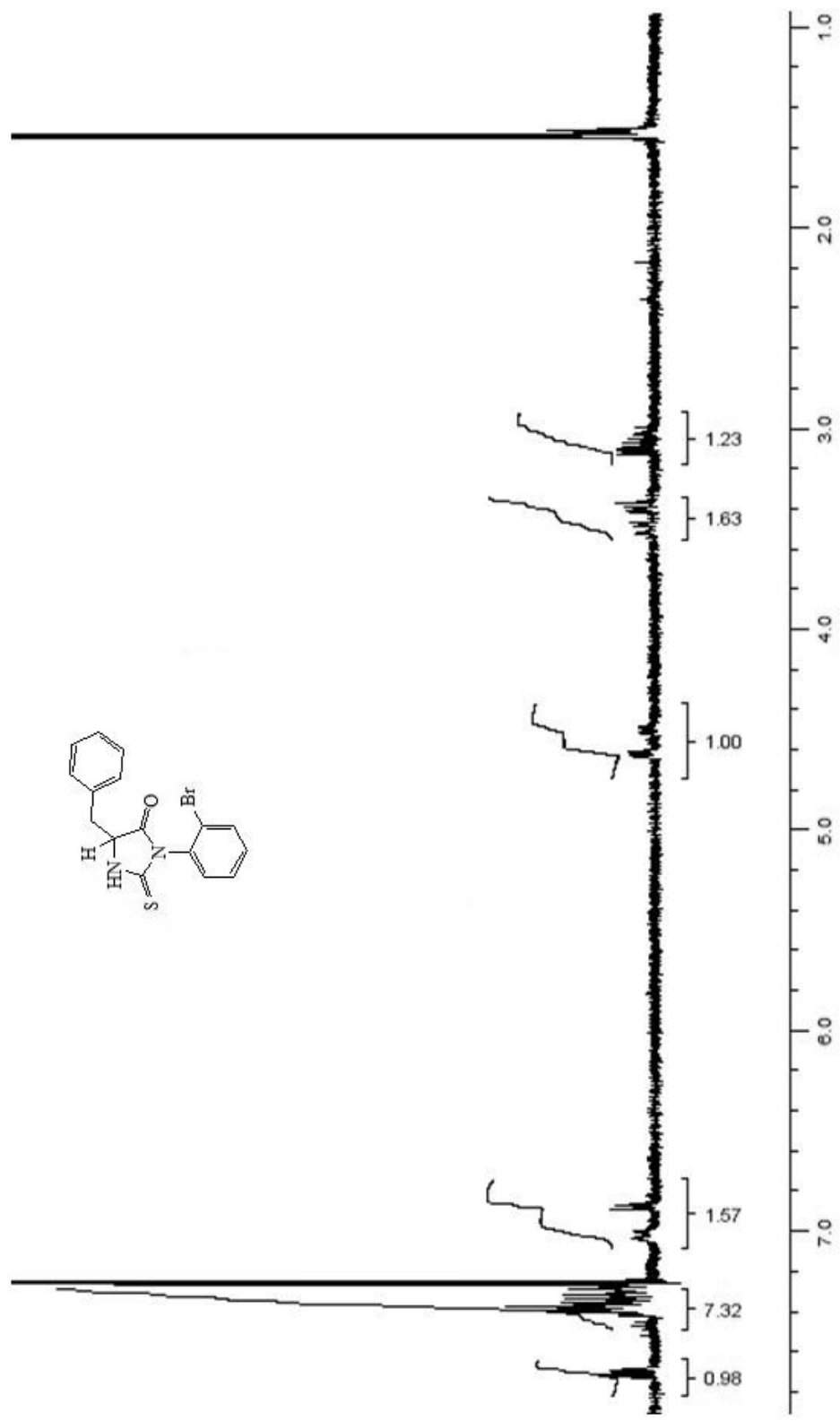
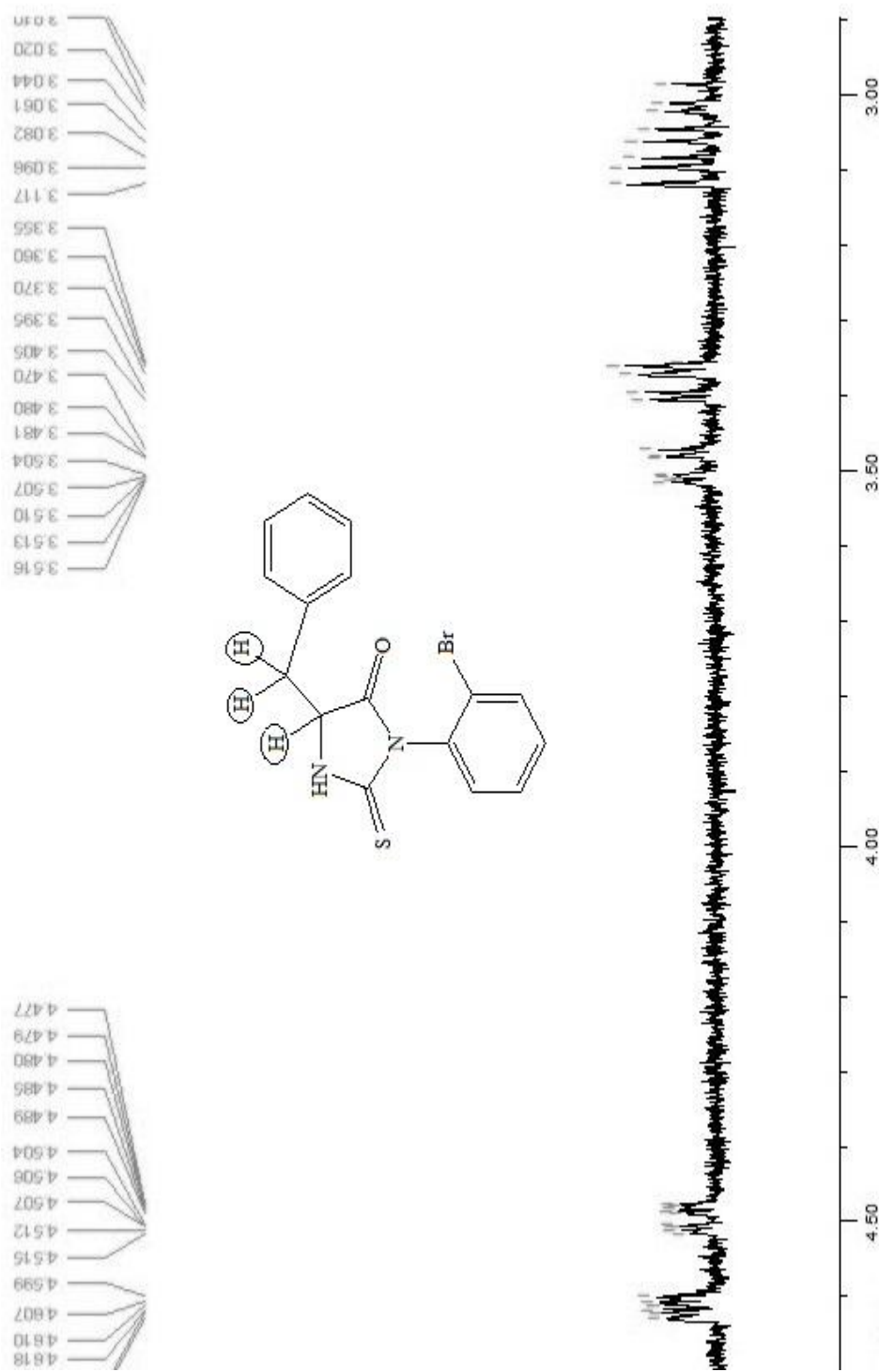


Figure A.7. The 400 MHz ¹H NMR spectrum of recrystallized 5-benzyl-3-(*o*-bromophenyl)-2-thiohydantoin in CDCl₃, used for assignment.



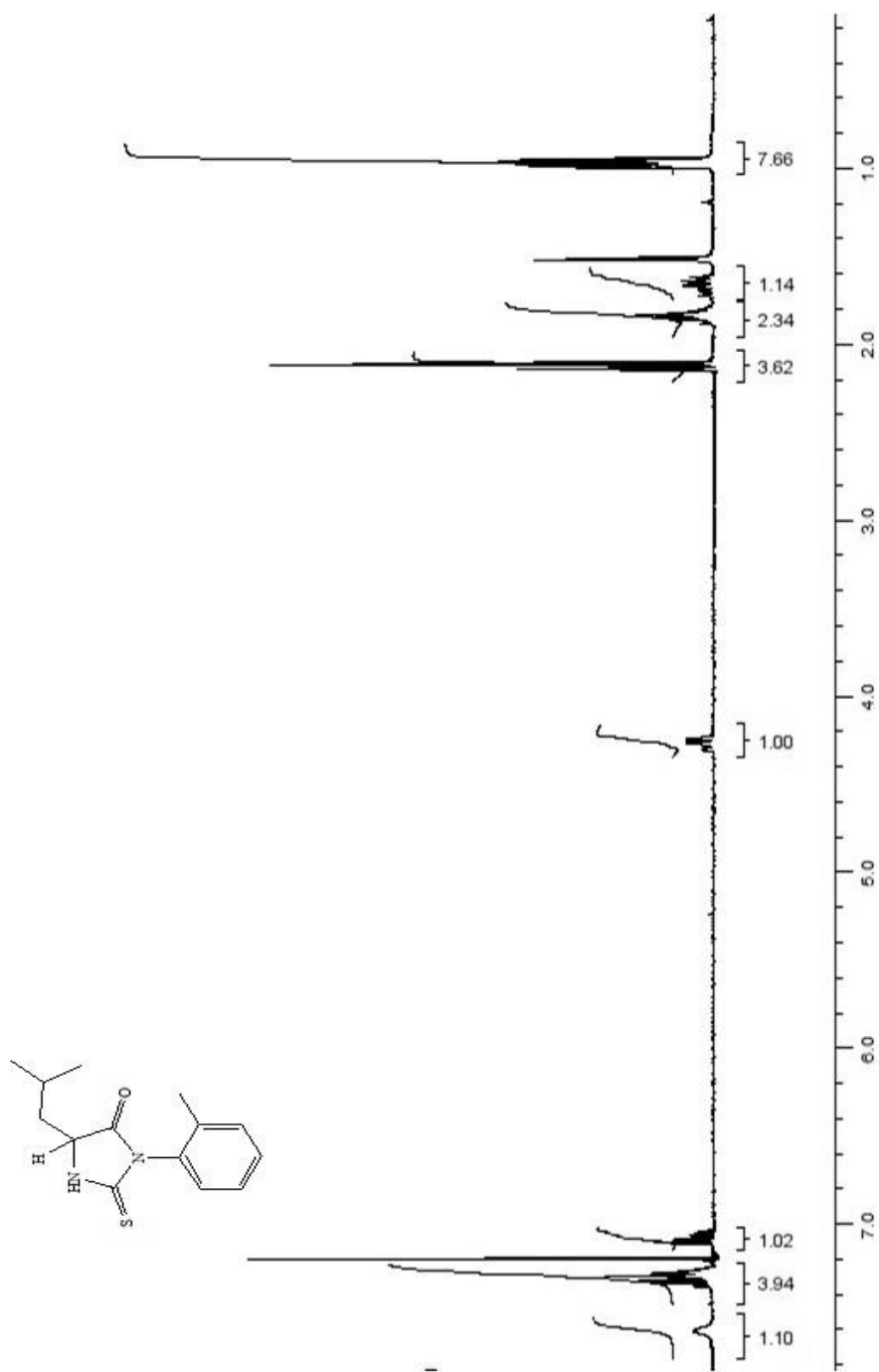


Figure A.9. The 400 MHz ¹H NMR spectrum of recrystallized 5-isobutyl-3-(*o*-tolyl)-2-thiohydantoin in CDCl₃, used for assignment.

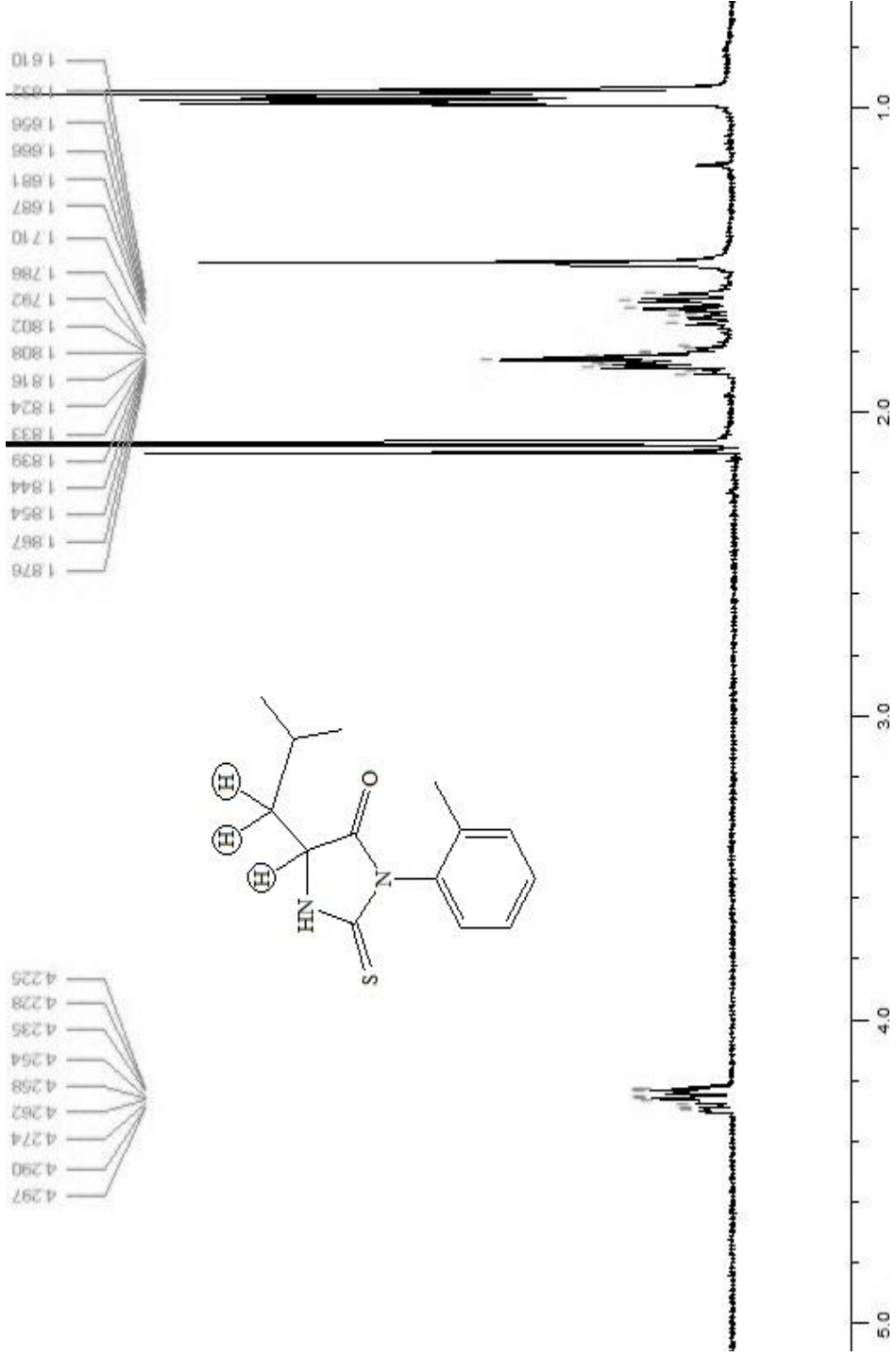


Figure A.10. The coupling constants of recrystallized 5-isobutyl-3-(*o*-tolyl)-2-thiohydantoin in CDCl_3 , used for assignment.

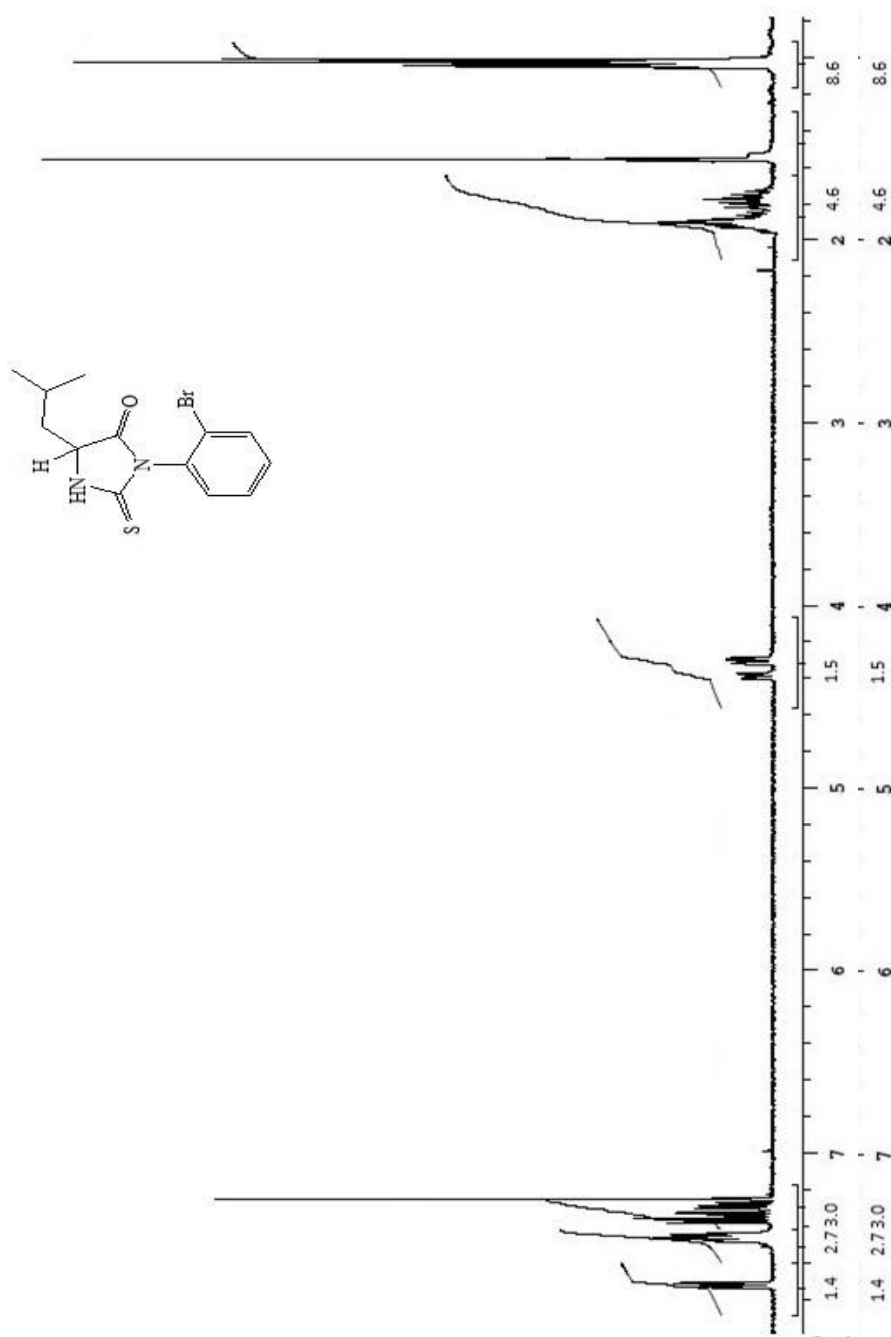


Figure A.11. The 400 MHz ¹H NMR spectrum of recrystallized 5-isobutyl-3-(*o*-bromophenyl)-2-thiohydantoin in CDCl₃, used for assignment

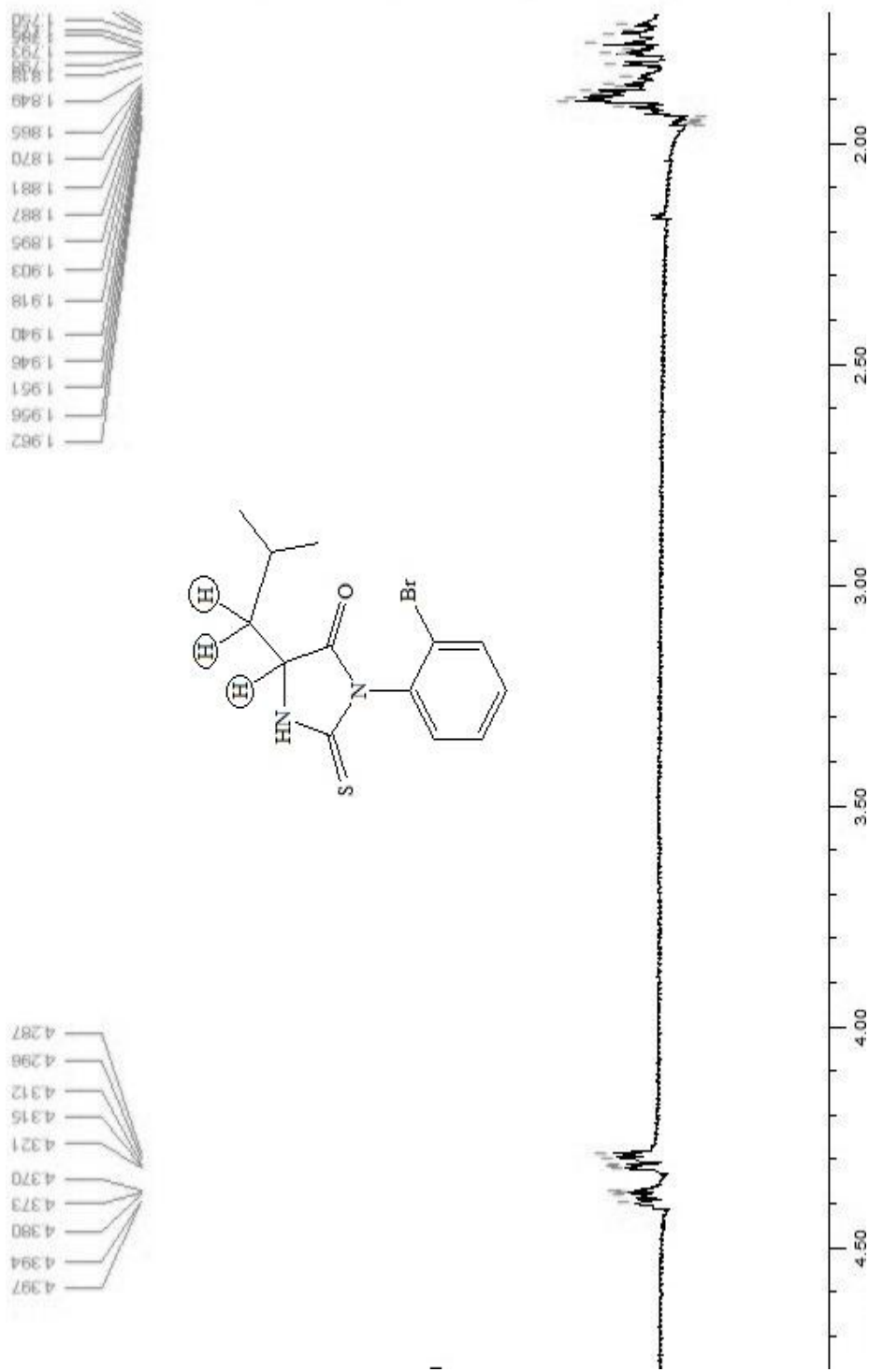


Figure A.12. The coupling constants of recrystallized 5-isobutyl-3-(*o*-bromophenyl)-2-thiohydantoin in CDCl₃, used for assignment.

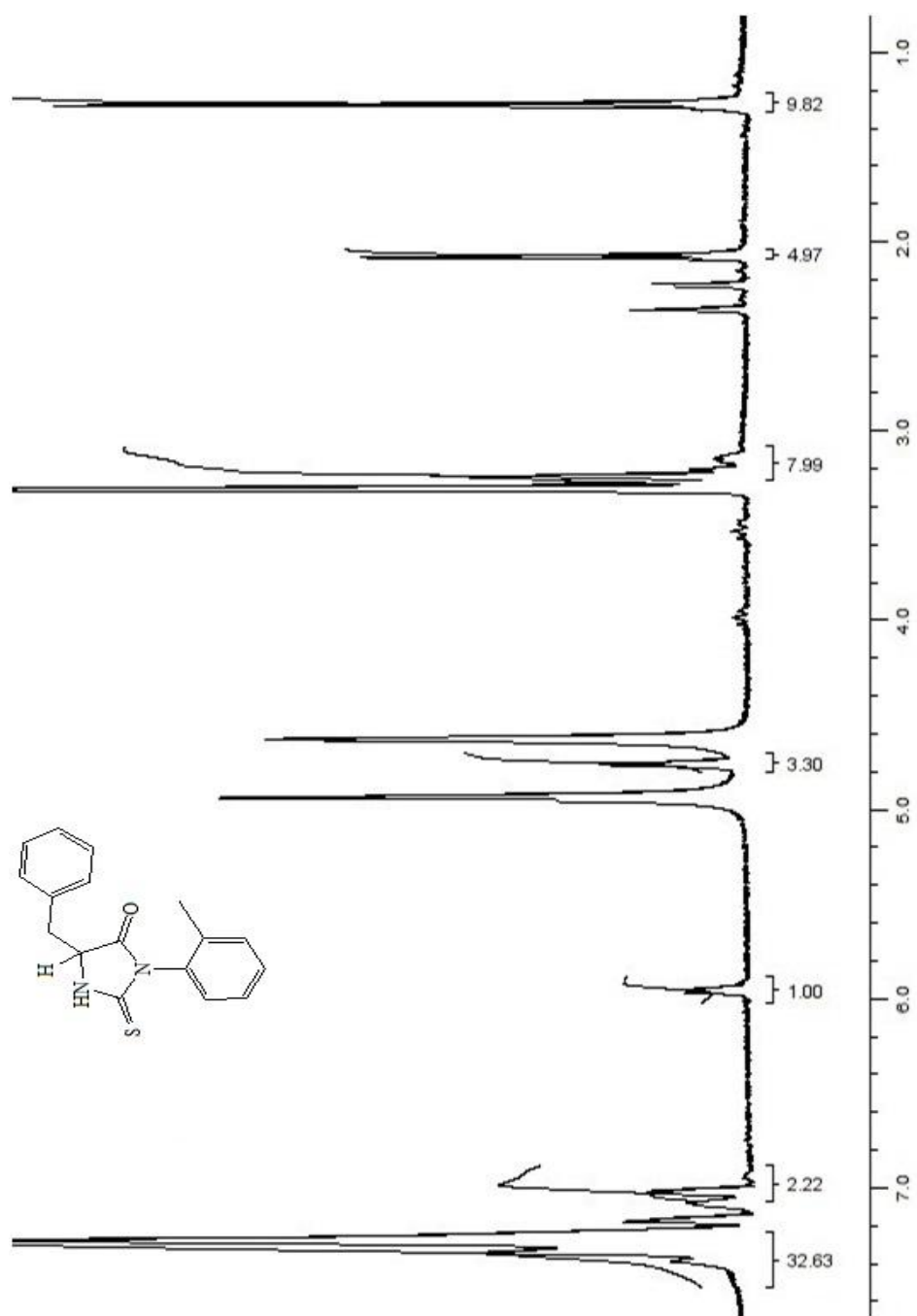


Figure A.13. The 400 MHz ¹H NMR spectrum of crude 5-benzyl-3-(*o*-tolyl)-2-thiohydantoin in CD₃OD, used for assignment.

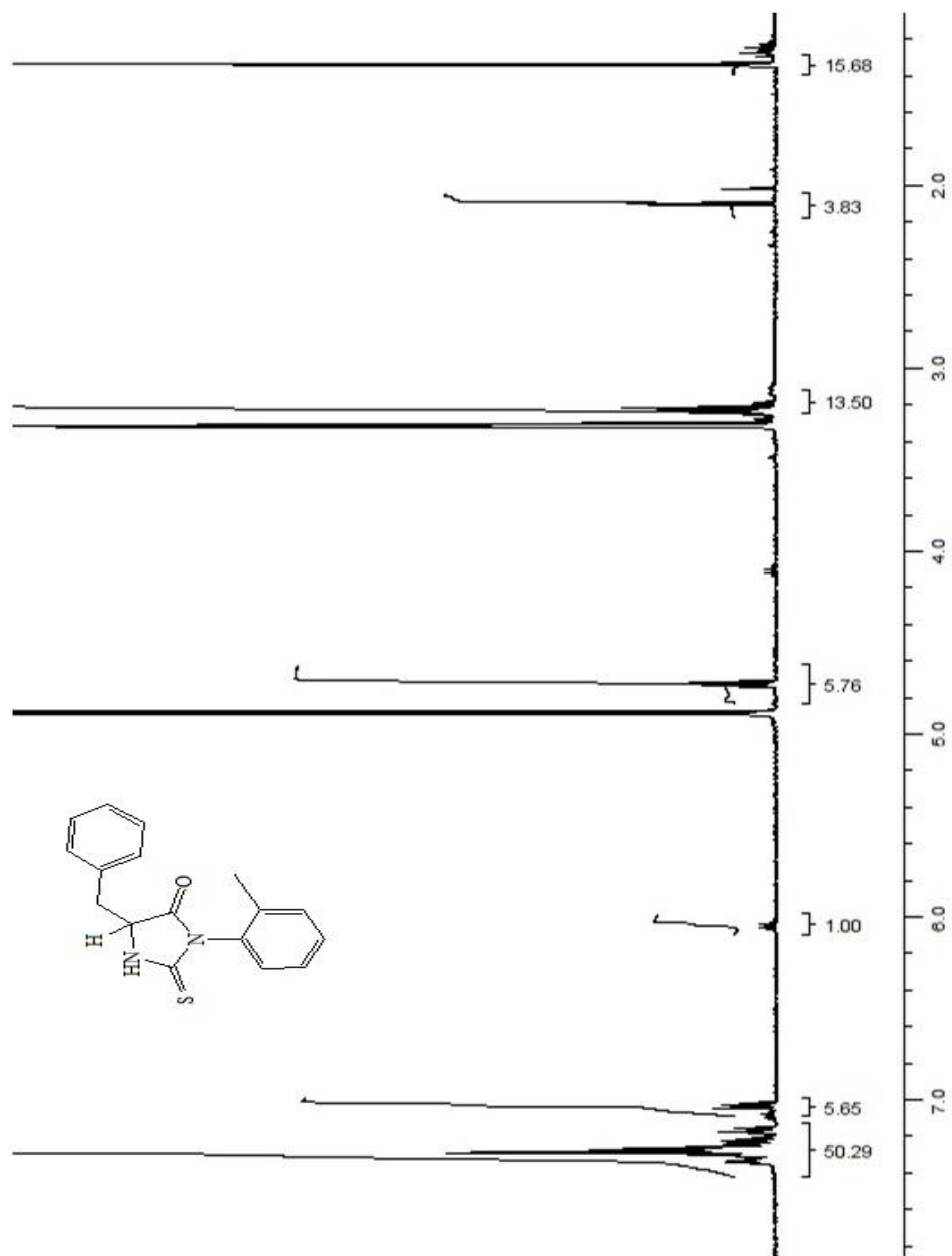


Figure A.14. The 400 MHz ¹H NMR spectrum of recrystallized 5-benzyl-3-(*o*-tolyl)-2-thiohydantoin in CD₃OD, used for assignment.

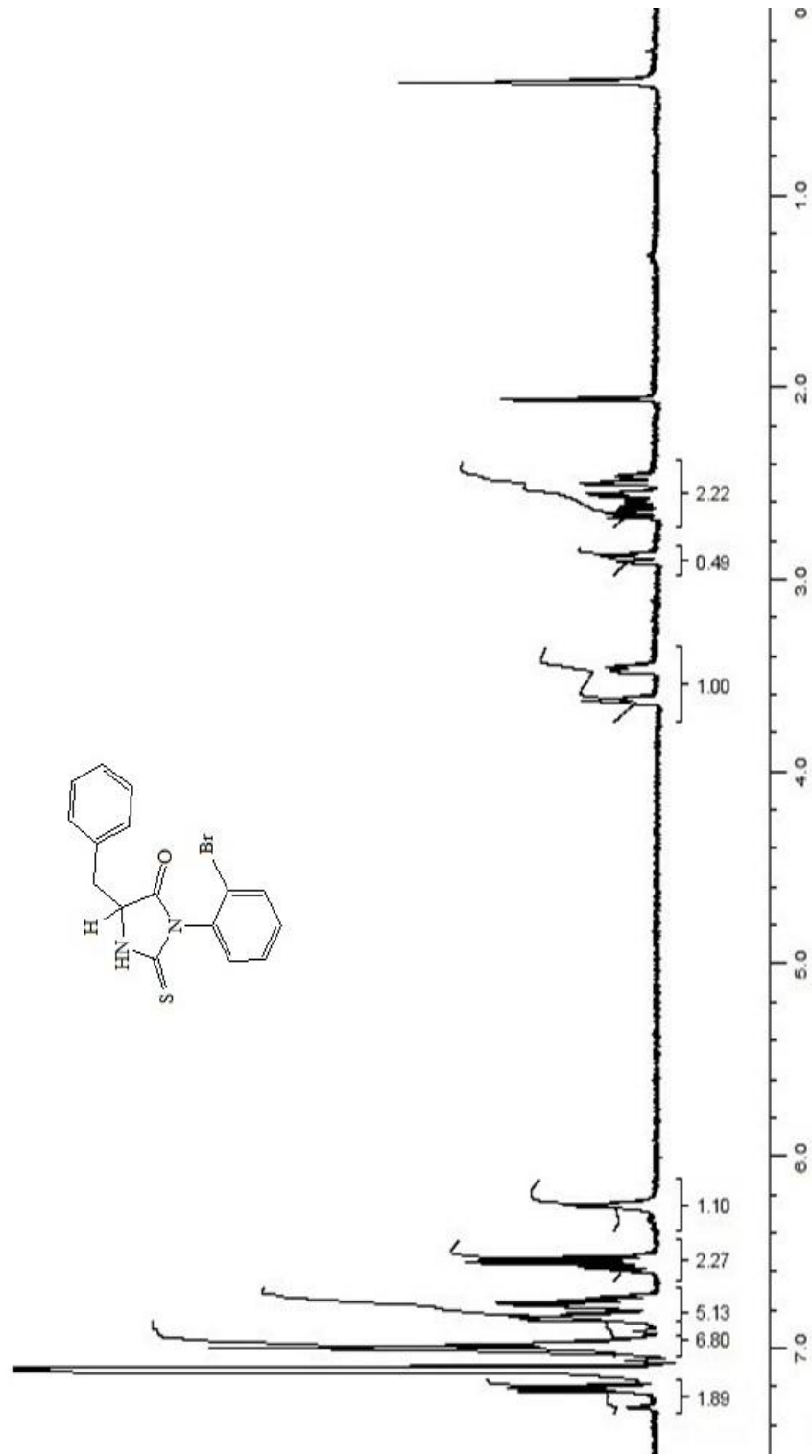


Figure A.15. The 400 MHz ^1H NMR spectrum of 5-benzyl-3-(*o*-bromophenyl)-2-thiohydantoin in C_6D_6 , not used for assignment.

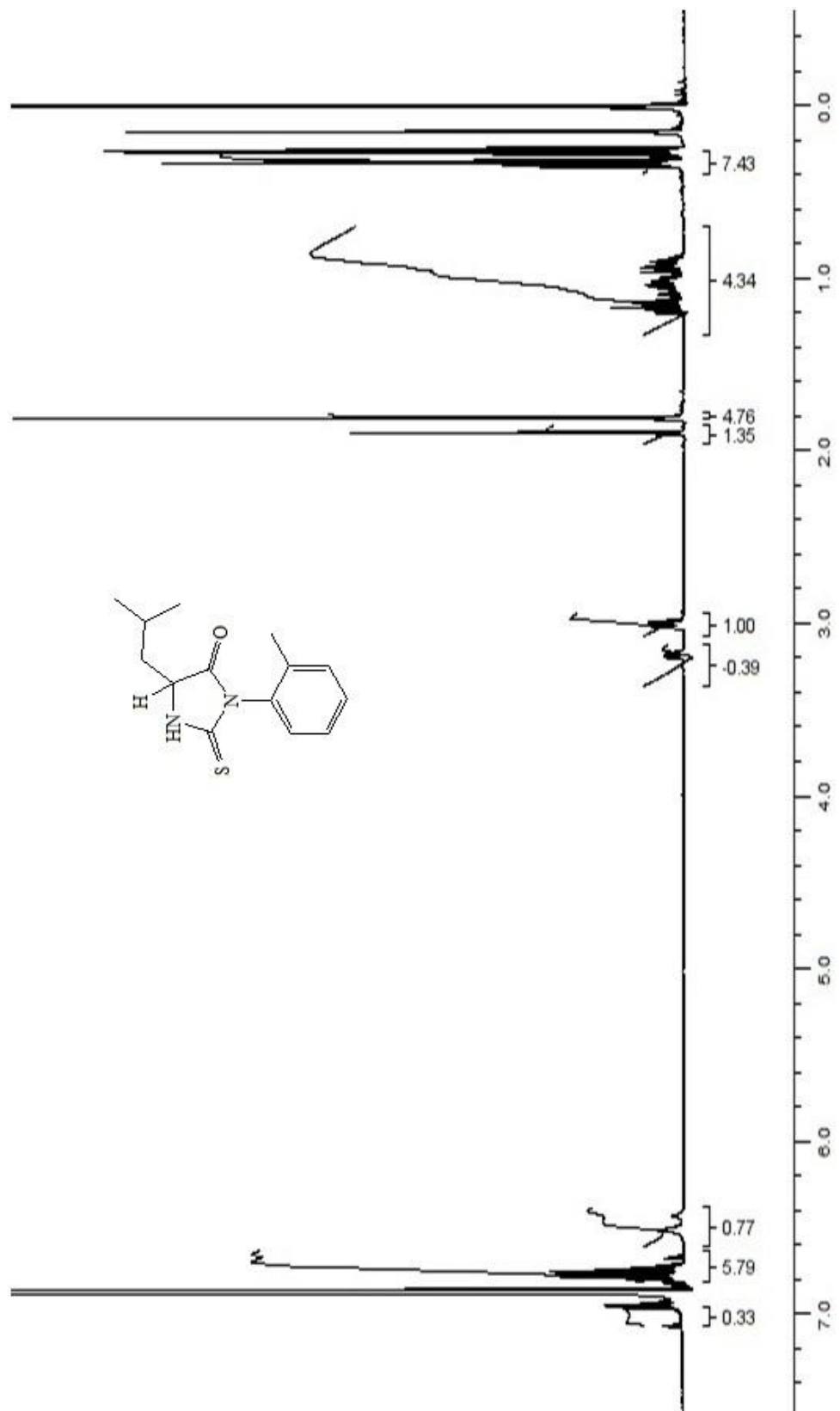


Figure A.16. The 400 MHz ¹H NMR spectrum of recrystallized 5-isobutyl-3-(*o*-tolyl)-2-thiohydantoin in C₆D₆, used for assignment.

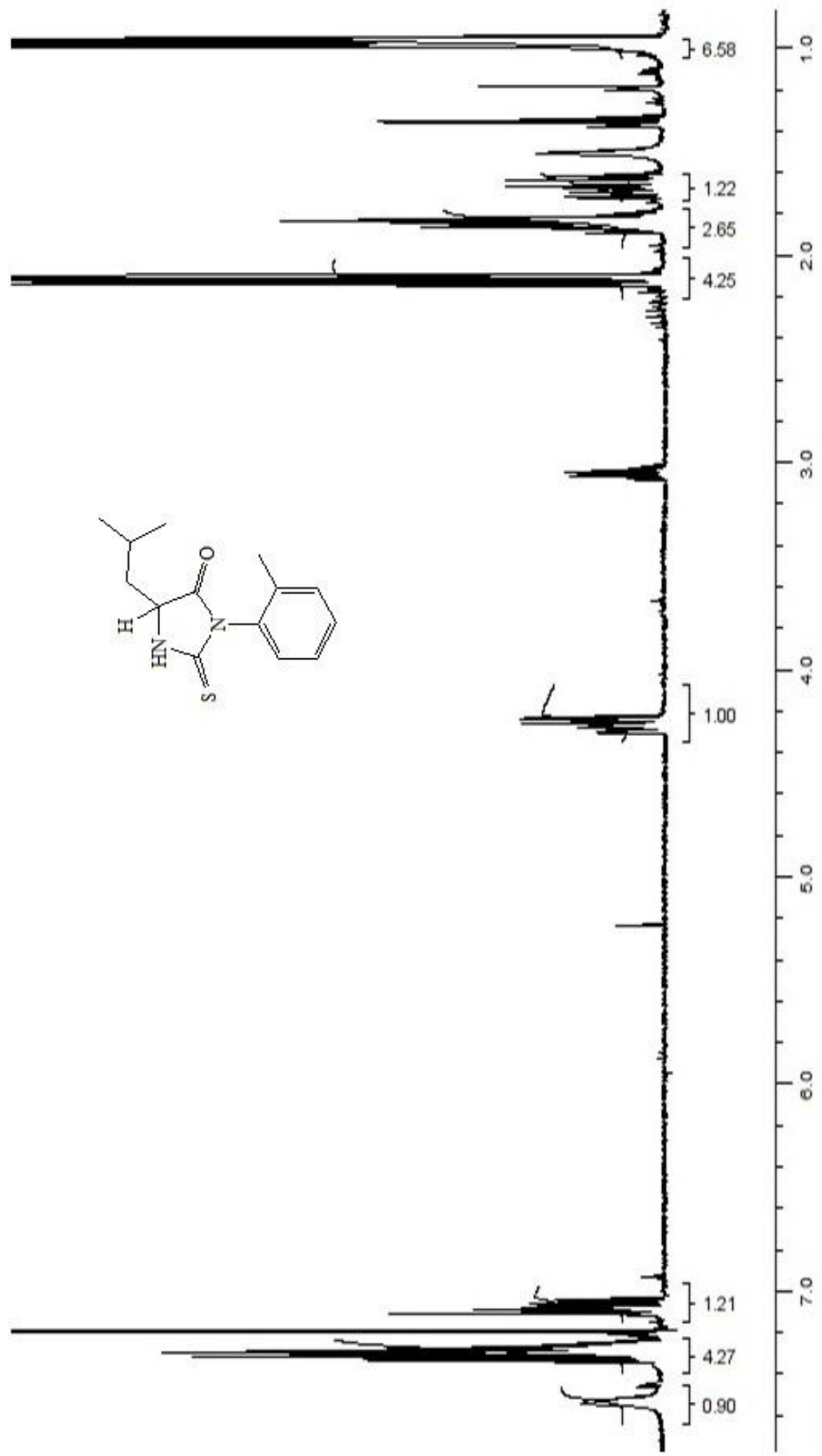


Figure A.17. The 400 MHz ¹H NMR spectrum of crude 5-isobutyl-3-(*o*-tolyl)-2-thiohydantoin in CDCl₃, used for assignment.

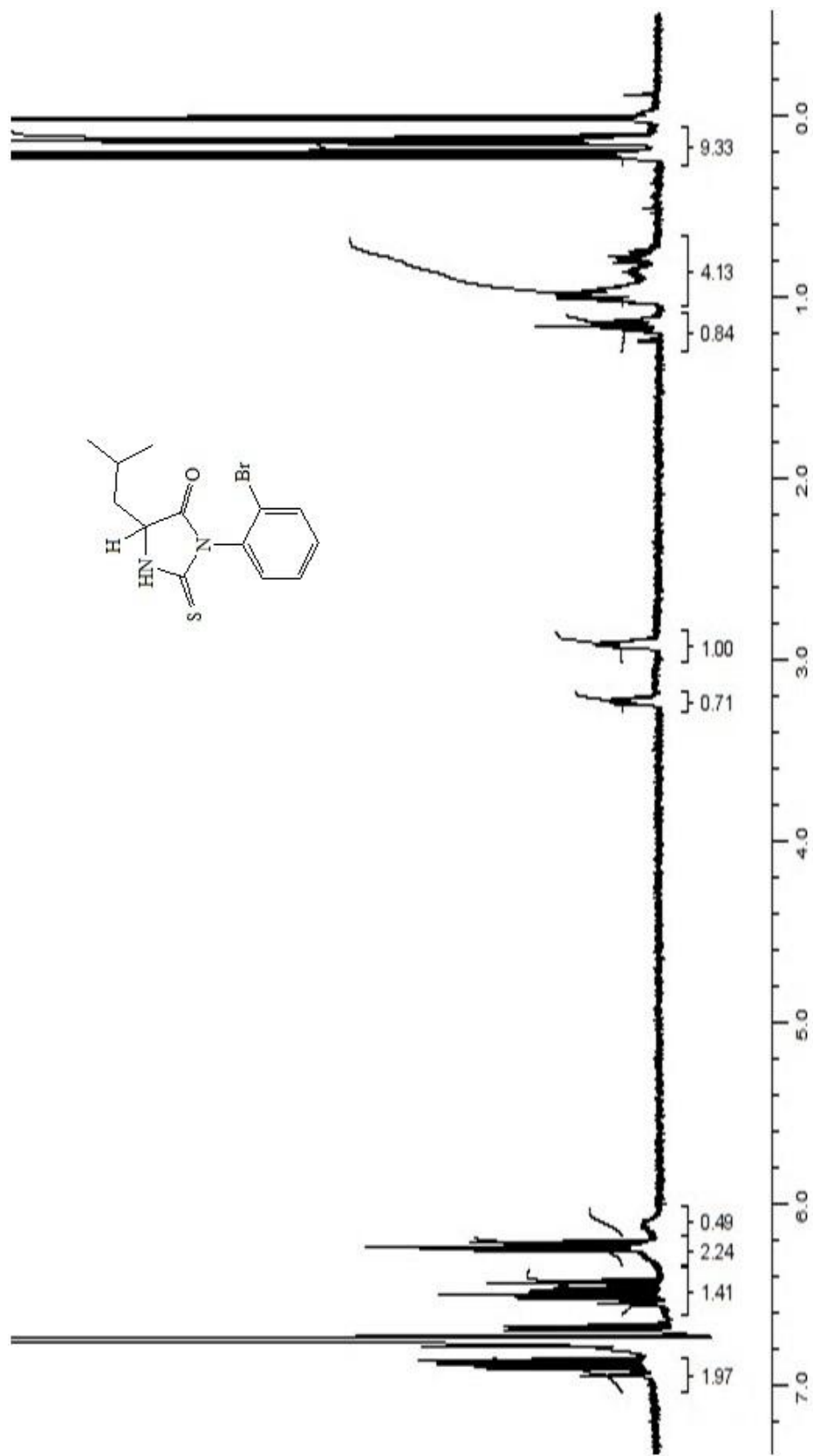


Figure A.18. The 400 MHz ^1H NMR spectrum of recrystallized 5-isobutyl-3-(*o*-bromophenyl)-2-thiohydantoin in C_6D_6 , used for assignment.